Leibniz-Gemeinschaft

Leibniz Institute for Solid State and Materials Research Dresden

Electron Holography

Axel Lubk

Converting phase shifts to contrasts: Fresnel imaging

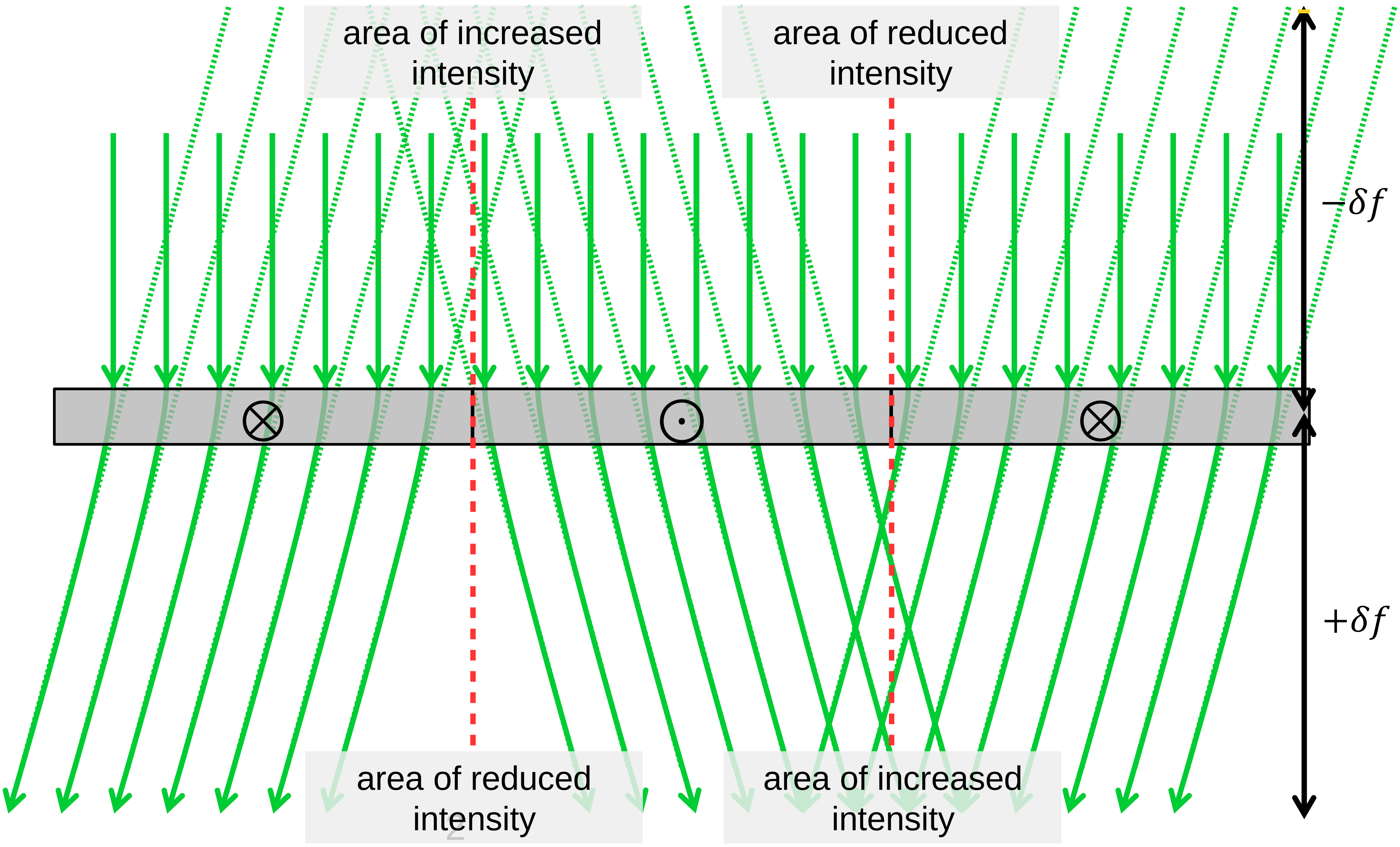

Fresnel imaging: Pros & Cons

Pro:

- simple
- fast
- sensitivity adjustable

Con:

- (partially) non-linear contrast
- defocus → unsharp images
- quantification difficult (but possible)
- sensitiv to dynamical scattering

Can be overcome by Holography! (now)

Recommended reading:

1. Völkl, Edgar, Allard, Lawrence F., Joy, David C. (Eds.) , Introduction to Electron Holography, Springer (1999).

1. **Fundamentals of electron scattering**
    a. **Axial scattering**
    b. **Magnetic and electric Ehrenberg–Siday–Aharonov–Bohm effect**

2. Fundamentals of Electron Holography and Tomography
    a. Holographic Principle (interference, reconstruction)
    b. Holographic Setups (inline, off-axis) and instrumental requirements
    c. Separation of electrostatic and magnetic contributions
    d. Tomographic reconstruction of 3D electric potential and magnetic induction vector field from tilt series of projections

How do fields act on electrons waves?

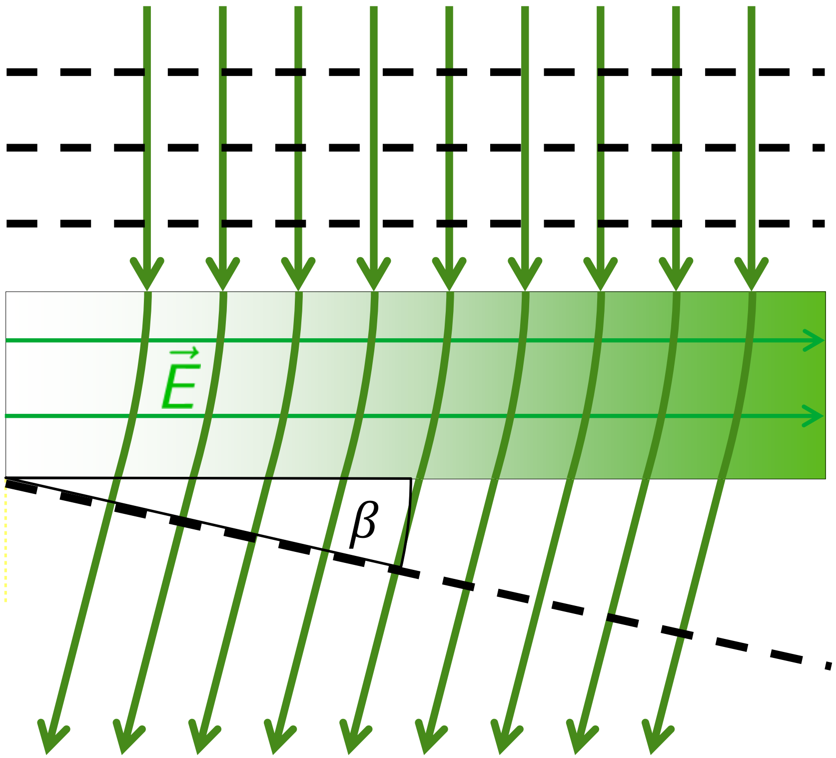

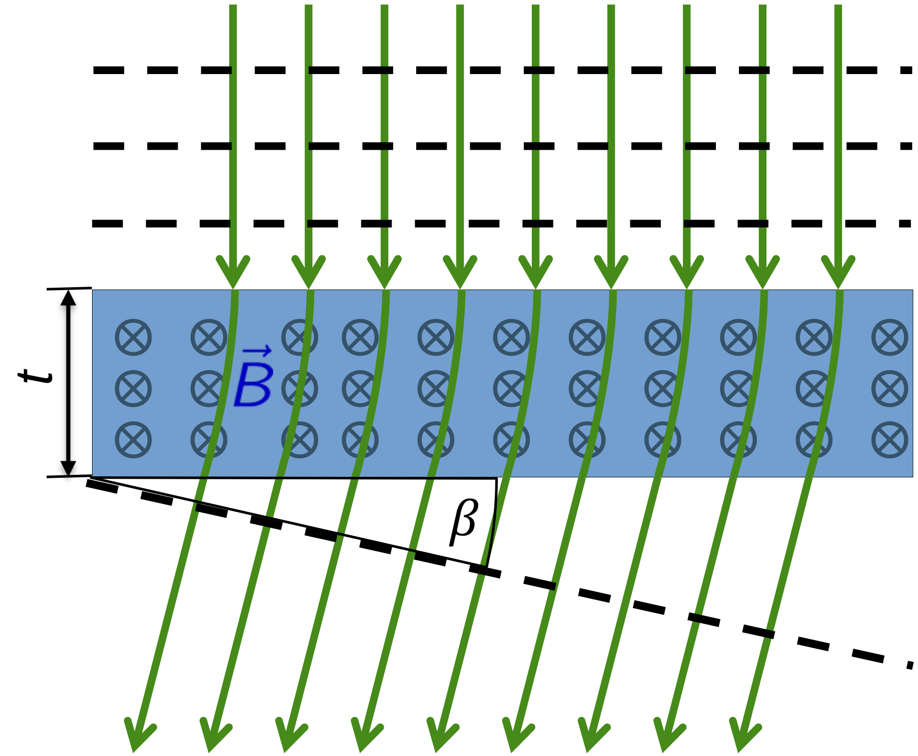

deflectio n angle

$$\beta = -\frac{et}{mv_0^2}\begin{pmatrix} E_x \\ E_y \end{pmatrix}$$

initial velocity

semiclassics

$$\beta = -\frac{et}{mv_0}\begin{pmatrix} -B_y \\ B_x \end{pmatrix}$$

$$\beta = \frac{1}{k}\nabla\varphi$$

phase shift

$$\varphi = \frac{et}{\hbar v_0}\Phi$$

electrostatic potential

$$p = mv_0 = \hbar k$$

momentum

wave number

$$\varphi = \frac{et}{\hbar}A_z$$

magnetic vector potential

How do fields act on electrons waves? *

reduced Klein-Gordon equation
(high-energy approximation)

$$E\Psi = \left[\frac{\hat{p}^2}{2m} - eV\right]\Psi$$

kinetic momentum operator

$$\hat{p} = -i\hbar\nabla + e\boldsymbol{A}$$

$$\Psi = e^{ik_z z}\psi$$

paraxial approximation

- small-angle scattering
- no backscattering

$$-2k_z\hbar\hat{p}_z\psi = \left[\hat{p}_\perp{}^2 - 2meV\right]\psi$$

$$\partial_z\psi \approx i\left[\frac{-\hat{p}_\perp{}^2}{2\hbar^2 k_z} + \sigma V - \frac{e}{\hbar}A_z\right]\psi$$

$\cong$ 2D time-dependent Schrödinger equation

axial approximation
(wavelength << object details)

- very small angle scattering

$$\partial_z\psi \approx i\left[\sigma V - \frac{e}{\hbar}A_z\right]\psi$$

$$\psi = e^{i\varphi}\psi_0 \rightarrow \varphi = \int_{\text{object}} \left(\frac{e}{\hbar v}V - \frac{e}{\hbar}A_z\right) dz$$

*** It is a good exercise to do derivation by yourself.**

Phase shift by electric potential

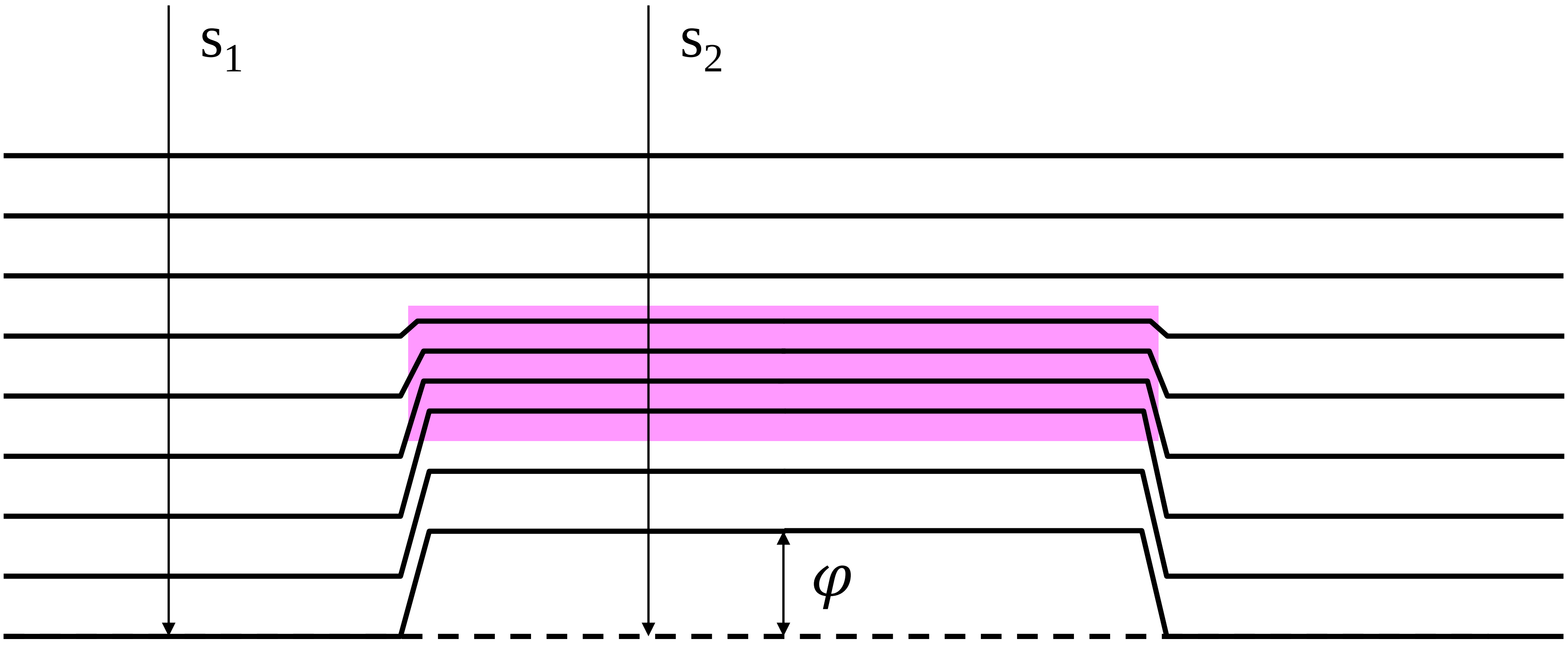

$$\varphi = k\left[\int_{s_2 - s_1} n\,ds\right] = \frac{e}{\hbar v}\int_{\mathrm{object}} V\,dz$$

refractive index

Detectable phase shift *

$$\underbrace{\Delta\varphi = \sigma \int_{s_2 - s_1} V \, ds}_{\text{electric}}$$

$$\Delta\varphi = \sigma \left(V_{\mathrm{p},1} - V_{\mathrm{p},2} \right)$$

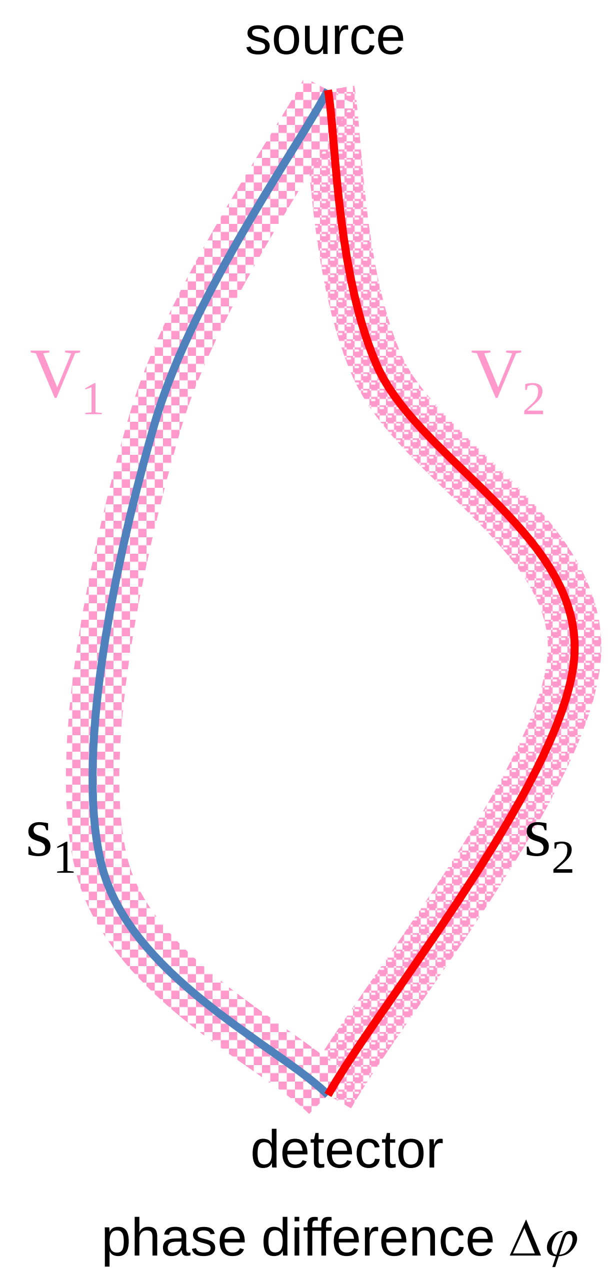

* Why can we only detect phase differences?

Detectable phase shift

$$\Delta\varphi = \underbrace{\sigma \int_{s_2-s_1} V\,ds}_{\text{electric}} - \underbrace{\frac{e}{\hbar}\oint_{s_2+s_1} \boldsymbol{A}\,d\boldsymbol{s}}_{\text{magnetic}}$$

$$\Delta\varphi = \sigma\left(V_{\mathrm{p},1} - V_{\mathrm{p},2}\right) - \frac{e}{\hbar}\Phi$$

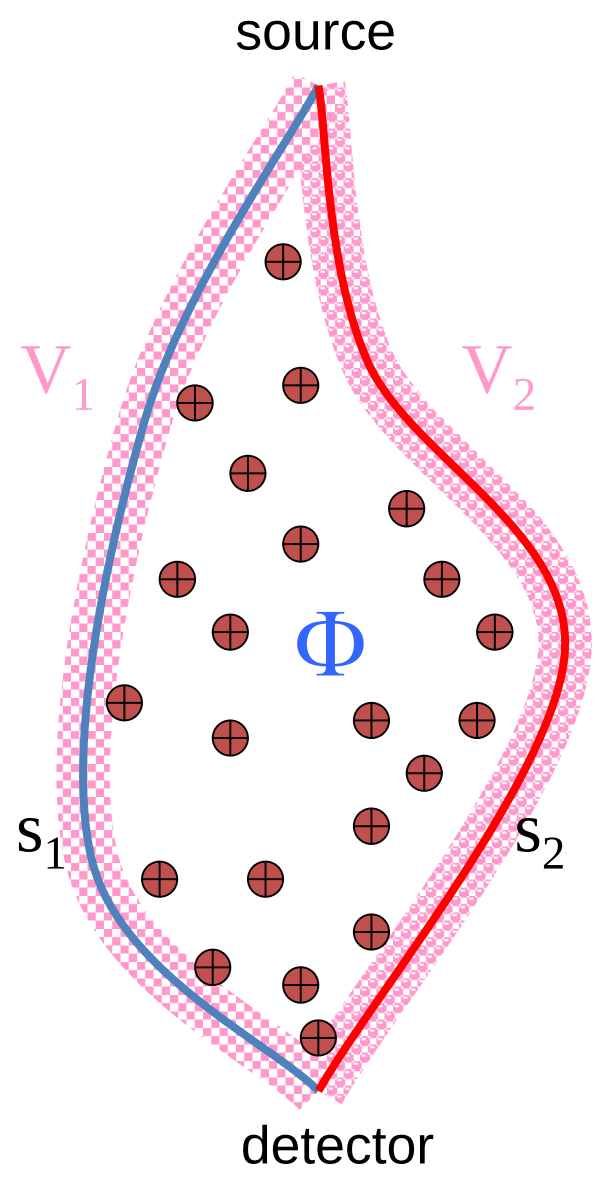

phase difference $\Delta\varphi$

Detectable phase shift

$$\Delta\varphi = \underbrace{\sigma \int_{s_2-s_1} V\,ds}_{\text{electric}} - \underbrace{\frac{e}{\hbar}\oint_{s_2+s_1} \boldsymbol{A}\,d\boldsymbol{s}}_{\text{magnetic}}$$

$$\Downarrow$$

$$\Delta\varphi = \sigma\left(V_{\mathrm{p},1} - V_{\mathrm{p},2}\right) - \frac{e}{\hbar}\Phi$$

For the magnetic phase shift a Lorentz force is not required at the electron trajectories !

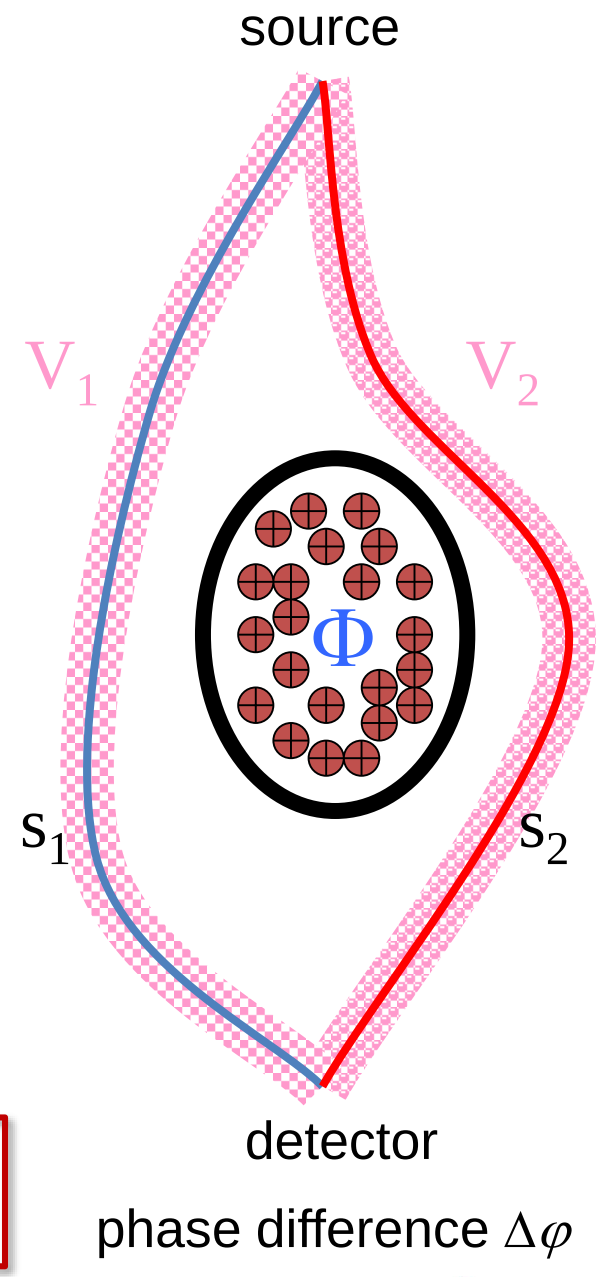

Ehrenberg - Siday – Aharonov - Bohm Effect

Proposal: Ehrenberg & Siday 1949

Aharonov & Bohm 1958

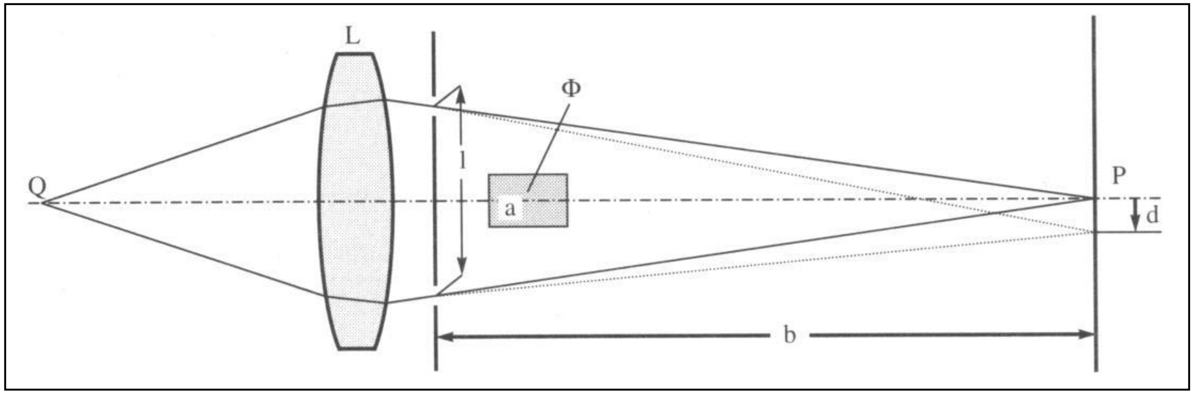

Experiment: Möllenstedt & Bayh 1962

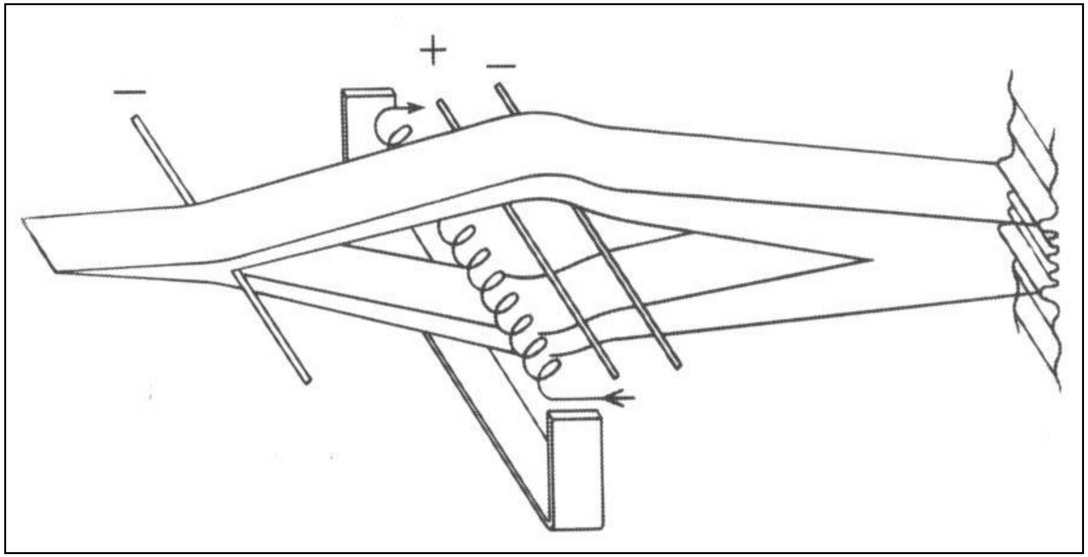

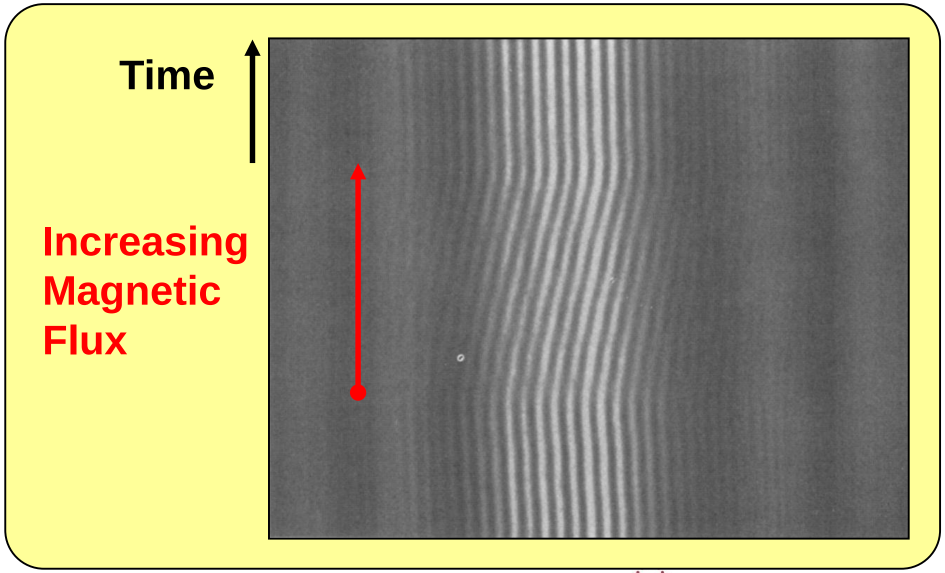

Magnetic phase shift

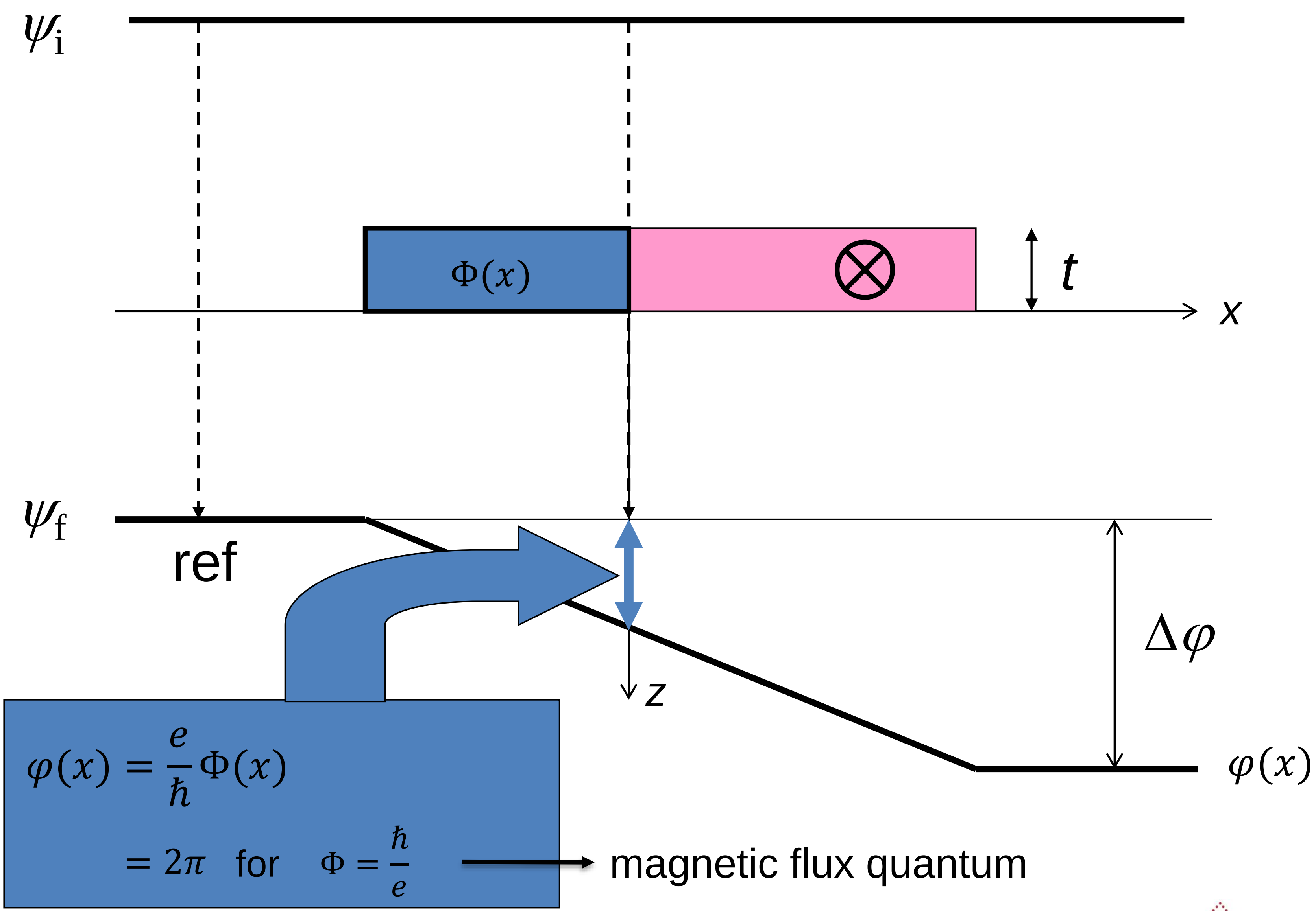

Summary: object exit wave

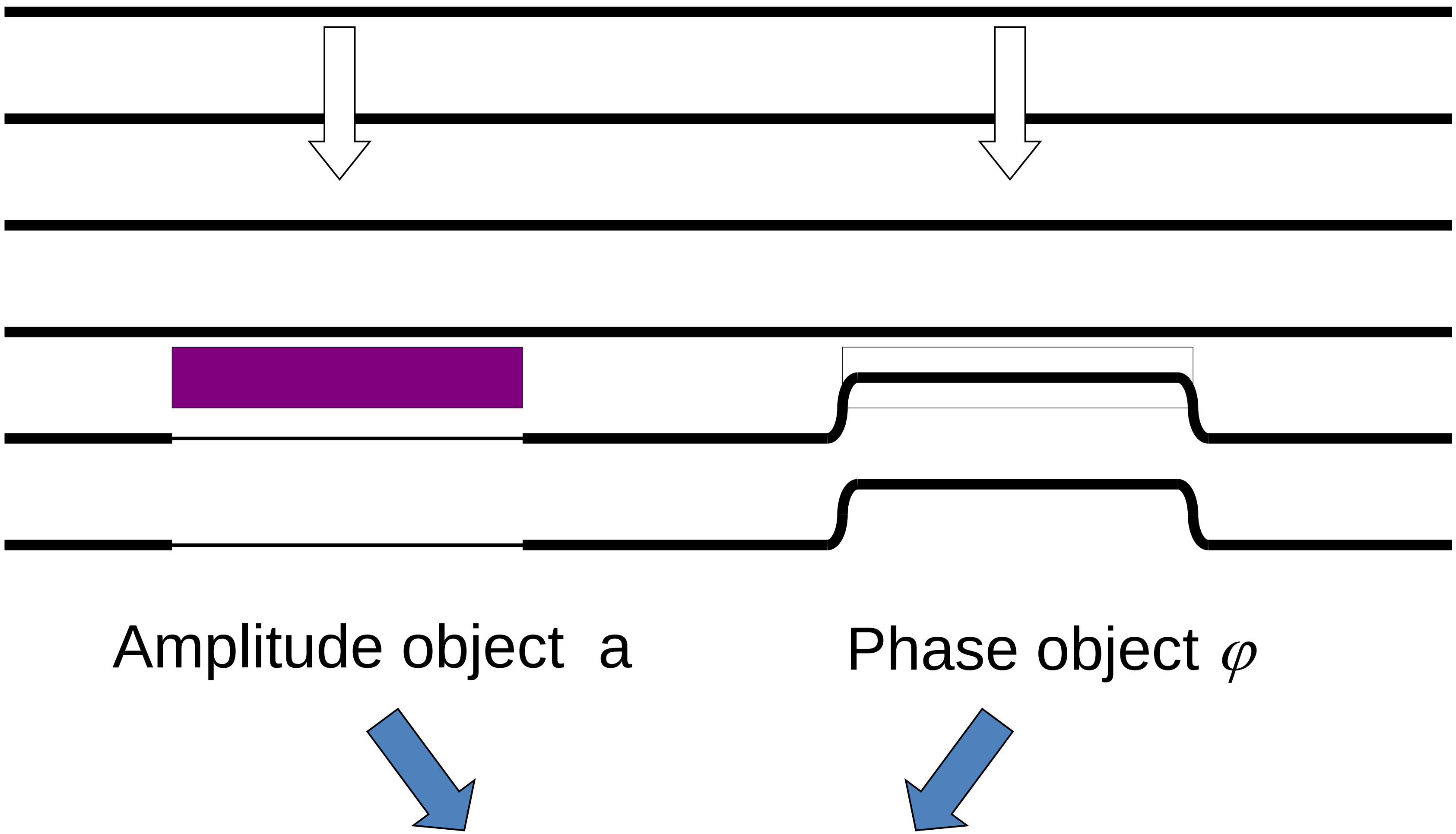

$$a \exp[i\,\varphi]$$

Summary: object exit wave

phase modulation $\varphi(x, y)$:

micro- /nanofields

- electric
- magnetic

amplitude modulation $a(x, y)$:

- scattering into large angles
- interference effects
- inelastic scattering

1. Fundamentals of electron scattering
    a. Axial scattering
    b. Magnetic and electric Ehrenberg–Siday–Aharonov–Bohm effect

2. Fundamentals of Electron Holography and Tomography
    a. Holographic Principle (interference, reconstruction)
    b. Holographic Setups (inline, off-axis) and instrumental requirements
    c. Separation of electrostatic and magnetic contributions
    d. Tomographic reconstruction of 3D electric potential and magnetic induction vector field from tilt series of projections

Dennis Gabor

1902-1979

Nobel Prize 1971

Easter 1947, on the tennis court:

... and all of sudden it came to me, without any effort on my side.

Interference and diffraction
are mutually inverse

Electron Holography
measures phases

Dennis Gabor

Holography

Object wave | hologram | Image wave

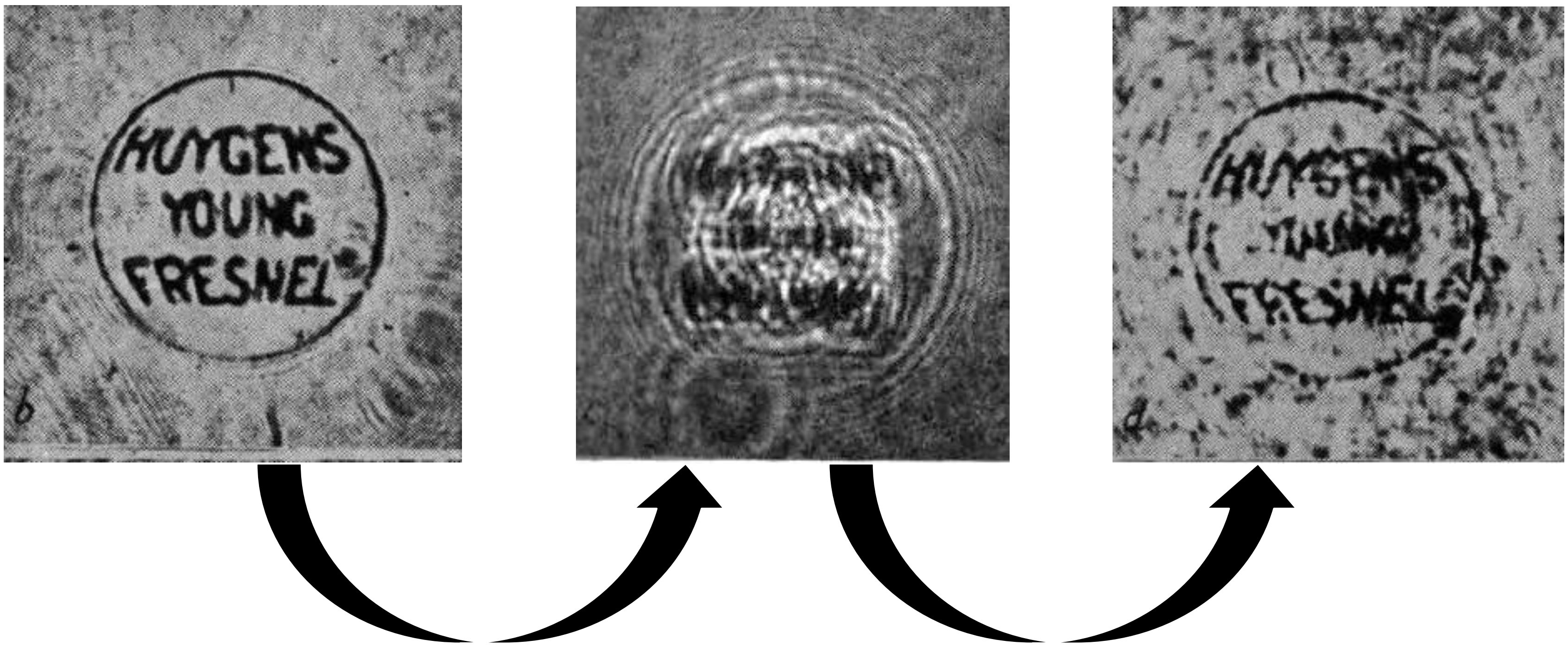

interference | diffraction

Common Forms of Electron Holography

focal series inline

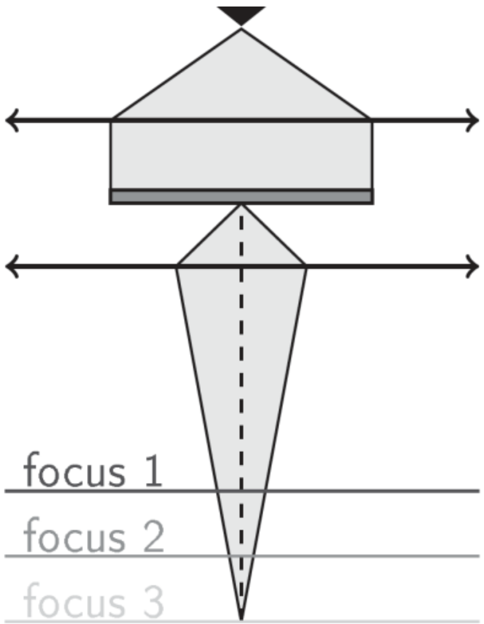

off-axis

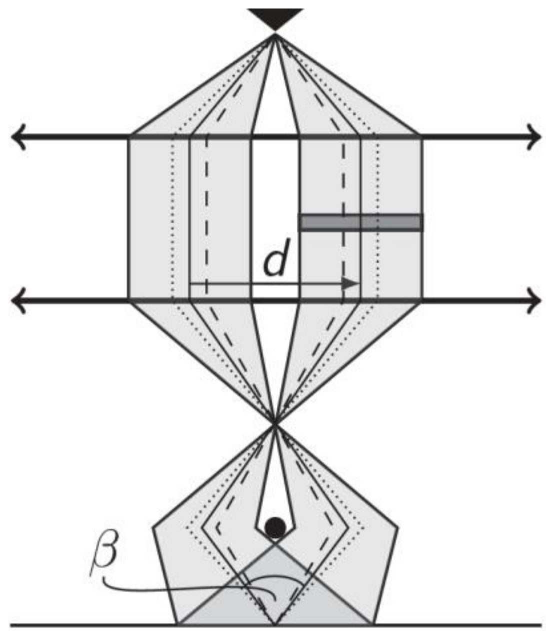

transport of intensity

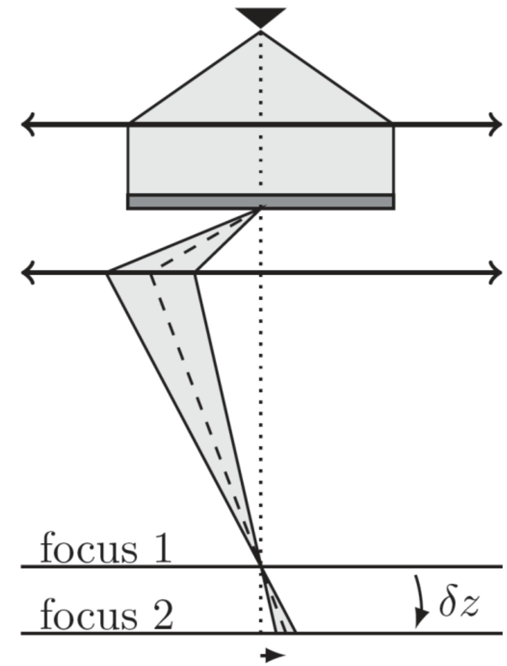

J.M. Cowley, *20 forms of holography*, Ultramicroscopy 41 (1992), 335-348

Holography - Dennis Gabor´s idea

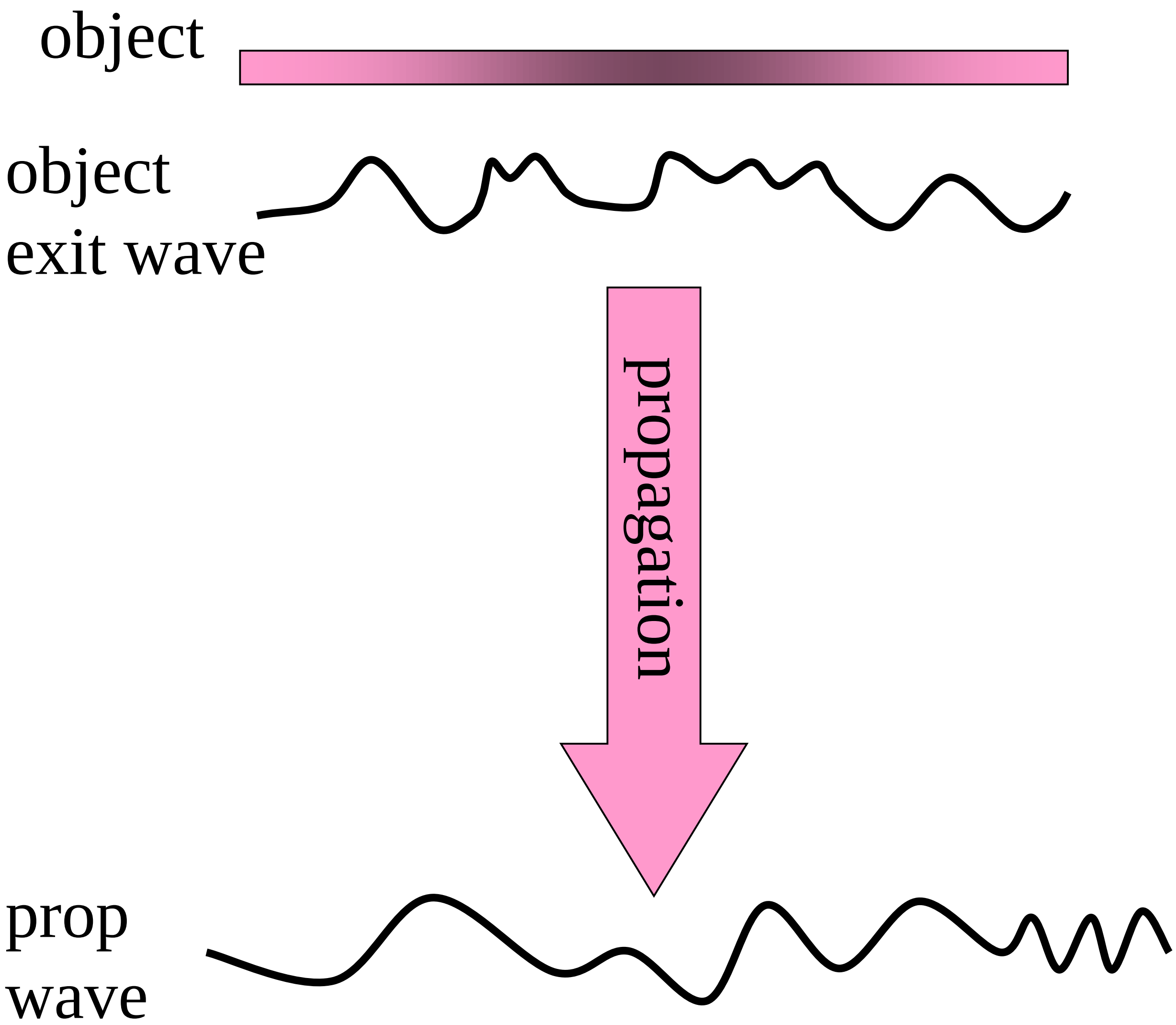

Holography - Dennis Gabor´s idea

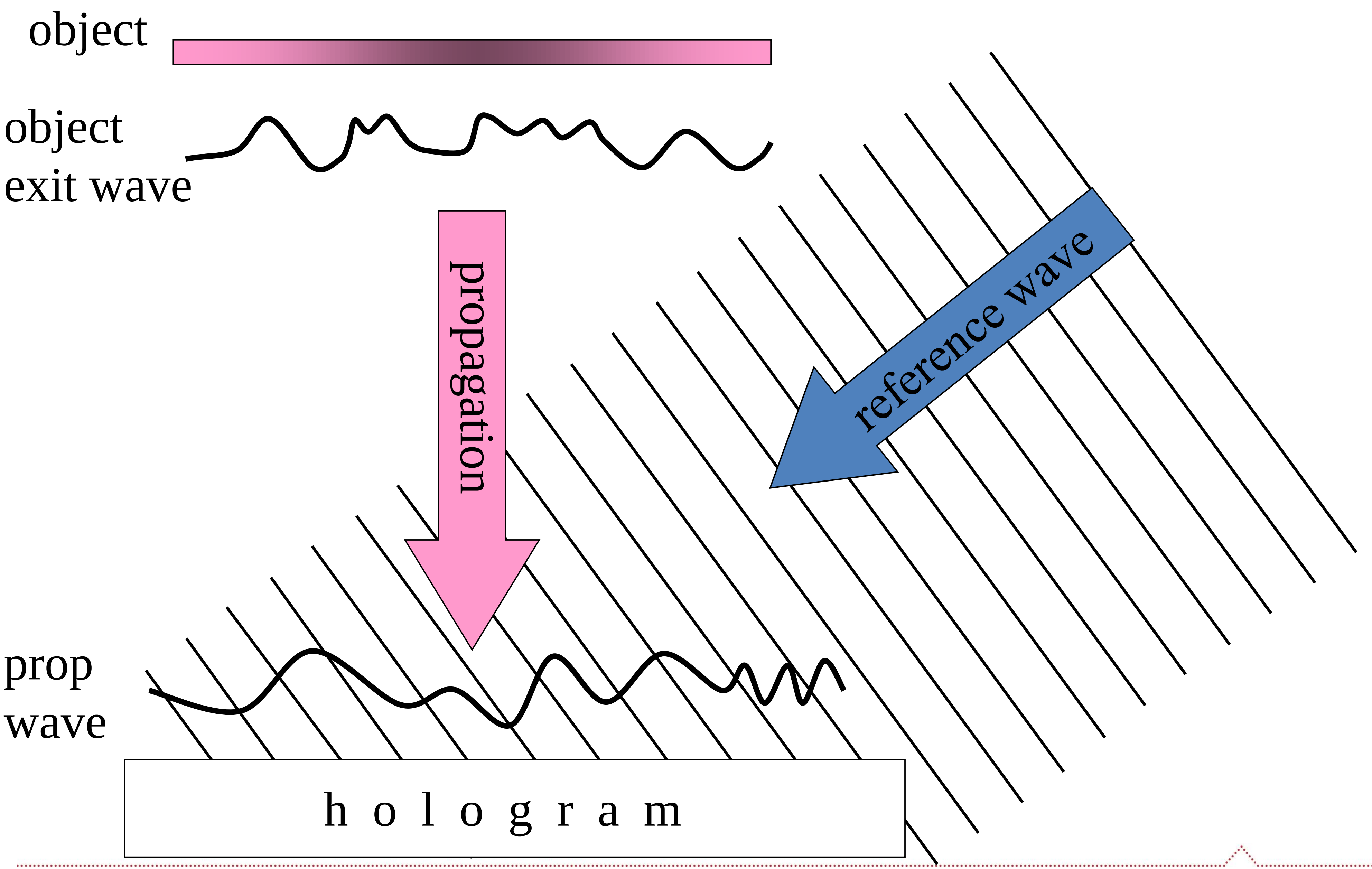

Holography - reconstruction of wave

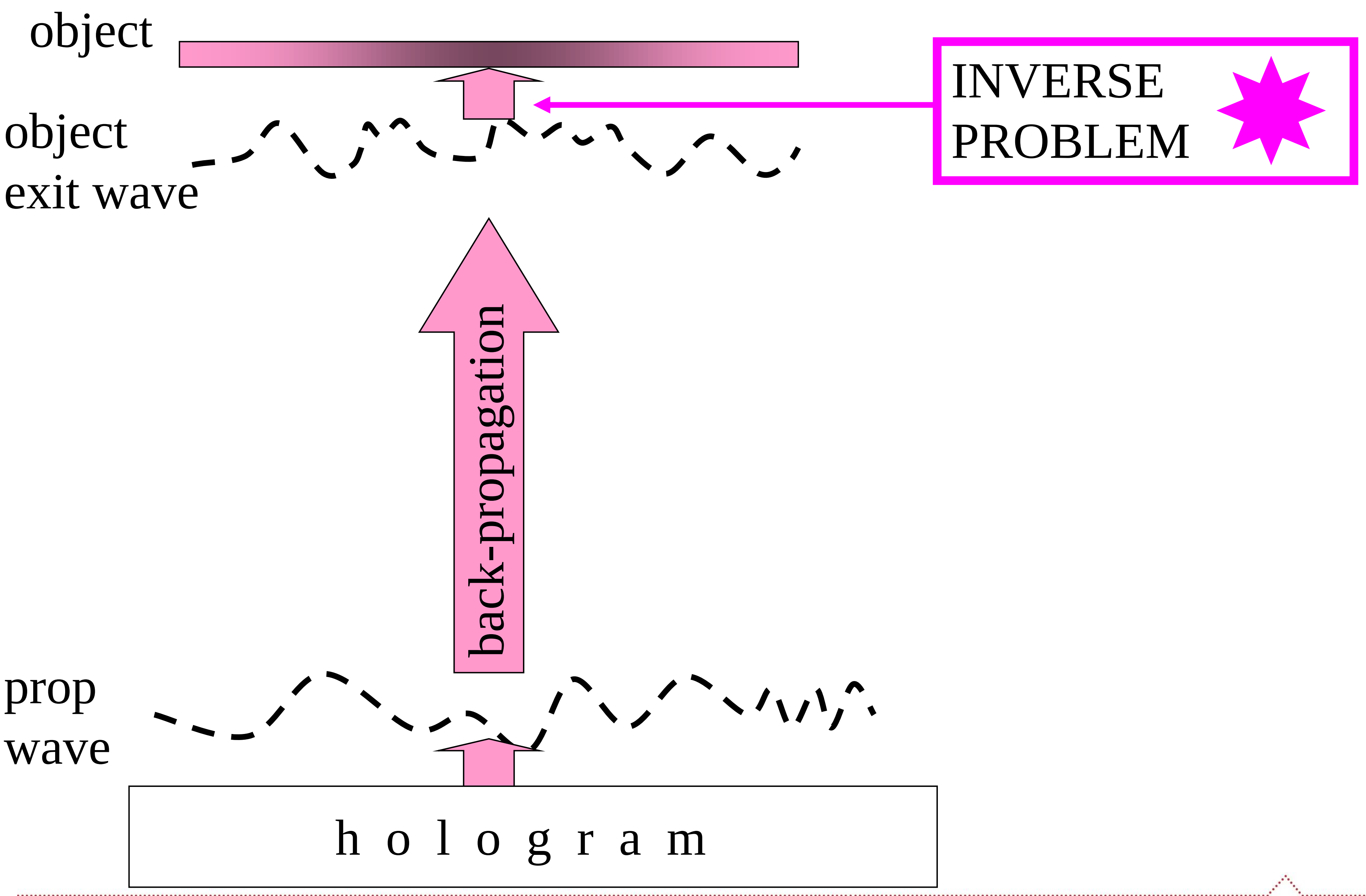

Holography: basic scheme

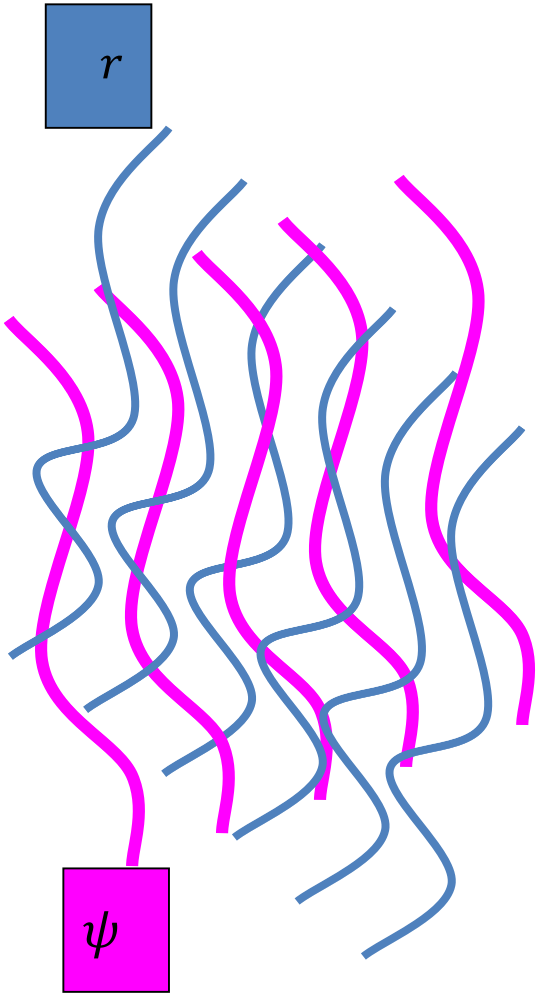

Holography: recording hologram

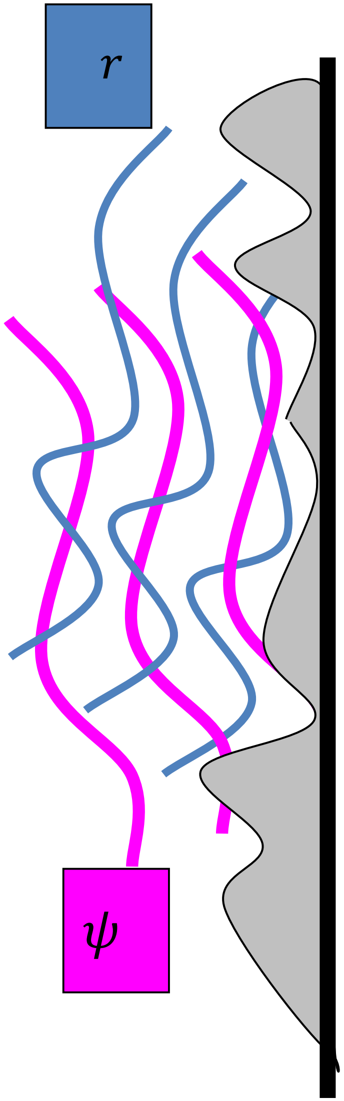

$$
\begin{aligned}
hol &= (\psi + r)(\psi + r)^* \\
&= \psi\psi^* + rr^* + \psi r^* + \psi^* r
\end{aligned}
$$

Holography: reconstruction of wave

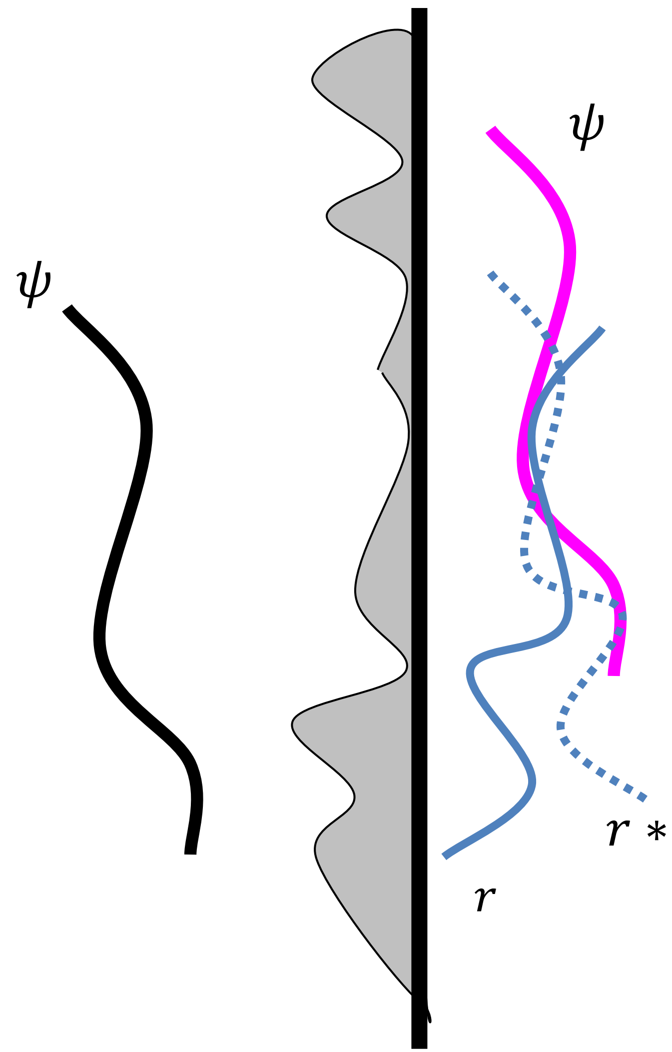

$$\psi \cdot hol = (\psi\psi^*)\psi + (rr^*)\psi + (\psi r^*)\psi + (\psi^* r)\psi$$

$$= \psi(\psi\psi^* + rr^*) + r^*(\psi\psi) + r(\psi\psi^*)$$

ψ-wave modulated in amp $\psi; r$

r^*-wave modulated in amp/phase ψ

r-wave modulated in amp ψ

Holography: reconstruction of wave

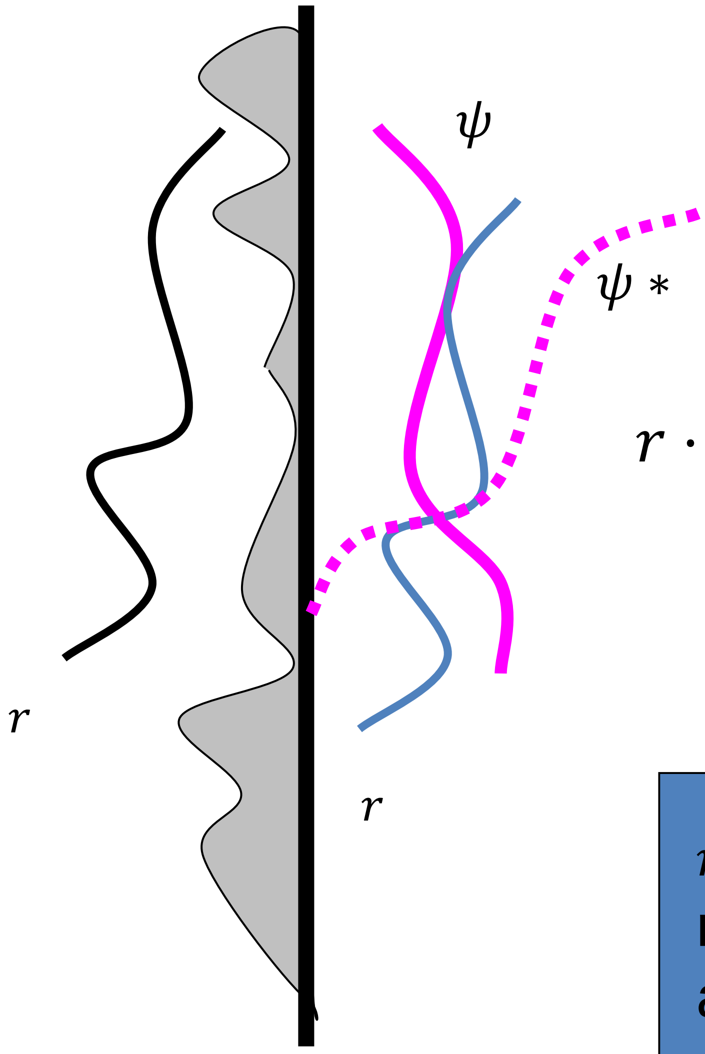

$$r \cdot hol = (\psi\psi^*)r + (rr^*)r + (\psi r^*)r + (\psi^* r)r$$
$$= r(\psi\psi^* + rr^*) + \psi(r^* r) + \psi^*(rr)$$

r-wave modulated in amp $\psi; r$

ψ-wave modulated in amp r

ψ^*-wave modulated in amp/phase r

Plane reference wave r

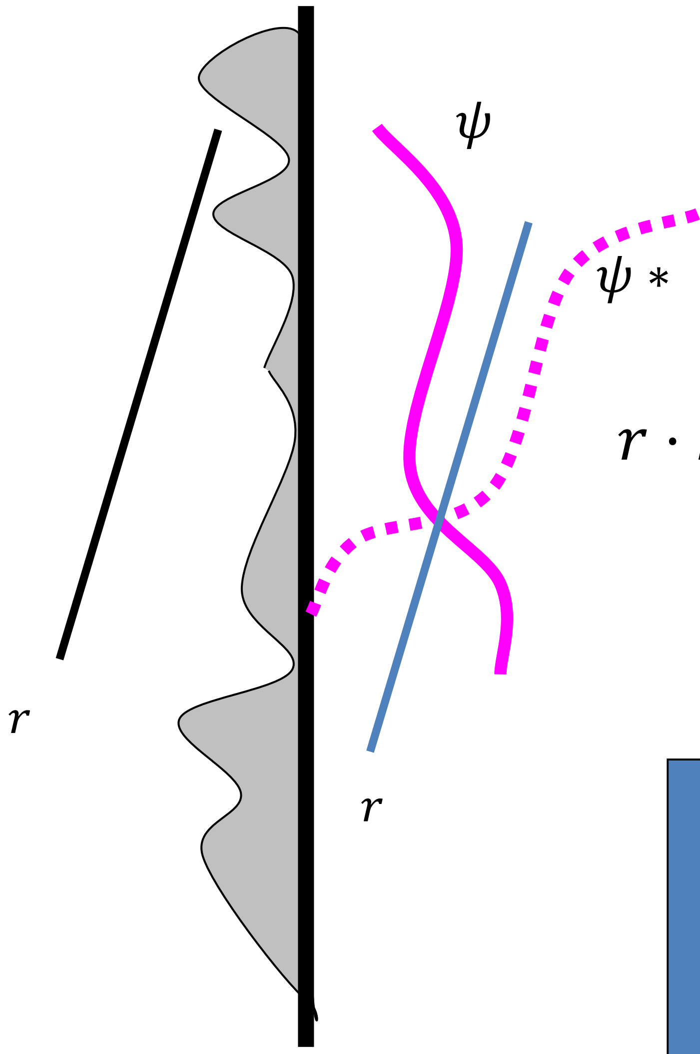

$$r \cdot hol = (\psi\psi^*)r + (rr^*)r + (\psi r^*)r + (\psi^* r)r$$

$$= \underbrace{r(\psi\psi^* + rr^*)} + \underbrace{\psi(r^* r)} + \underbrace{\psi^*(rr)}$$

r -wave modulated in amp ψ

ψ -wave

ψ * -wave modulated in phase r

Where to take the hologram ?

Object plane

Fresnel region

Fraunhofer region

Fourier plane

?

In principle: „where“ is not essential,

but with electrons we are „coherency-limited“

.....

Where to take the hologram ?

Inline Holography

Scattering Regimes

Reconstruction Schemes

Illumination $k = 2\pi / \lambda$

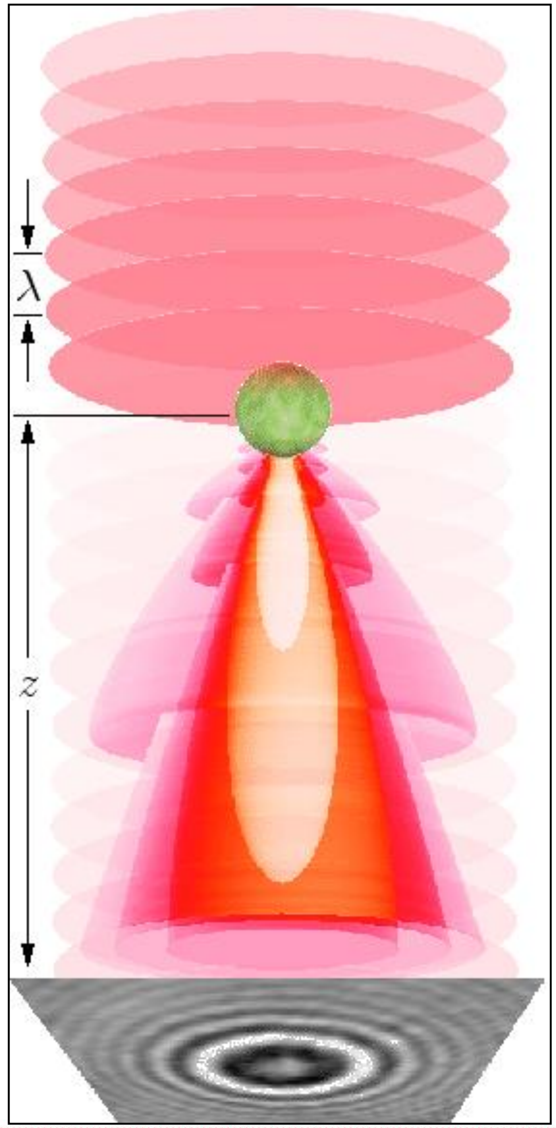

Differential Defocus / Transport of Intensity Reconstruction

Fresnel (near field)

Defocus Series Reconstruction

Fraunhofer (far field)

Fraunhofer Holography

Figure from Lee, Optics Express Vol. 15, Issue 26, pp. 18275-18282 (2007)

1. Fundamentals of electron scattering
    a. Axial scattering
    b. Magnetic and electric Ehrenberg–Siday–Aharonov–Bohm effect

2. Fundamentals of Electron Holography and Tomography
    a. Holographic Principle (interference, reconstruction)
    b. Holographic Setups (inline, off-axis) and instrumental requirements
    c. Separation of electrostatic and magnetic contributions
    d. Tomographic reconstruction of 3D electric potential and magnetic induction vector field from tilt series of projections

Transport of Intensity Reconstruction

Paraxial Eq.

$$\boxed{\frac{\partial \Psi(\mathbf{r}_\perp, z)}{\partial z} = \frac{i}{2k} \Delta_\perp \Psi(\mathbf{r}_\perp, z)}$$

Continuity Eq. / Transport of Intensity Eq.

density / intensity

$$\boxed{\rho \equiv |\Psi|^2}$$

$$\boxed{\begin{aligned} \frac{\partial \rho(\mathbf{r}_\perp, z)}{\partial z} &= -\frac{1}{k} \nabla_\perp \cdot j_\perp(\mathbf{r}_\perp, z) \\ &= -\frac{1}{k} \nabla_\perp \cdot \left(\rho(\mathbf{r}_\perp, z) \nabla_\perp \varphi(\mathbf{r}_\perp, z) \right) \end{aligned}}$$

phase

$$\boxed{\varphi \equiv \arg \Psi}$$

experimental data from 2 slightly defocussed images

$$\boxed{\rho(z+\delta z),\ \rho(z-\delta z)}$$

$$\boxed{\begin{aligned} \frac{\partial \rho(z)}{\partial z} &= \frac{\rho(z+\delta z) - \rho(z-\delta z)}{2\delta z} + O\left(\delta z^2\right) \\ \rho(z) &= \frac{\rho(z+\delta z) + \rho(z-\delta z)}{2} + O\left(\delta z^2\right) \end{aligned}}$$

Transport of Intensity Reconstruction

simplified TIE reconstruction

$$\boxed{\begin{aligned}\frac{\partial\rho(\mathbf{r}_\perp,z)}{\partial z} &= -\frac{1}{k}\nabla_\perp\cdot j_\perp(\mathbf{r}_\perp,z)\\ &= -\frac{1}{k}\nabla_\perp\cdot\left(\rho(\mathbf{r}_\perp,z)\nabla_\perp\varphi(\mathbf{r}_\perp,z)\right)\end{aligned}}$$

phase object

$$\boxed{\rho(\mathbf{r}_\perp,z)=\text{const.}}$$

$$\boxed{\frac{\partial\rho(\mathbf{r}_\perp,z)}{\partial z} = -\frac{\rho}{k}\Delta_\perp\varphi(\mathbf{r}_\perp,z)}$$

Poisson problem
(e.g., solve with periodic boundary conditions)

minimal model

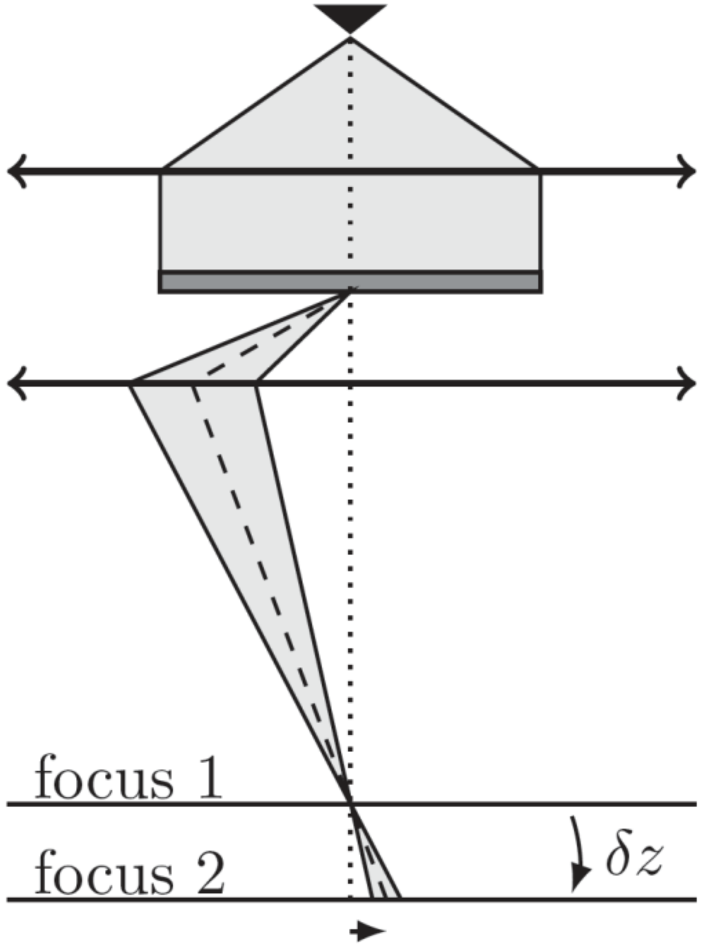

TIE: Pros & Cons

Pro:

- linear signal
- simple reconstruction
- simple experiment
- no external reference / vacuum required
- works at moderate coherency

Con:

- not so fast (2 recordings)
- not sensitiv to small spatial frequencies (large scale variations)
- ambiguous result (because of unknown boundary conditions)

Inline Holography

minimal model

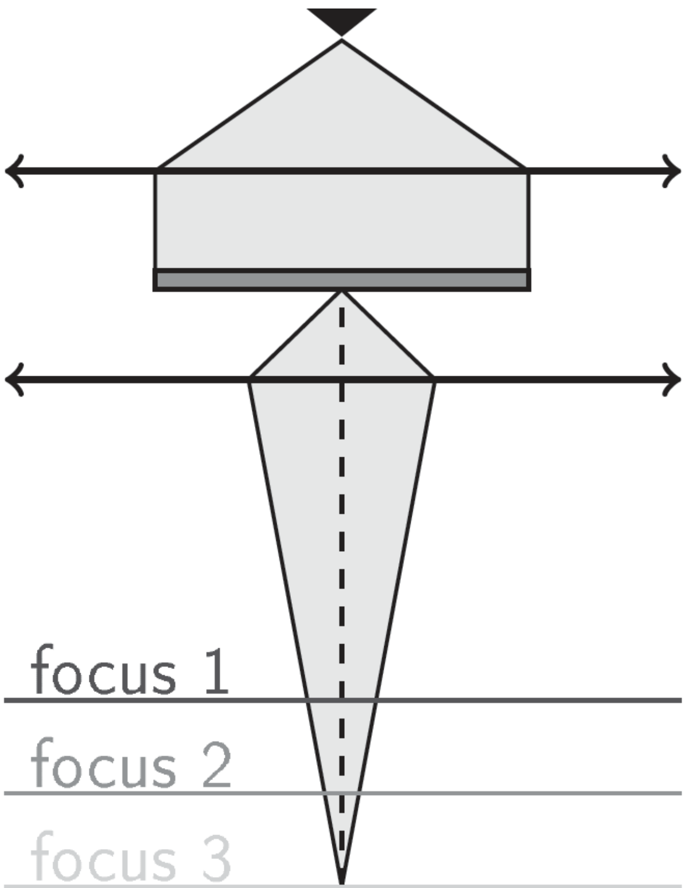

reconstruction algorithm

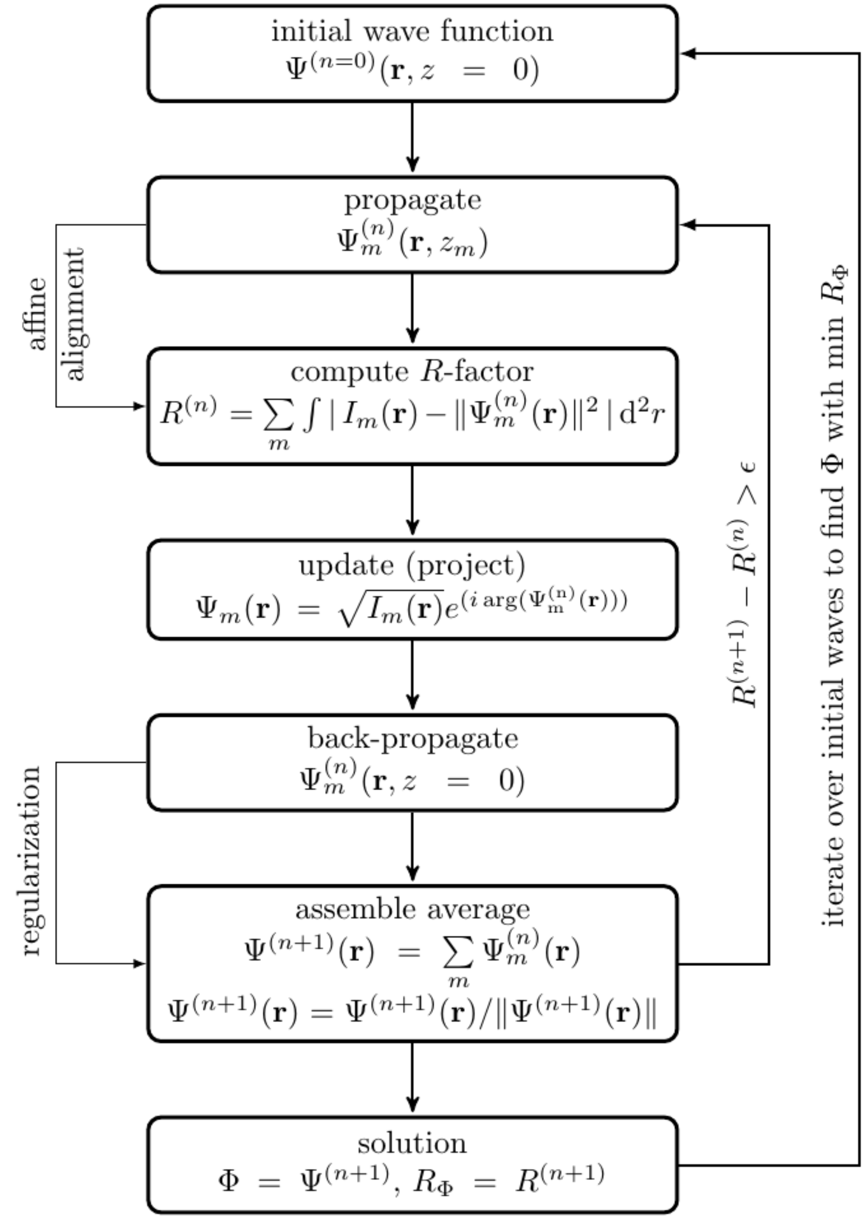

Focal Series Reconstruction

Experimental focus series

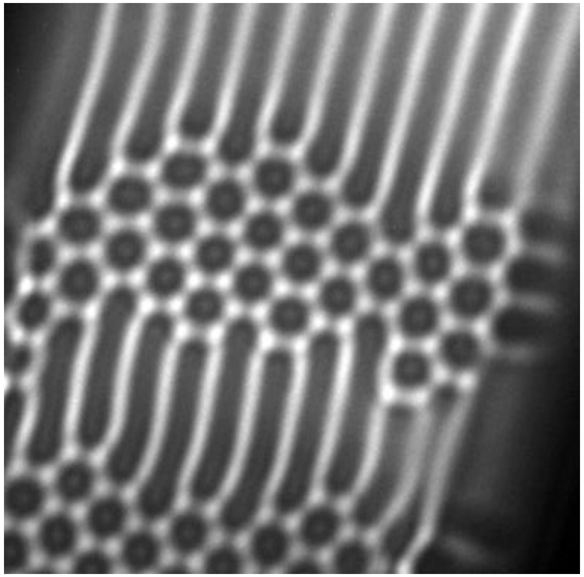

Reconstruction of B-Field

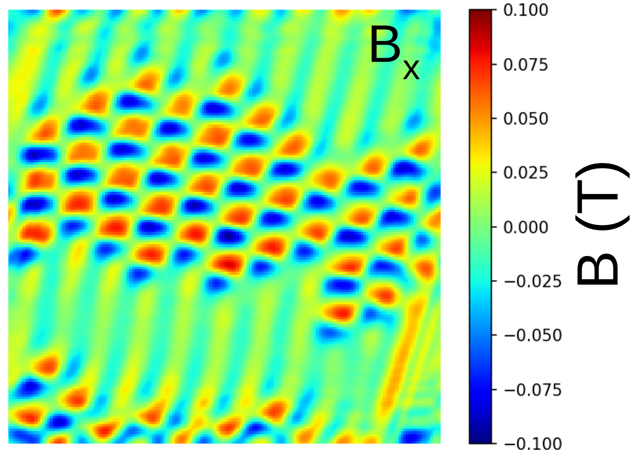

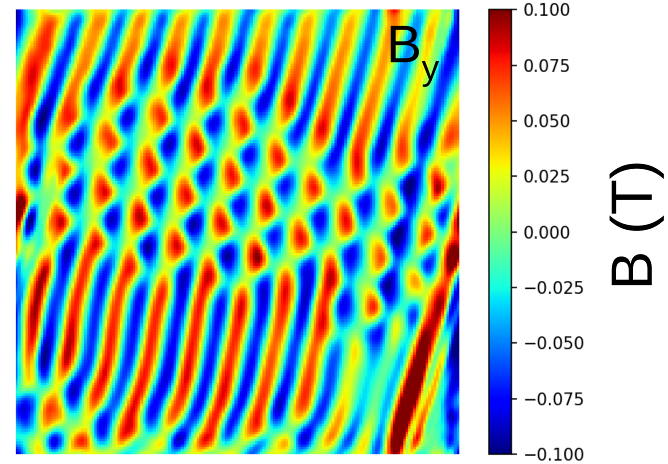

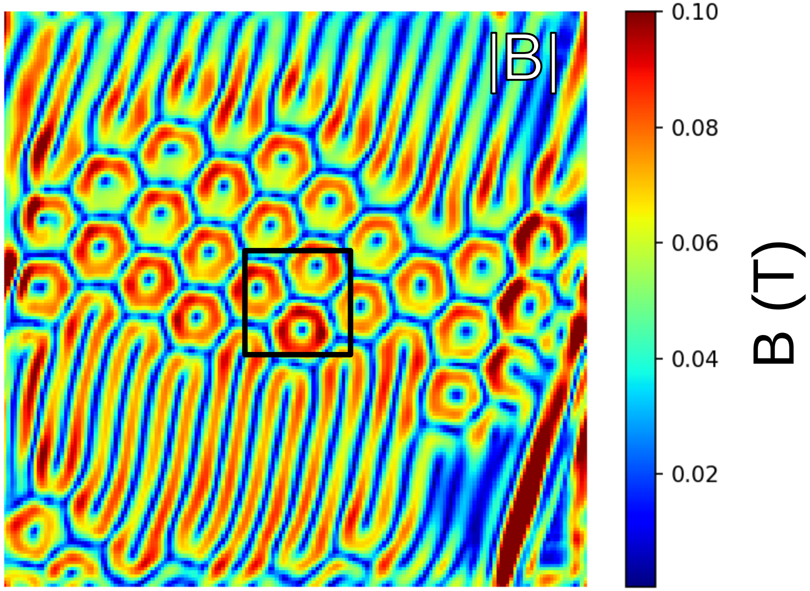

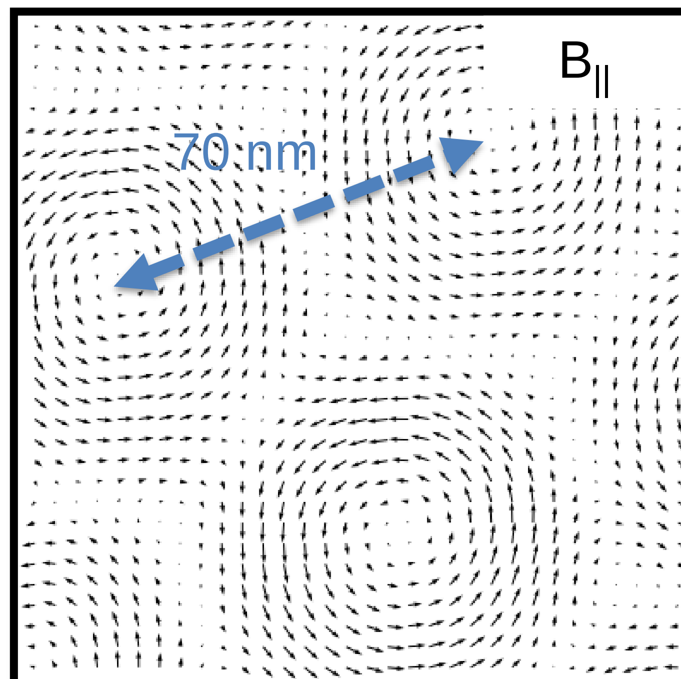

Focal Series: Pros & Cons

Pro:

- sensitiv to smaller (but still not very small) spatial frequencies
- works at every TEM
- no external reference / vacuum required

Con:

- very slow
- ambiguous result (depending on starting guess)
- complicated reconstruction

Off-axis electron holography

Hologram

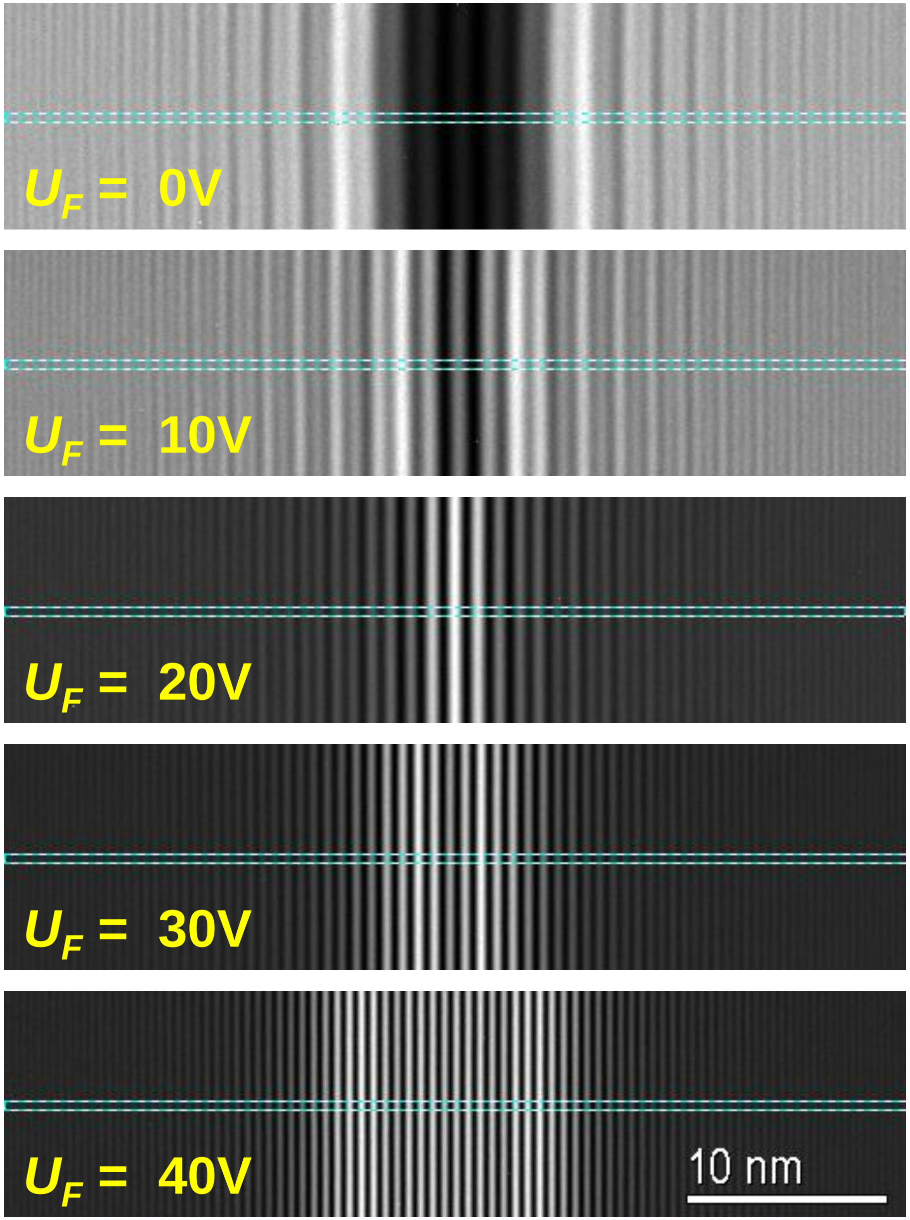

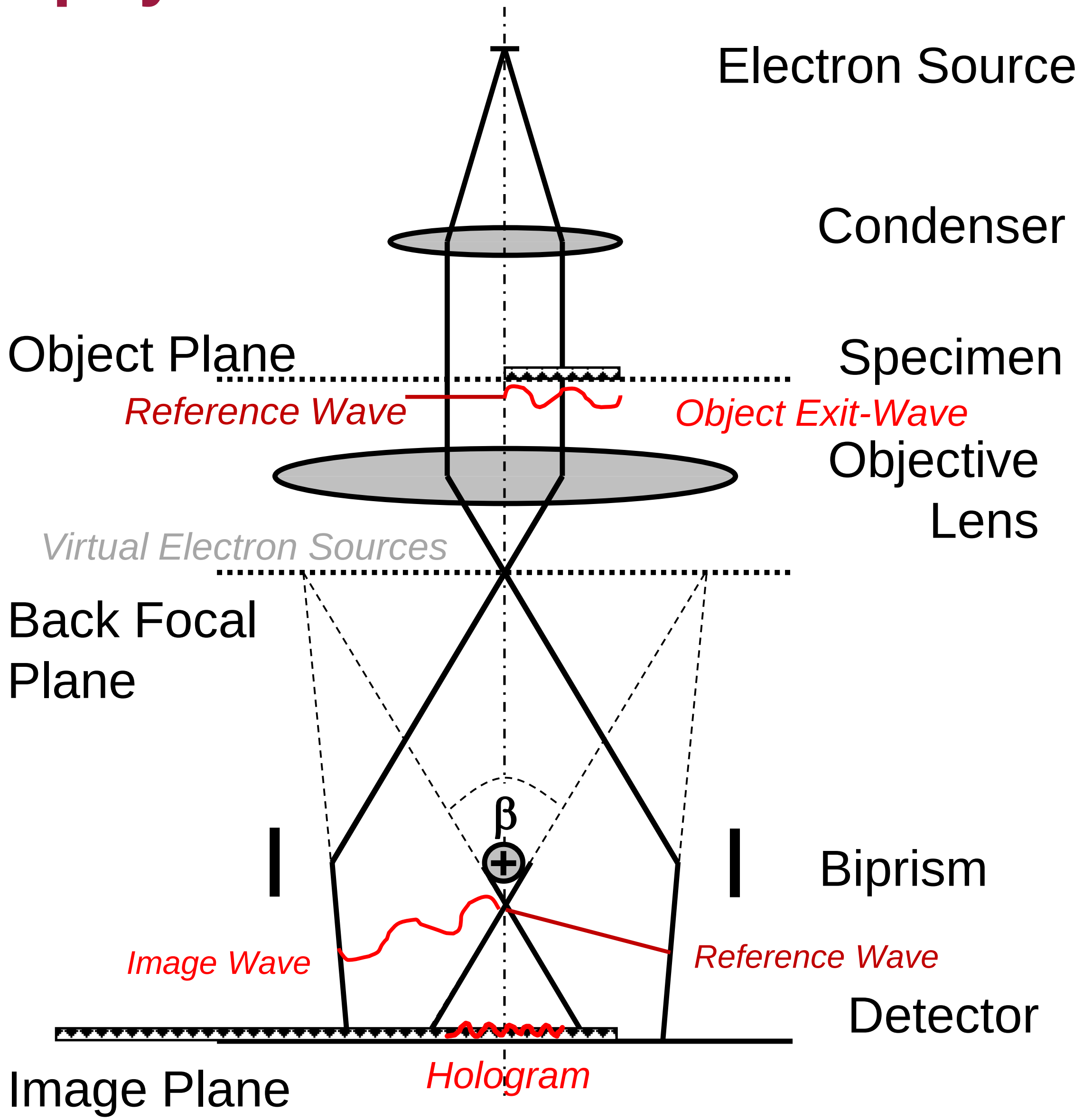

$$I_{\mathrm{hol}}(\mathbf{r}) = I_{\mathrm{CB}}(\mathbf{r}) + 2\mu_c I_{\mathrm{SB}}(\mathbf{r}) \cos\left(\mathbf{q}_{\mathrm{c}}\mathbf{r} + \varphi(\mathbf{r})\right)$$

Biprism-Holder

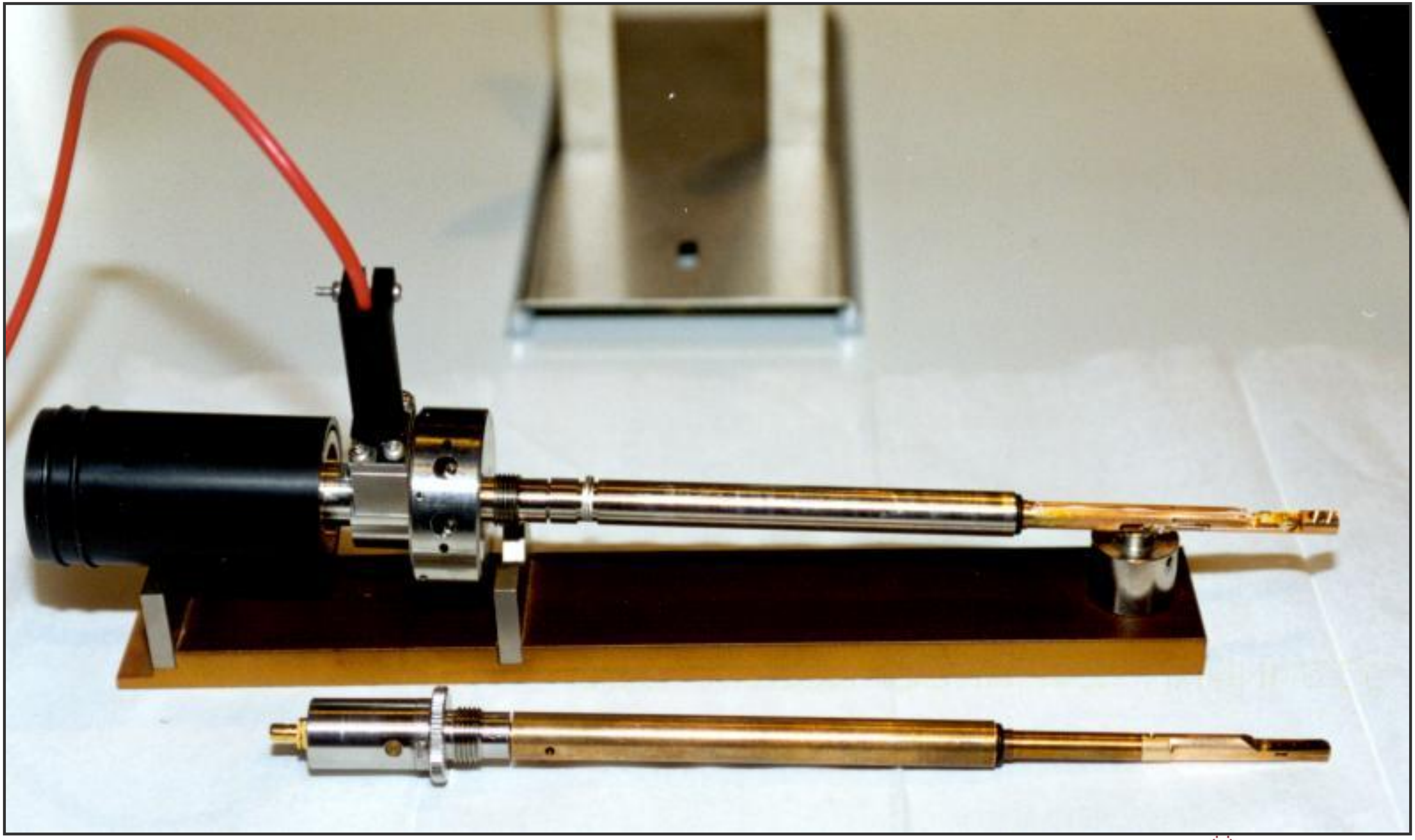

Biprism-Holder

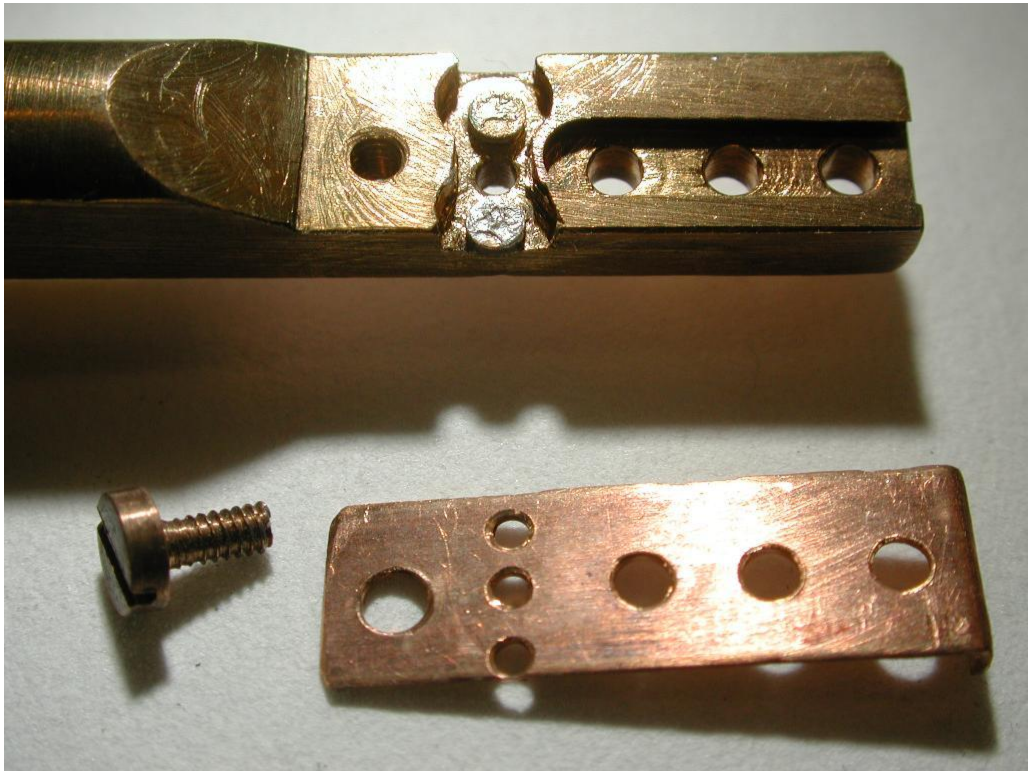

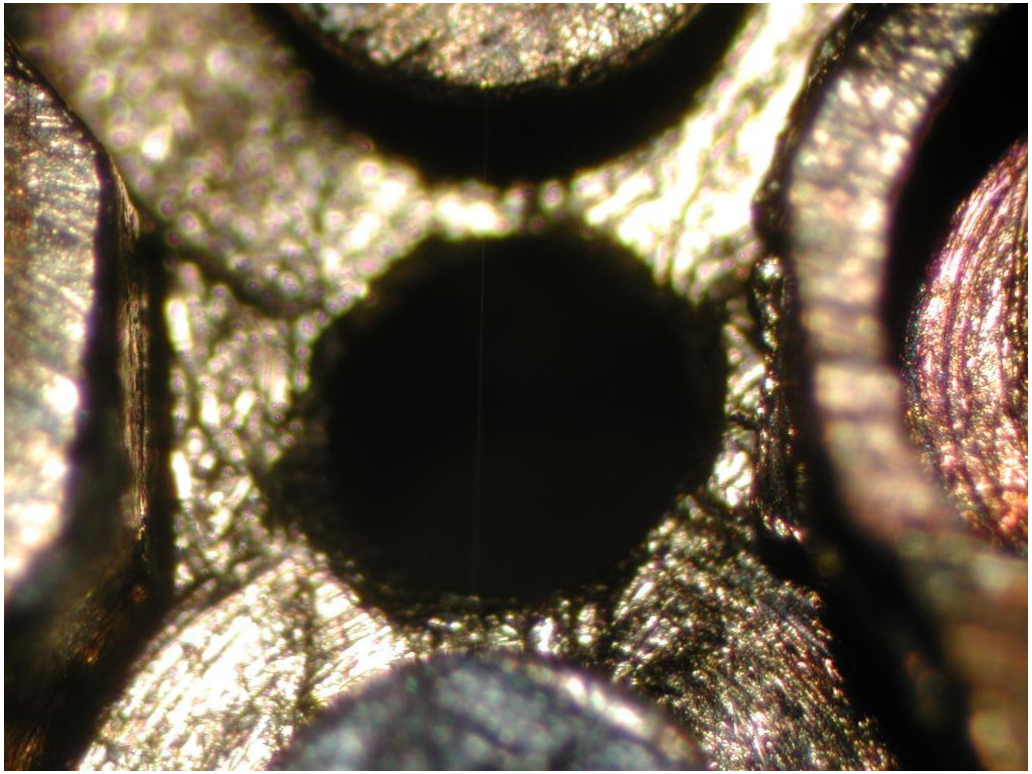

Off-axis electron holography

Hologram

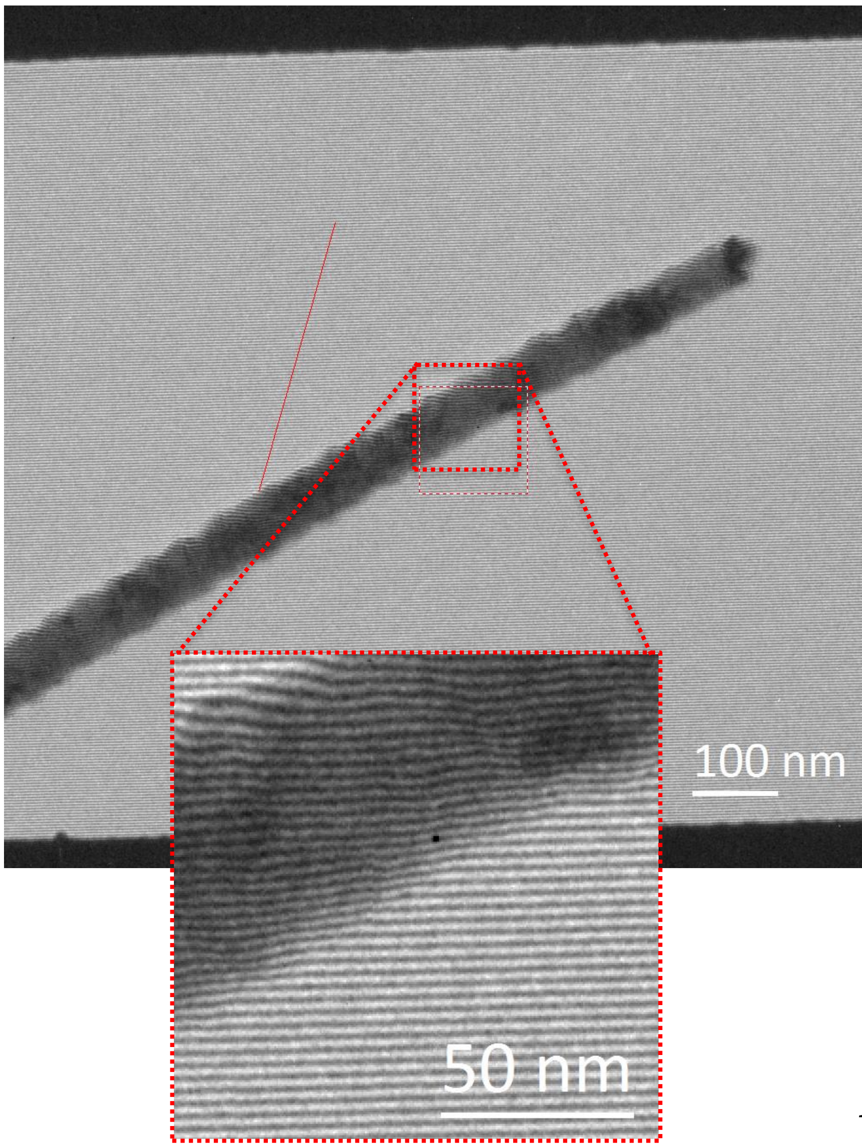

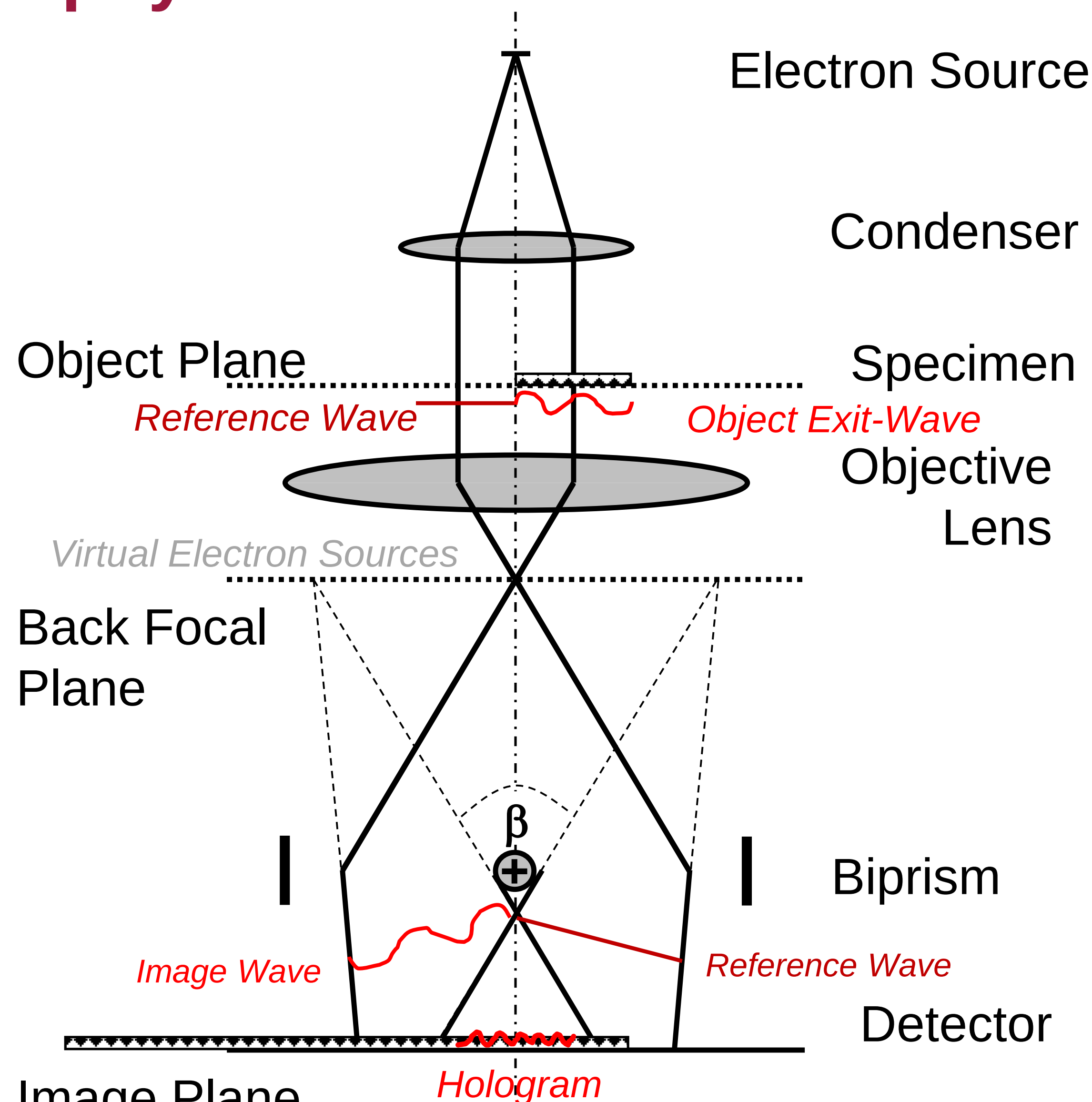

$$I_{\mathrm{hol}}(\mathbf{r}) = I_{\mathrm{CB}}(\mathbf{r}) + 2\mu_c I_{\mathrm{SB}}(\mathbf{r})\cos\left(\mathbf{q}_{\mathrm{c}}\mathbf{r} + \varphi(\mathbf{r})\right)$$

Magnetic phase shift in Cobalt stripe domains

Amplitude image

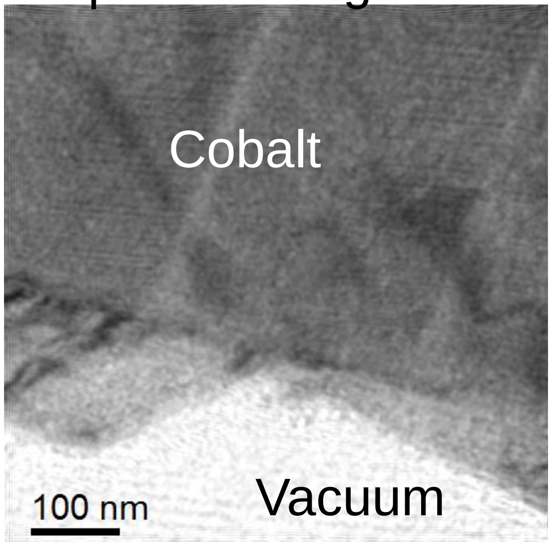

Phase image

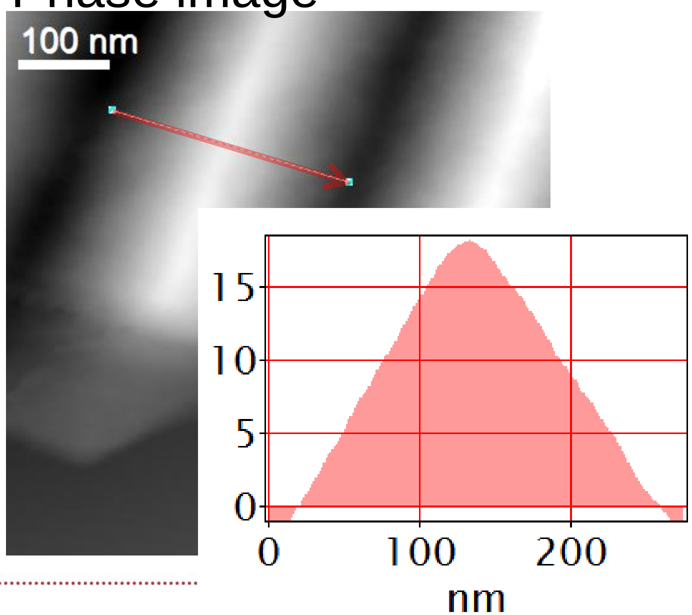

$$\frac{\partial \varphi_{\mathrm{mag}}}{\partial x} = -\frac{e}{\hbar}\int B_y(x,y,z)\,\mathrm{d}z$$

Projected B-field

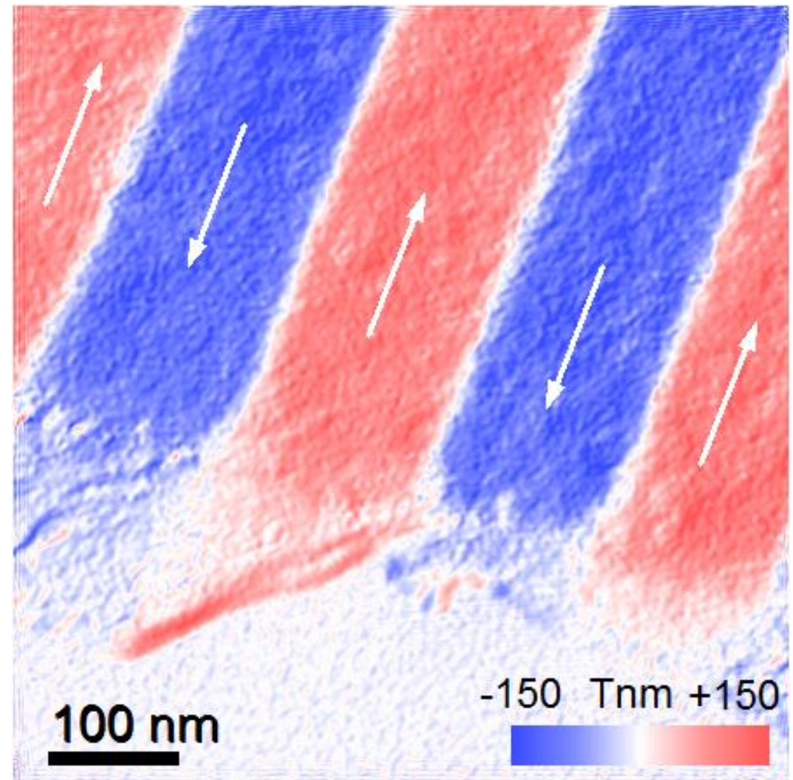

Electric and magnetic phase shift

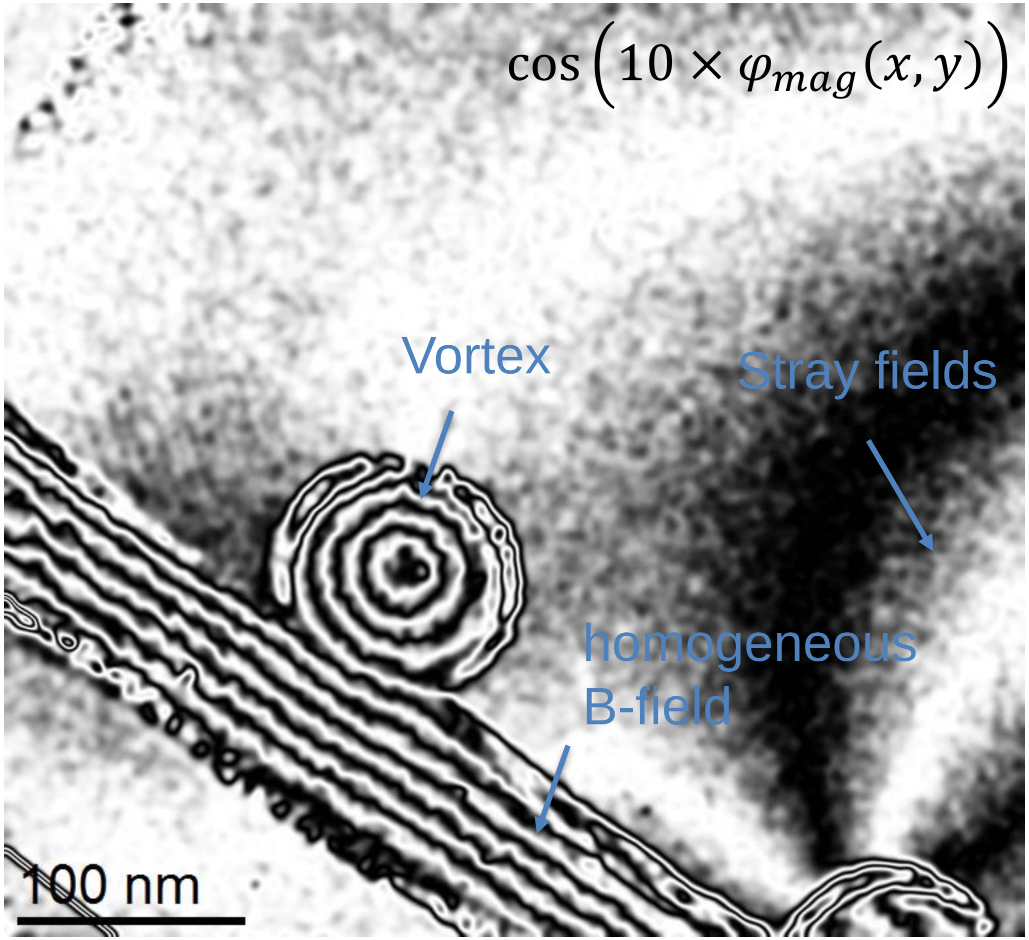

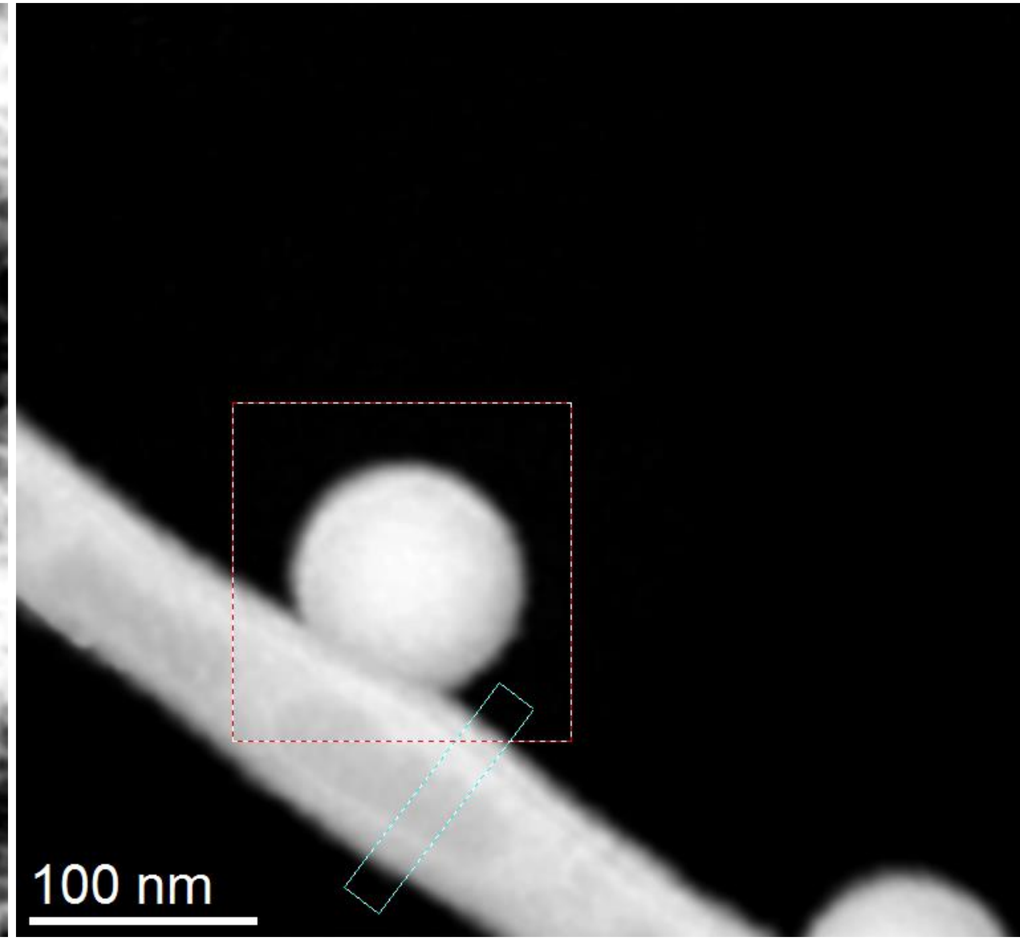

$$\begin{pmatrix} \partial_x \varphi_{mag} \\ \partial_y \varphi_{mag} \end{pmatrix} = -\frac{e}{\hbar} \int \begin{pmatrix} B_y(x,y,z) \\ -B_x(x,y,z) \end{pmatrix} \mathrm{d}z$$

$$\varphi_{el}(x,y) = C_E \int_{-\infty}^{+\infty} V(x,y,z) \mathrm{d}z$$

Sample provided by Denys Makarov, Helmholtz-Zentrum Dresden-Rossendorf.

Electric and magnetic phase shift

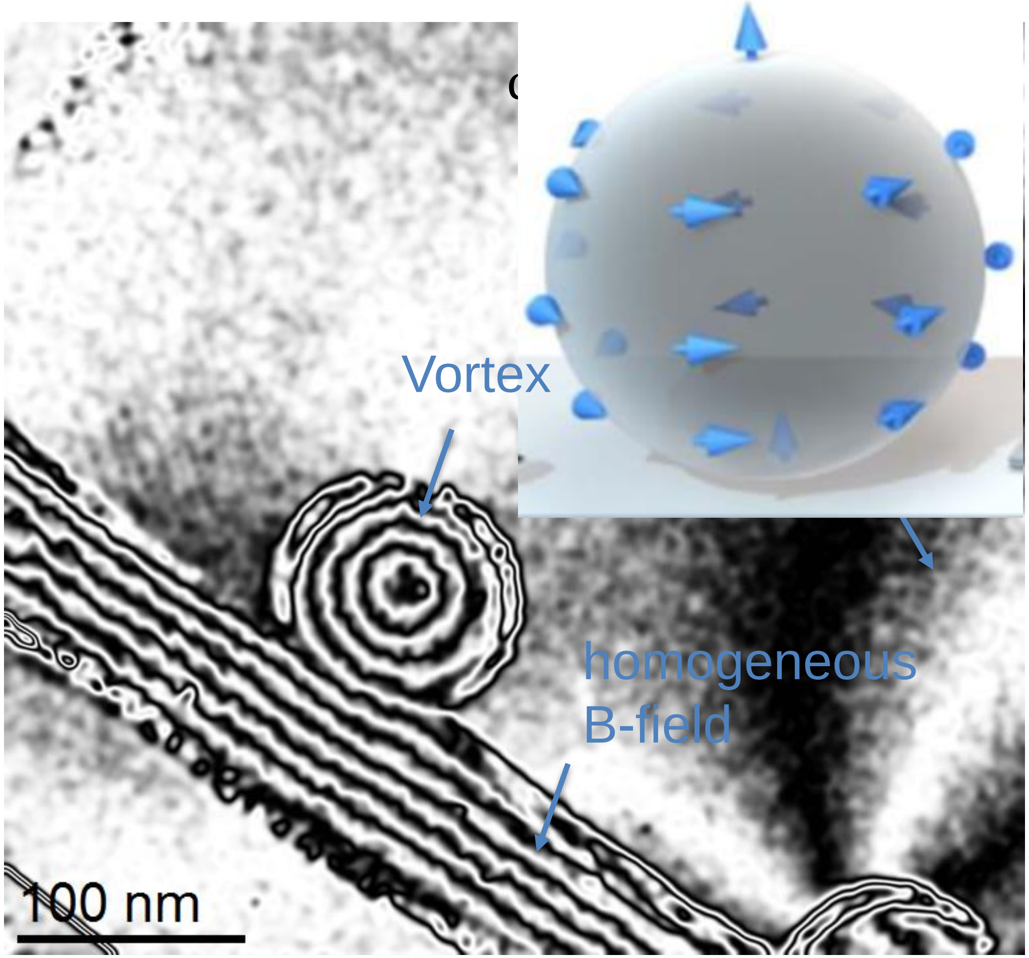

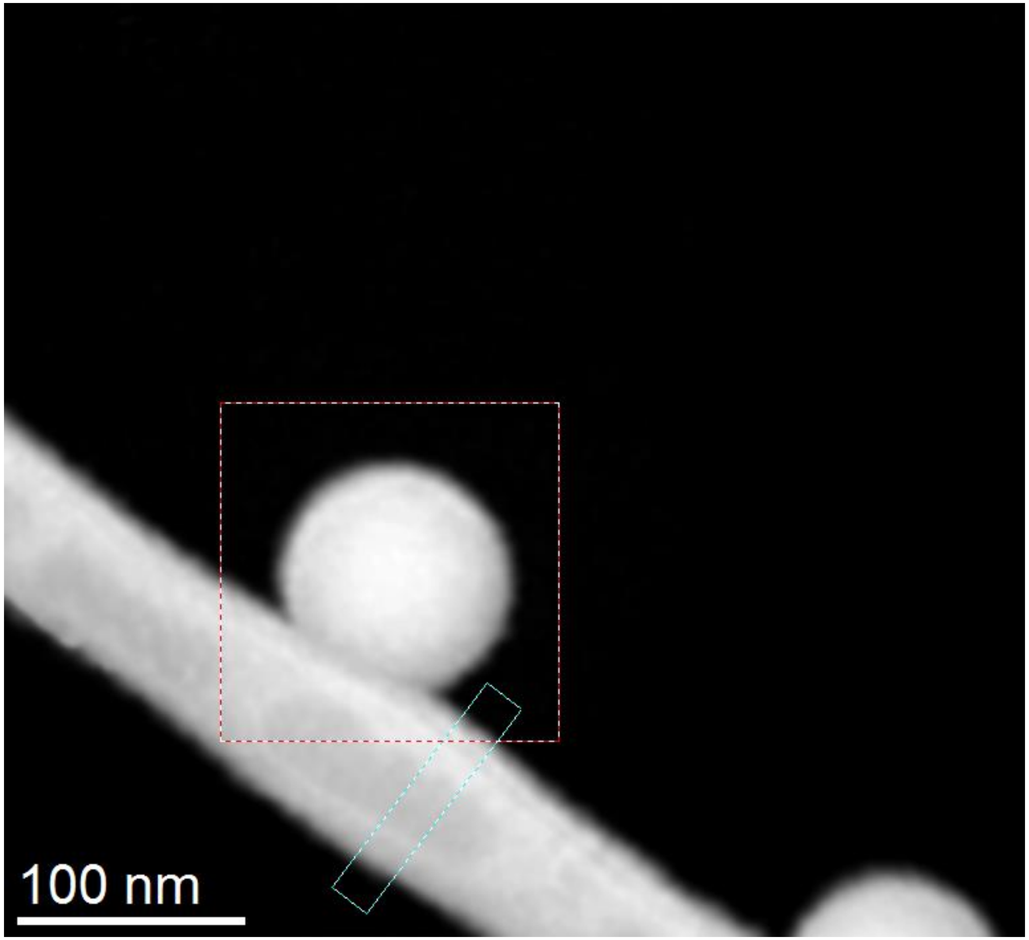

$$\begin{pmatrix} \partial_x \varphi_{mag} \\ \partial_y \varphi_{mag} \end{pmatrix} = -\frac{e}{\hbar} \int \begin{pmatrix} B_y(x,y,z) \\ -B_x(x,y,z) \end{pmatrix} \mathrm{d}z$$

$$\varphi_{el}(x,y) = C_E \int_{-\infty}^{+\infty} V(x,y,z) \mathrm{d}z$$

Fernandez-Pacheco, A. et al. , *Nat Commun* **2017,** *8*, 15756.
Sample provided by Denys Makarov, Helmholtz-Zentrum Dresden-Rossendorf.

Liquid Helium Cryostage

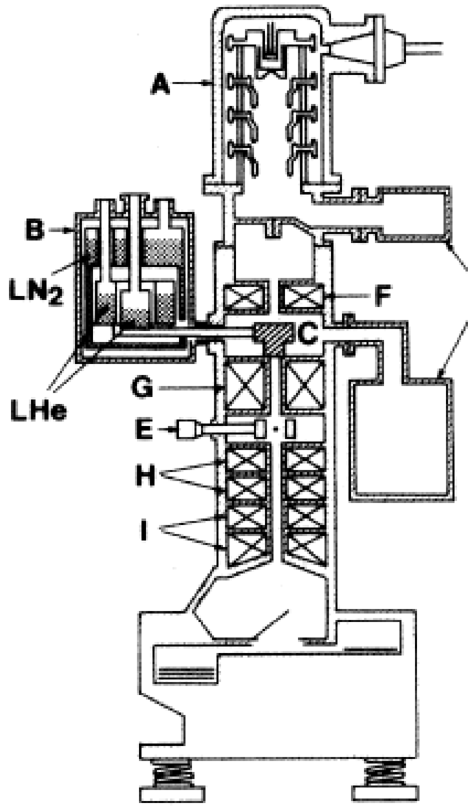

FIG. 4. Cross section of electron microscope with cooling apparatus. *A*, field emission gun; *B*, liquid-He reservoir; *C*, cooling stage; *D*, ion pumps; *E*, biprism; *F*, condenser lens; *G*, objective lens; *H*, intermediate lenses; *I*, projector lenses.

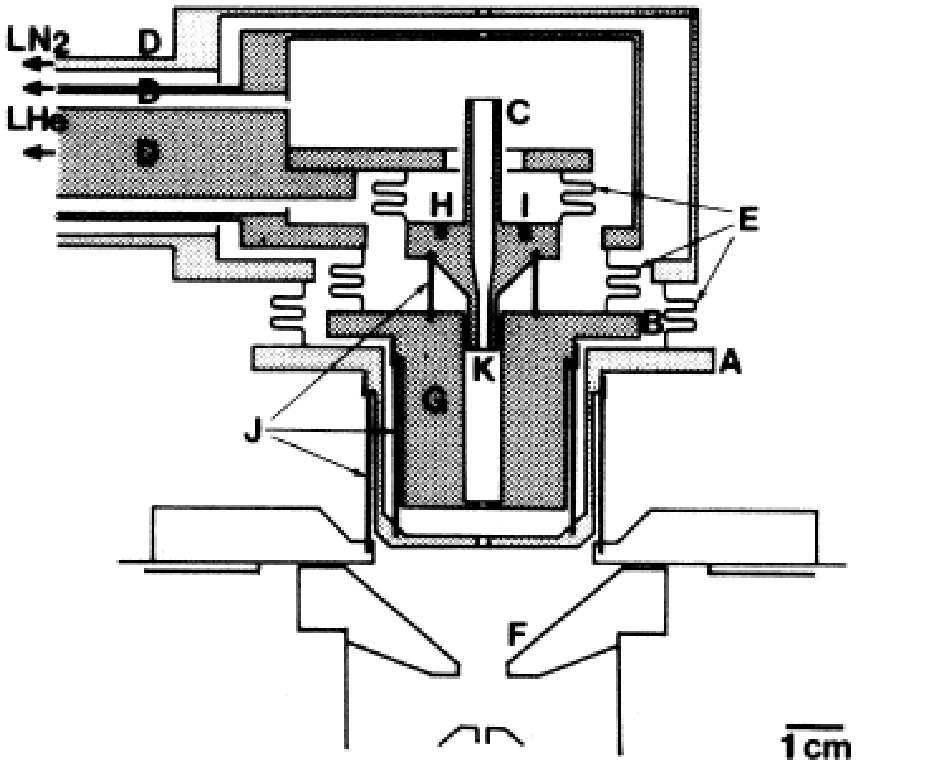

FIG. 5. Cross section of cooling stage. *A*, second shield; *B*, first shield; *C*, specimen holder; *D*, conducting rods; *E*, heater; *F*, objective pole-piece; *G*, superconducting coil; *H*, heater; *I*, Ge resistor; *J*, insulating supports; *K*, specimen.

N. Osakabe, T. Matsuda, T. Kawasaki, J. Endo and A. Tonomura, Phys.Rev. A 34(1986), 815

Superconductivity: Vortex lattice

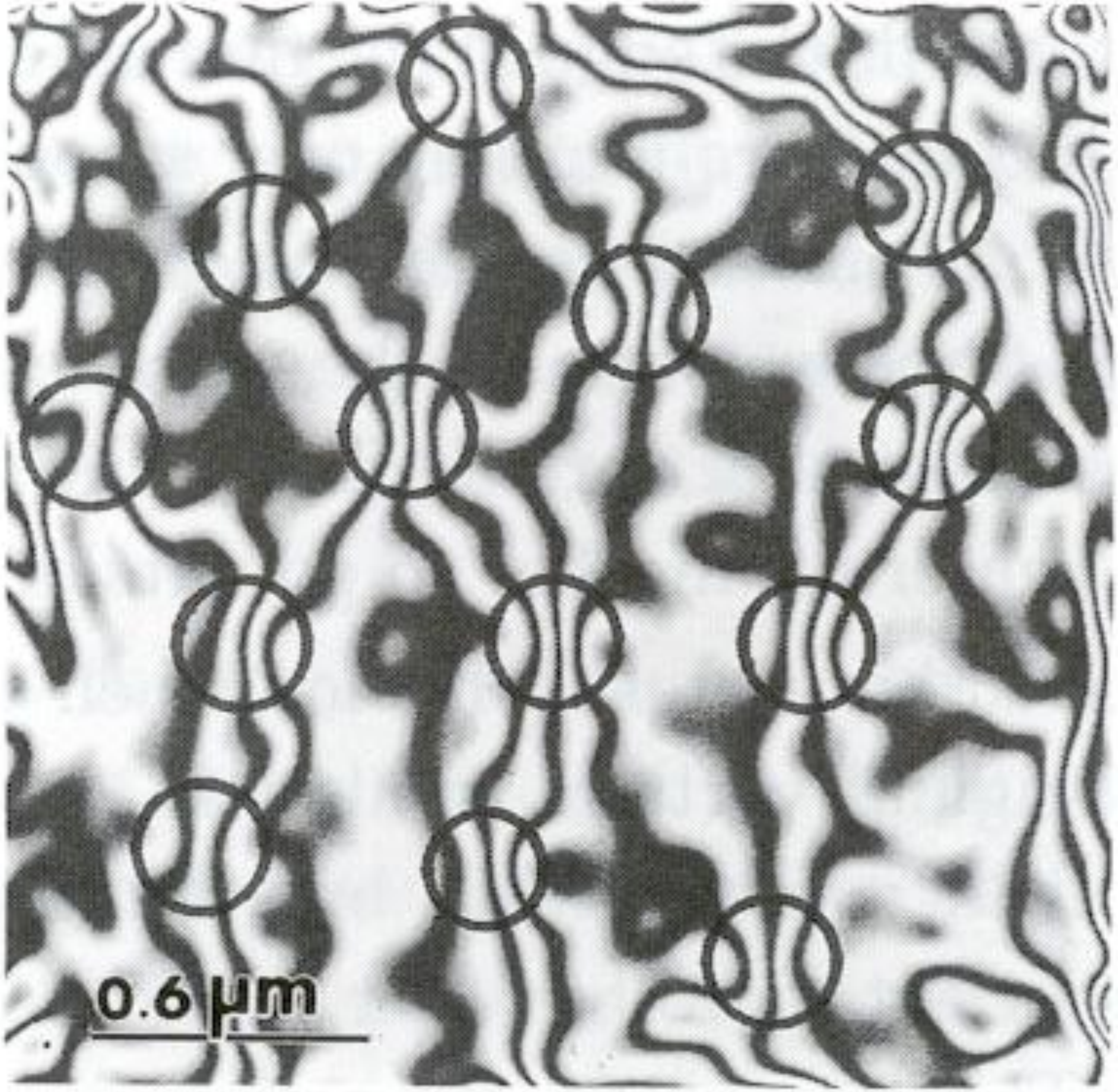

Nb-film
T=4.5K < Tc=9.2K
B=15 mT (150 Gauss)
Phase amplification 16*

J.E. Bonevich, K. Harada, T. Matsuda, H. Kasai, T. Yoshida, G. Pozzi and A. Tonomura, Phys.Rev.Letters, 70 (1993), 2952

Off-axis: Pros & Cons

Pro:

- linear signal
- simple reconstruction
- unambiguous result
- sensitiv to the whole spatial frequency range

Con:

- (multiple) biprisms required
- reference (vacuum) required
- large coherency requirements

1. Fundamentals of electron scattering
    a. Axial scattering
    b. Magnetic and electric Ehrenberg–Siday–Aharonov–Bohm effect

2. Fundamentals of Electron Holography and Tomography
    a. Holographic Principle (interference, reconstruction)
    b. Holographic Setups (inline, off-axis) and instrumental requirements
    c. Separation of electrostatic and magnetic contributions
    d. Tomographic reconstruction of 3D electric potential and magnetic induction vector field from tilt series of projections

3. Magnetic fields and textures in solids
    a. Magnetization, Magnetic induction, Magnetic field
    b. Magnetostatics
    c. Micromagnetics

Separation of magnetic and electric phase shift *

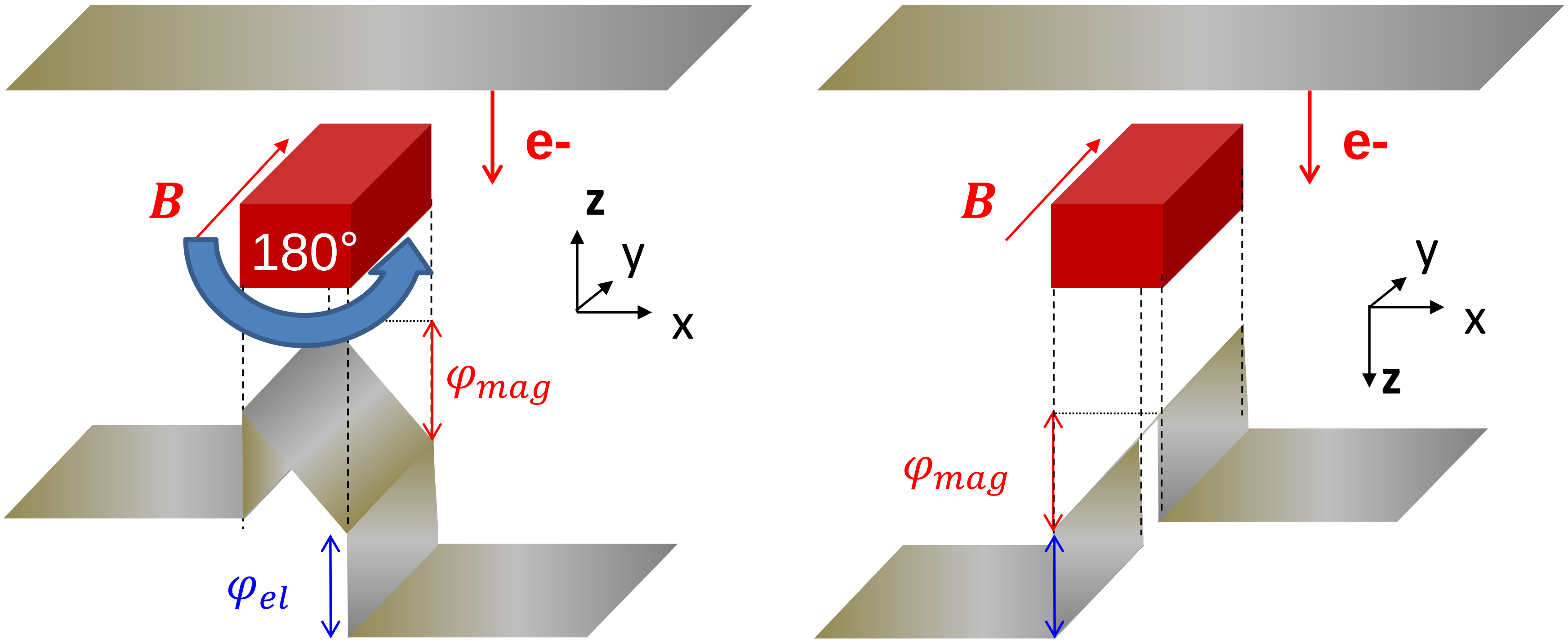

$$\varphi_1(x,y) = \varphi_{el}(x,y) + \varphi_{mag}(x,y) \qquad \varphi_2(x,y) = \varphi_{el}(x,y) - \varphi_{mag}(x,y)$$

$$\varphi_{mag}(x,y) = \big(\varphi_1(x,y) - \varphi_2(x,y)\big)/2$$
$$\varphi_{el}(x,y) = \big(\varphi_1(x,y) + \varphi_2(x,y)\big)/2$$

* What does it have to do with time-inversion symmetry?

1. Fundamentals of electron scattering
    a. Axial scattering
    b. Magnetic and electric Ehrenberg–Siday–Aharonov–Bohm effect

2. **Fundamentals of Electron Holography and Tomography**
    a. Holographic Principle (interference, reconstruction)
    b. Holographic Setups (inline, off-axis) and instrumental requirements
    c. Separation of electrostatic and magnetic contributions
    d. **Tomographic reconstruction of 3D electric potential and magnetic induction vector field from tilt series of projections**

Separation of magnetic and electric phase shift

$$\varphi_{mag} = (\varphi_1 - \varphi_2)/2$$

$$\varphi_{el} = (\varphi_1 + \varphi_2)/2$$

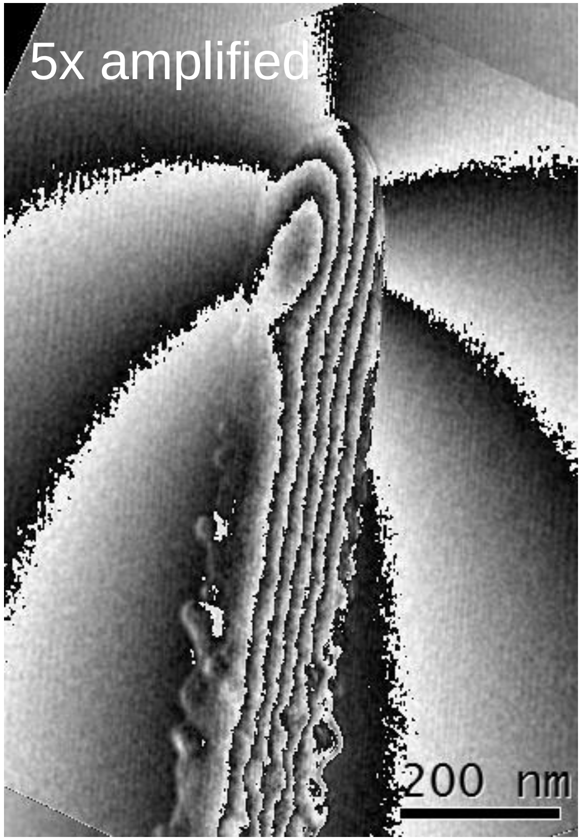

$$\begin{pmatrix} \partial_x \varphi_{mag} \\ \partial_y \varphi_{mag} \end{pmatrix} = -\frac{e}{\hbar} \int \begin{pmatrix} B_y(x,y,z) \\ -B_x(x,y,z) \end{pmatrix} \mathrm{d}z$$

$$\varphi_{el}(x,y) = C_E \int_{-\infty}^{+\infty} V(x,y,z) \mathrm{d}z$$

Towards 3D nanomagnetism

+ structural, chemical data

Reyes et al., Nano Lett. 16 (2016) 1230

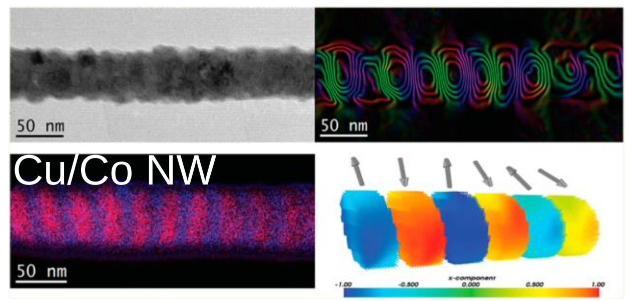

Biziere et al., Nano Lett. 13 (2013) 2053

2D Magnetic phase maps by TEM holography

3D modelling of M,B (eg. micromagnetic simulation)

Comparison

Projection

Towards 3D nanomagnetism

+ structural, chemical data

2D Magnetic phase maps by TEM holography

3D modelling of M,B (eg. micromagnetic simulation)

Reyes et al., Nano Lett. 16 (2016) 1230

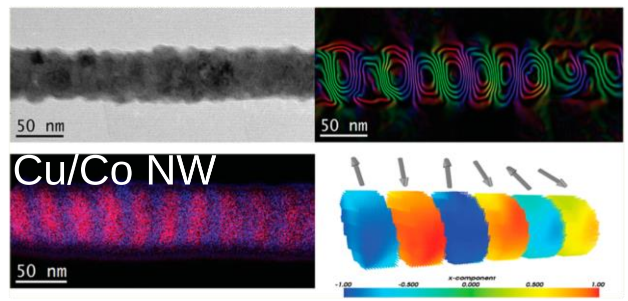

Biziere et al., Nano Lett. 13 (2013) 2053

Comparison

Projection

Loss of 3D-information!

Towards 3D nanomagnetism

+ structural, chemical data

Reyes et al., Nano Lett. 16 (2016) 1230

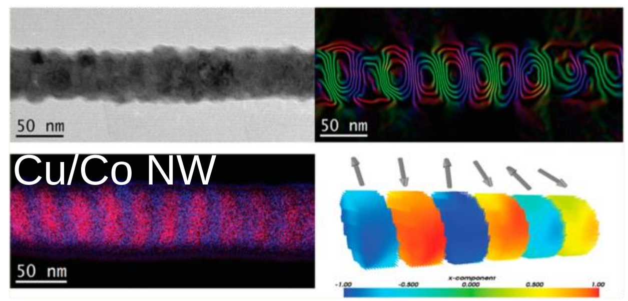

Biziere et al., Nano Lett. 13 (2013) 2053

3D reconstruction by electron holographic vector field tomography of B-fields

3D modelling of M,B (eg. micromagnetic simulation)

Comparison

Single tilt axis holographic tomography of nanomagnets

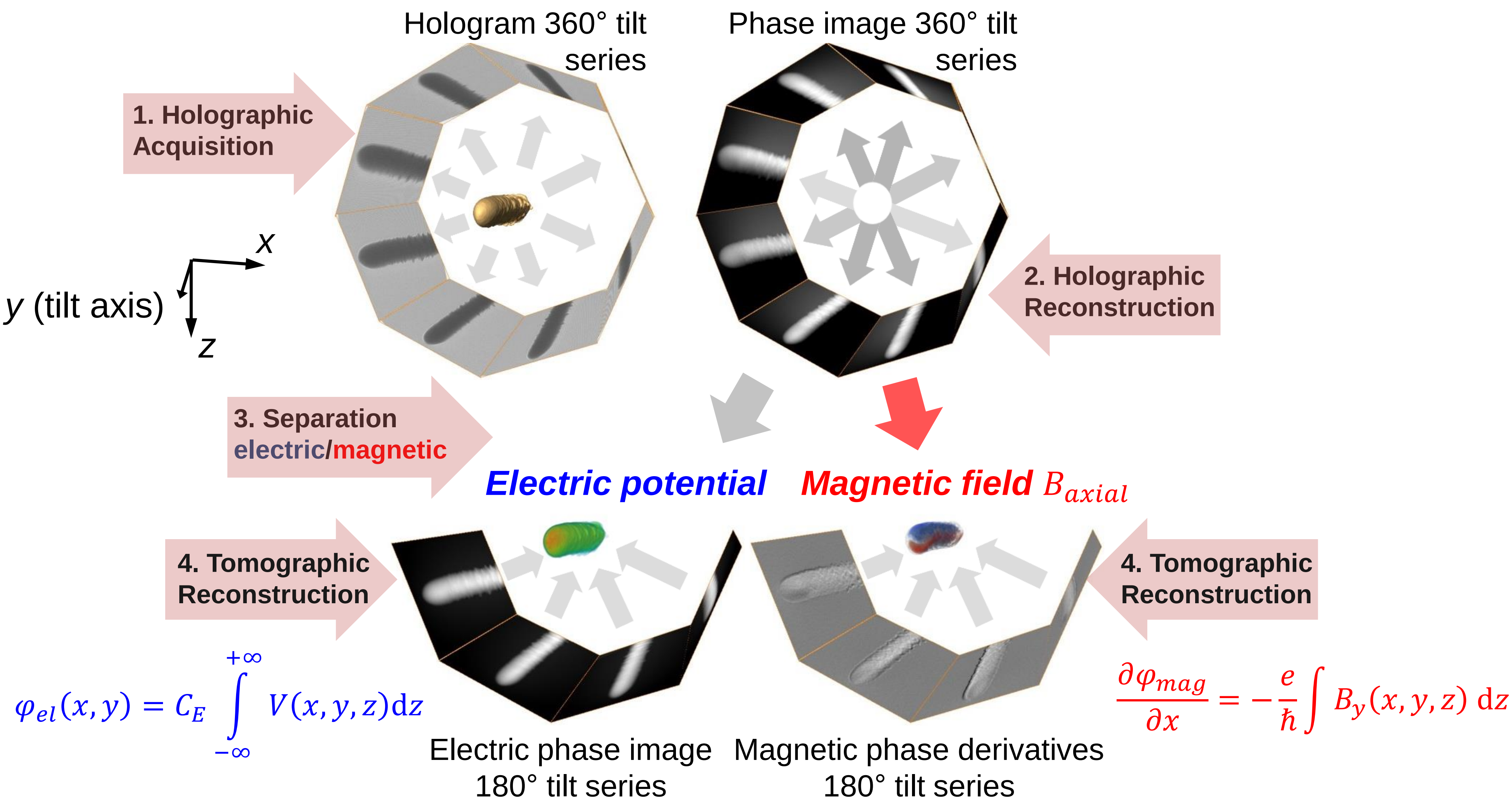

Wolf et al., *Chem. Mater.* **27** (2015) 6771
Simon, Wolf et al., *Nano Lett.* **16** (2016) 114

Electron holographic tomography of magnetic samples

3D reconstruction of $V(x,y,z)$ and $\boldsymbol{B}(x,y,z)$

1. **Tilt series acquisition** of off-axis electron holograms: Two 360° tilt series around x- and y-axis (gaps due to experimental limitations)
2. **Phase shift retrieval** from electron holograms
3. **Separation** of **electric** and **magnetic** phase shift and alignment
4. **Tomographic reconstruction** of
   $V(x,y,z)$ from φ_{el},
   $B_x(x,y,z)$ from $\frac{\partial \varphi_{mag}}{\partial y}$,
   $B_y(x,y,z)$ from $\frac{\partial \varphi_{mag}}{\partial x}$
5. **Computation** of $B_z(x,y,z)$ from $\nabla \cdot \boldsymbol{B}(x,y,z) = 0$

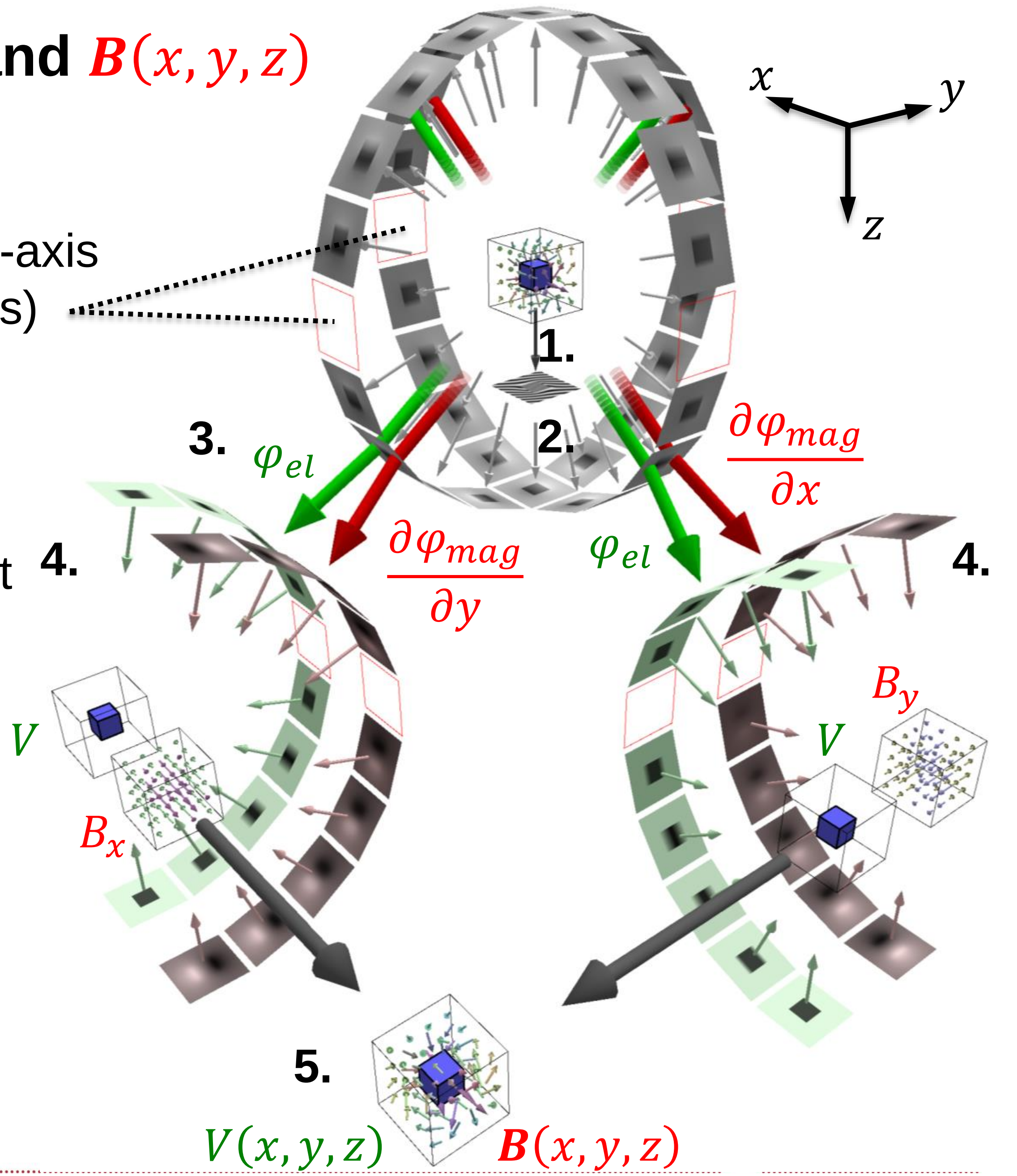

Dual tilt axis holographic tomography of nanomagnets

Electron Holographic Tomography

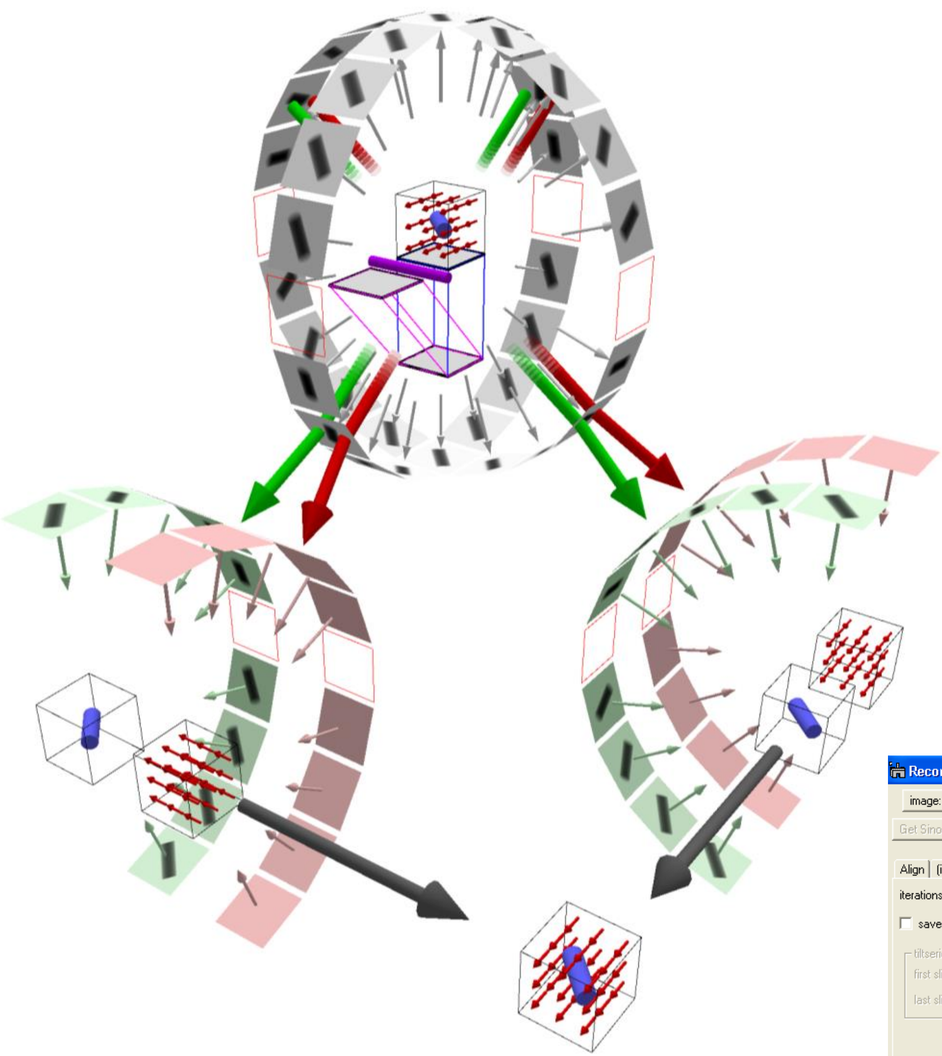

Implementation

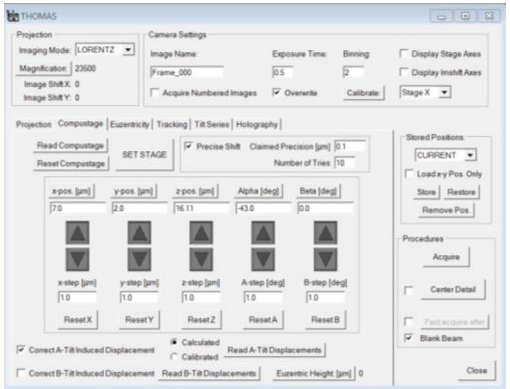

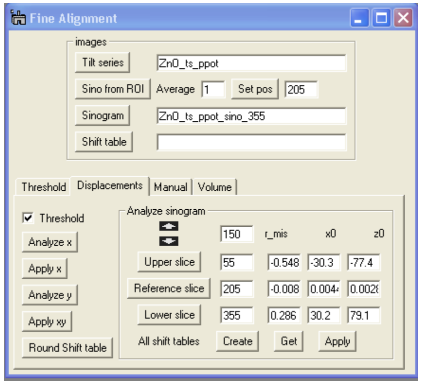

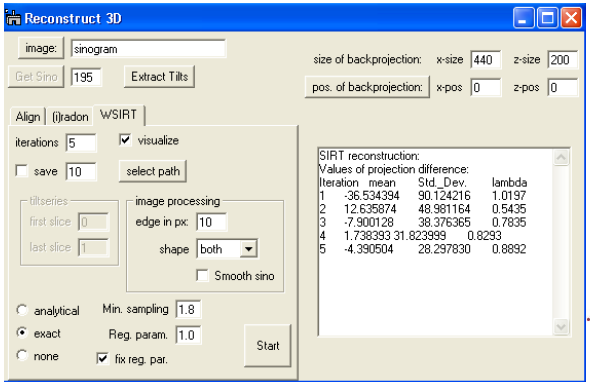

Automated tomographic tilt series acquisition

- Installed at NCEM Berkeley, U Antwerp, TU Berlin
- Adapted for different TEMs

Wolf et al. *Ultramic.* **110** (2010) 390

Alignment

- Displacement correction
- Tilt axis finding

Wolf et al., *Chem. Mater.* **27** (2015) 6771

“Reconstruct 3D” software package

- Documentation at www.triebenberg.de/wolf

Wolf et al. *Ultramic.* **136** (2014) 15

Challenges and problems of 3D B field mapping

Challenges	Problems
Magnetic sample	• beam damage • diffraction contrast • stray fields • magnetization by Lorentz lens

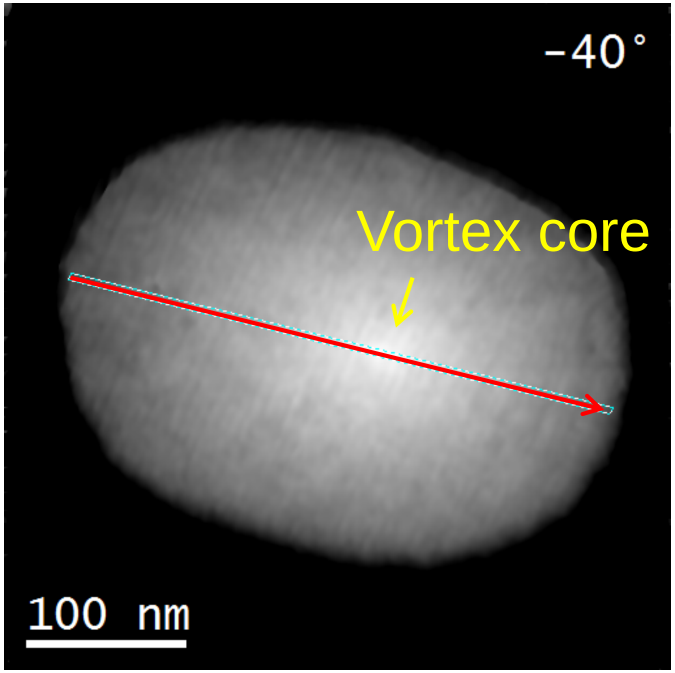

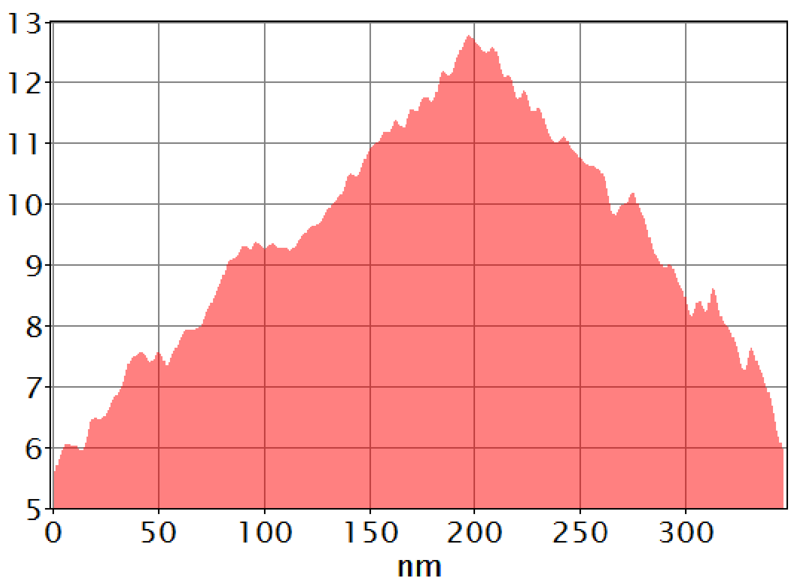

Permalloy disks
provided by J. Zweck, Regensburg

Challenges and problems of 3D B field mapping

Challenges	Problems
Magnetic sample	• beam damage • diffraction contrast • stray fields • magnetization by Lorentz lens

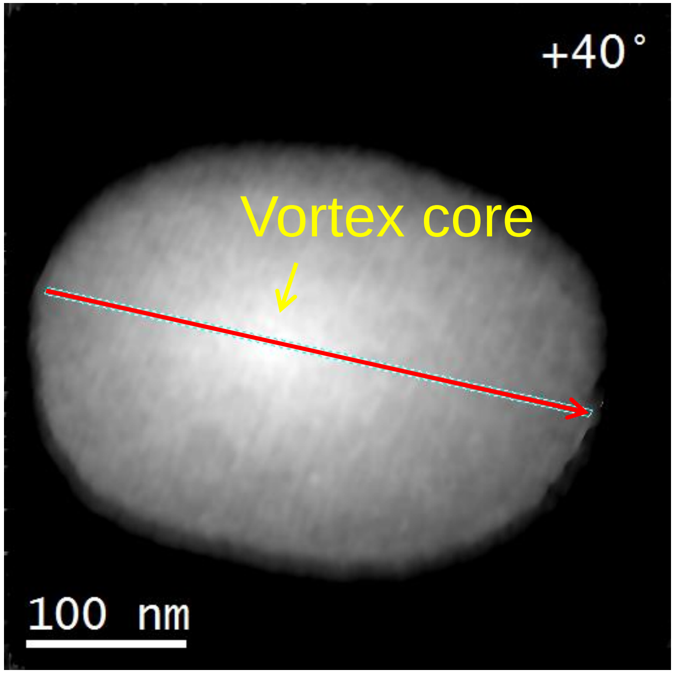

Permalloy disks
provided by J. Zweck, Regensburg

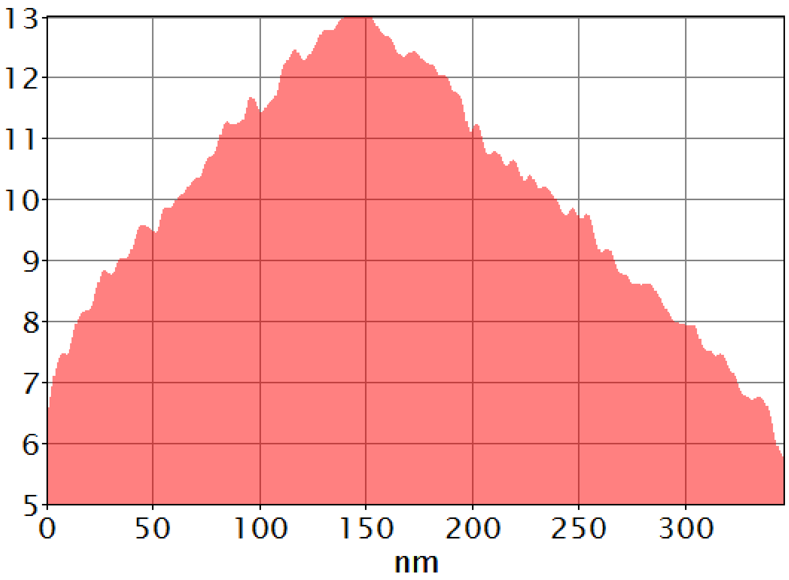

R. E. Dunin-Borkowski and T. Kasama, *Microscopy and Microanalysis* **10** (2004) 1010.

Challenges and problems of 3D B field mapping

Challenges	Problems
Magnetic sample	• beam damage • diffraction contrast • stray fields • magnetization by Lorentz lens
$\int B_y(x(\alpha), y, z(\alpha))\,\mathrm{d}z = -\frac{\hbar}{e}\frac{\partial\varphi}{\partial x(\alpha)}$ y in the direction of tilt axis	• derivation enhances noise • only B_y, i.e., parallel to tilt axis

R. E. Dunin-Borkowski and T. Kasama, *Microscopy and Microanalysis* **10** (2004) 1010.

Challenges and problems of 3D B field mapping

Challenges	Problems
Magnetic sample	• beam damage • diffraction contrast • stray fields • magnetization by Lorentz lens
$\int B_y\big(x(\alpha), y, z(\alpha)\big)\,\mathrm{d}z = -\frac{\hbar}{e}\frac{\partial\varphi}{\partial x(\alpha)}$ y in the direction of tilt axis	• derivation enhances noise • only B_y, i.e., parallel to tilt axis
Two ultra-high-tilt series ($\pm 90°$) about orthogonal axes to get B_x and B_y	• sample geometry • holder design • stability

R. E. Dunin-Borkowski and T. Kasama, *Microscopy and Microanalysis* **10** (2004) 1010.

Challenges and problems of 3D B field mapping

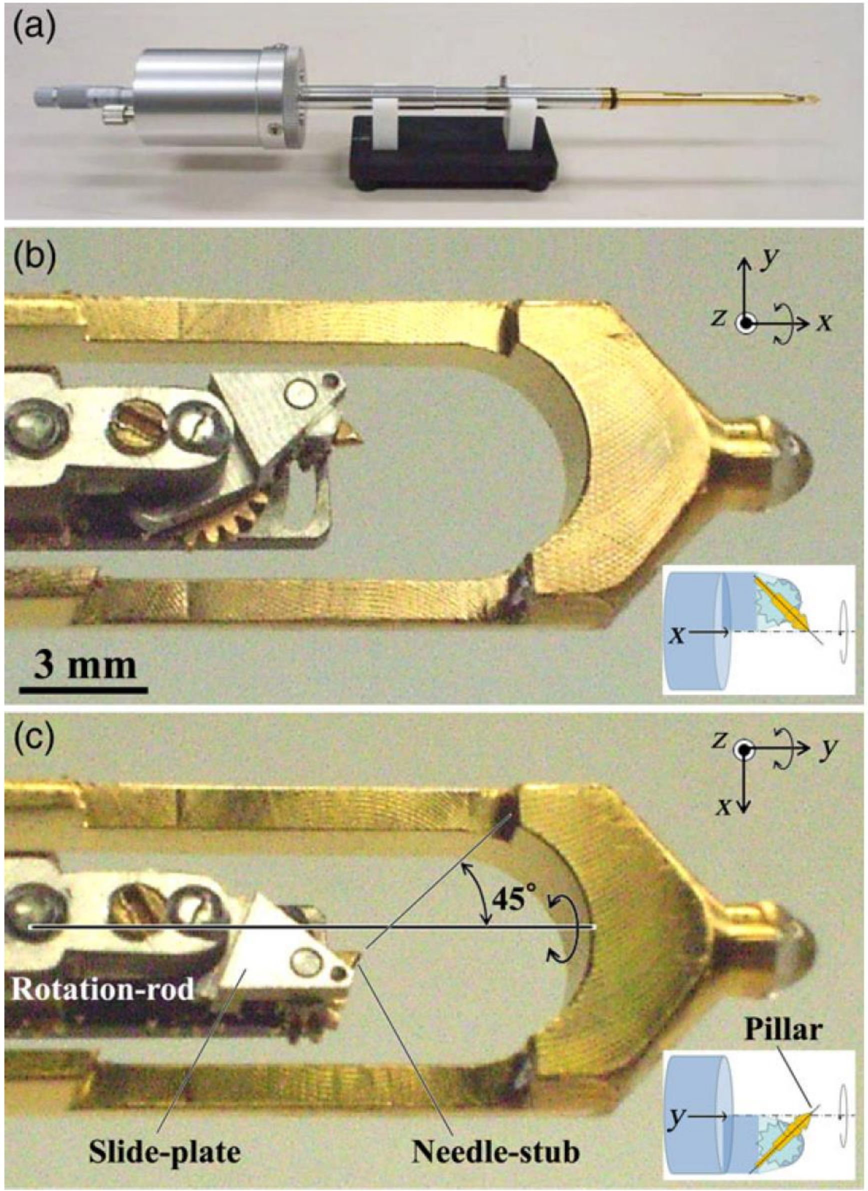

Tsuneta et al., Microscopy **63** (2014) p. 469

Solution

- preparation of free-standing samples combined with special holder designs

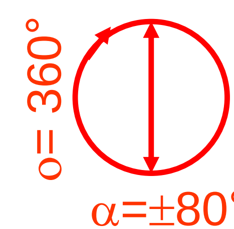

Dual-Axis Tomography Holder
Model 2040, Fischione Instruments

Multiple-axis rotation holder

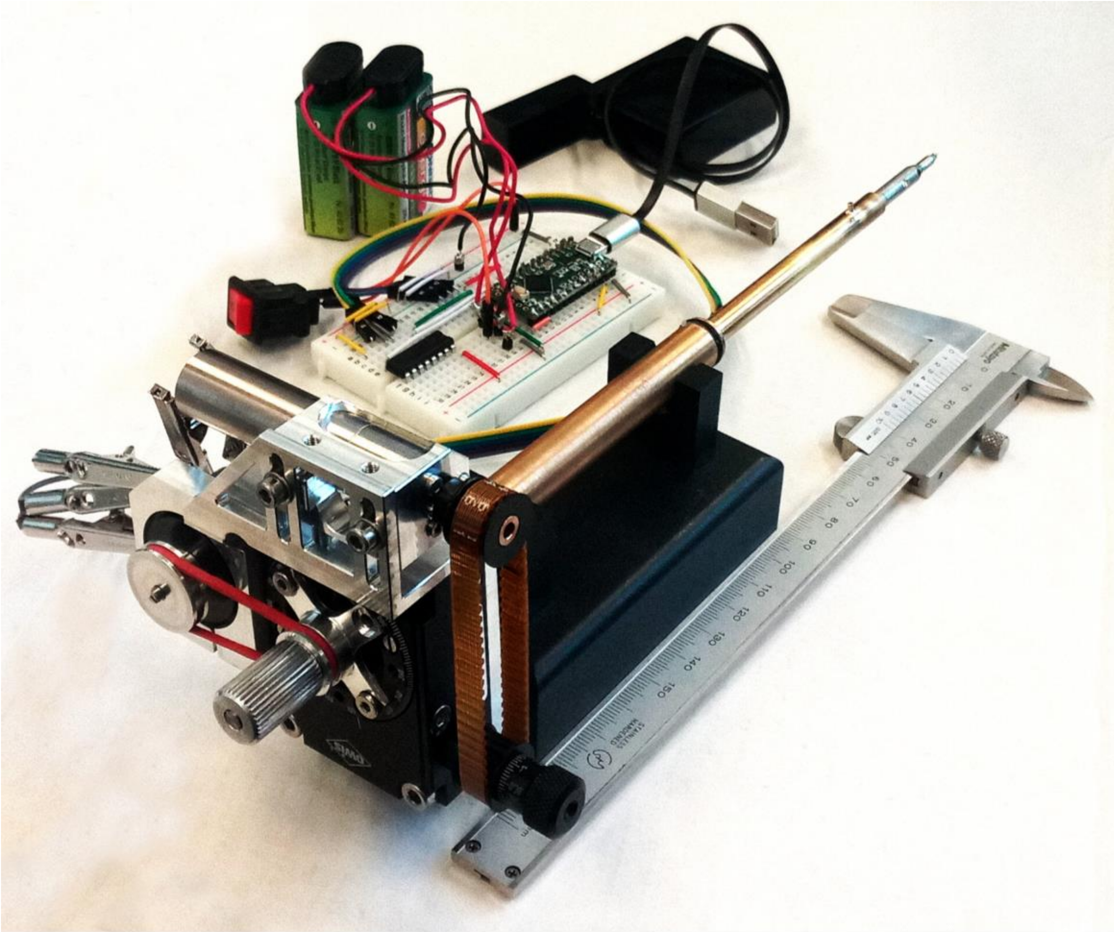

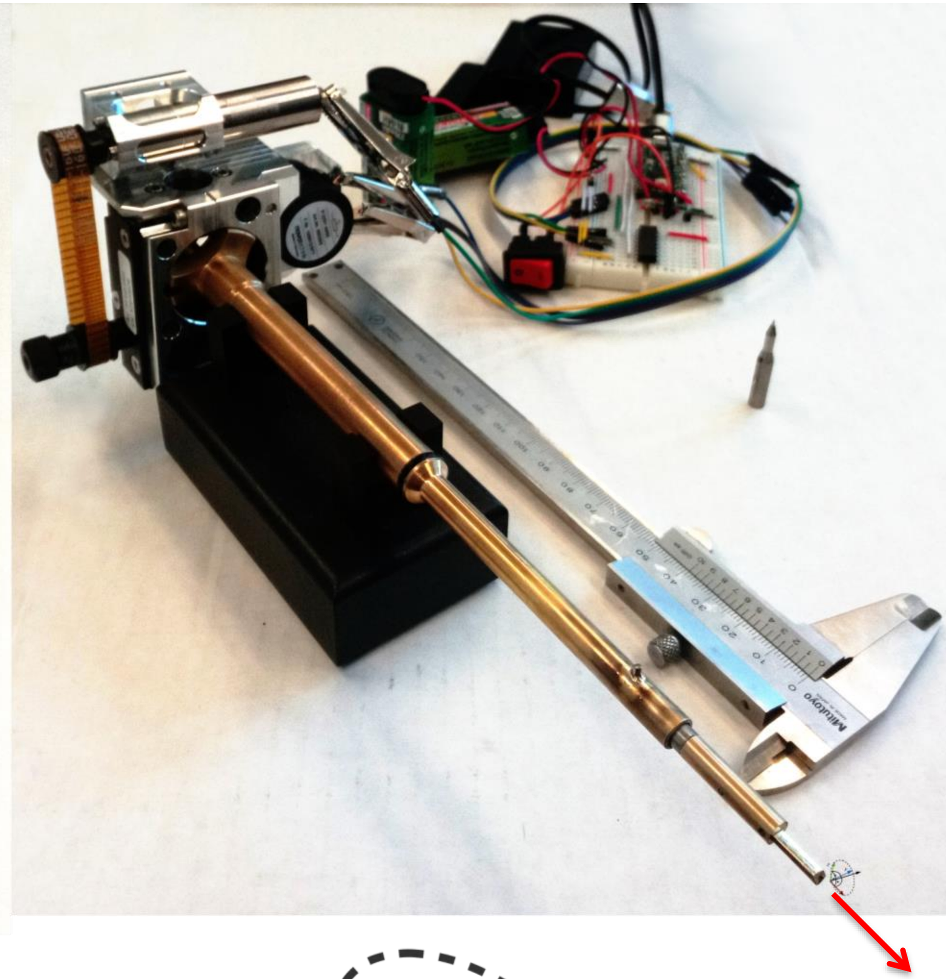

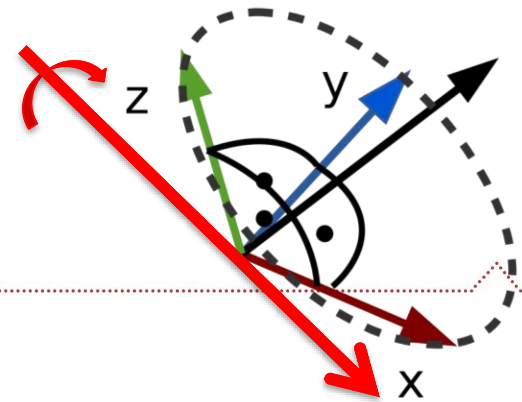

IFW Forschungstechnik:
Steffen Ziller, Nico Richter, Rolf Morgner

Challenges and problems of 3D B field mapping

Challenges	Problems
Magnetic sample	• beam damage • diffraction contrast • stray fields • magnetization by Lorentz lens
$\int B_y(x(\alpha), y, z(\alpha))\,\mathrm{d}z = -\frac{\hbar}{e}\frac{\partial\varphi}{\partial x(\alpha)}$ y in the direction of tilt axis	• derivation enhances noise • only B_y, i.e., parallel to tilt axis
Two ultra-high-tilt series ($\pm 90°$) about orthogonal axes to get B_x and B_y	• sample geometry • holder design • stability
Separation electric (MIP contribution) magnetic phase shift	• acquisition of additional two tilt series with reversed magnetization • precise alignment (2D Affine transformation)

R. E. Dunin-Borkowski and T. Kasama, *Microscopy and Microanalysis* **10** (2004) 1010.

Challenges and problems of 3D B field mapping

Challenges	Problems
Magnetic sample	• beam damage • diffraction contrast • stray fields • magnetization by Lorentz lens
$\int B_y(x(\alpha), y, z(\alpha))\,\mathrm{d}z = -\frac{\hbar}{e}\frac{\partial\varphi}{\partial x(\alpha)}$ y in the direction of tilt axis	• derivation enhances noise • only B_y, i.e., parallel to tilt axis
Two ultra-high-tilt series ($\pm 90°$) about orthogonal axes to get B_x and B_y	• sample geometry • holder design • stability
Separation electric (MIP contribution) magnetic phase shift	• acquisition of additional two tilt series with reversed magnetization • precise alignment
B_z from $\boldsymbol{\nabla} \cdot \boldsymbol{B} = 0$ with B_x and B_y inserted	• second derivation enhances noise further • unknown boundary conditions

R. E. Dunin-Borkowski and T. Kasama, *Microscopy and Microanalysis* **10** (2004) 1010.

Vectorfield tomography of Cu/Co multi-stacked NWs: Phase diagram for a single Co-disk from micromag simulation

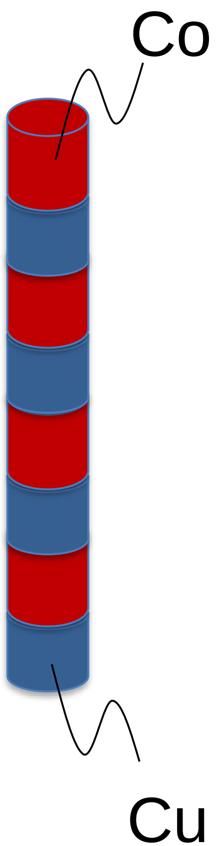

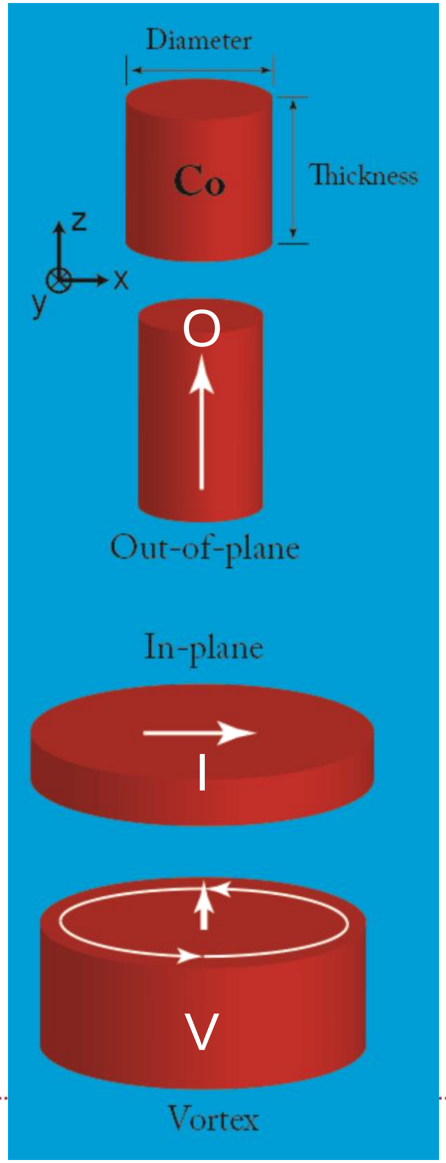

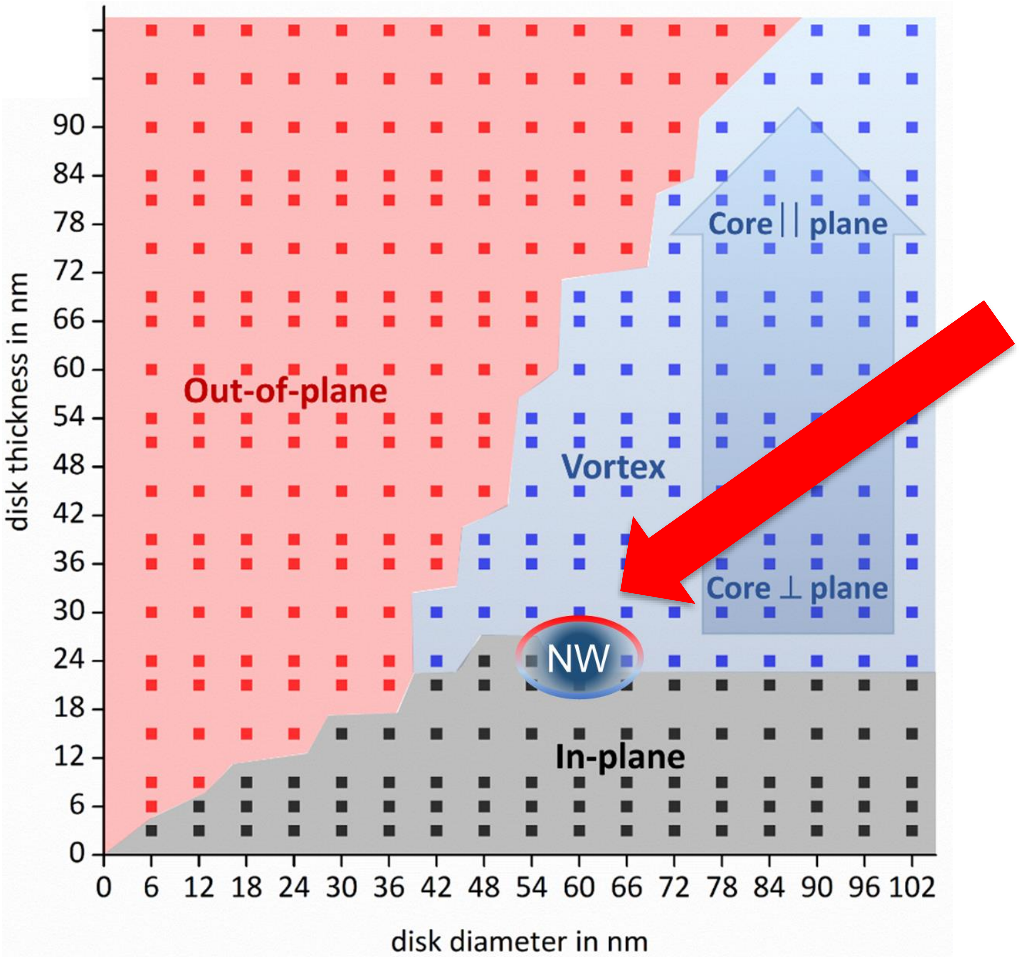

Vectorfield tomography of Cu/Co multi-stacked NWs:

Hologram tilt series

Tilt range -69° to +72°

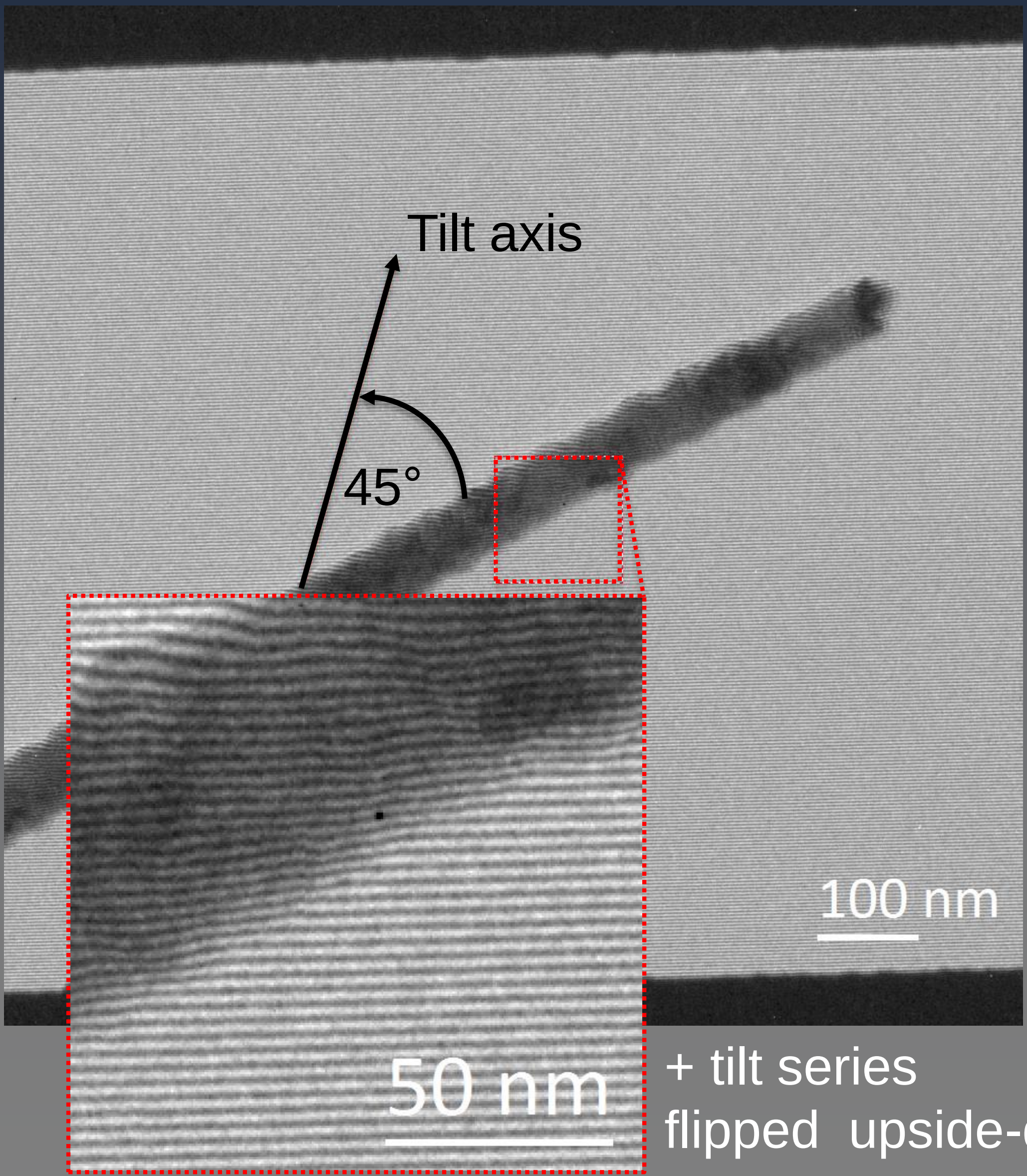

+ tilt series
flipped upside-down

Rotated 90° in-plane: Tilt range -69° to +72°

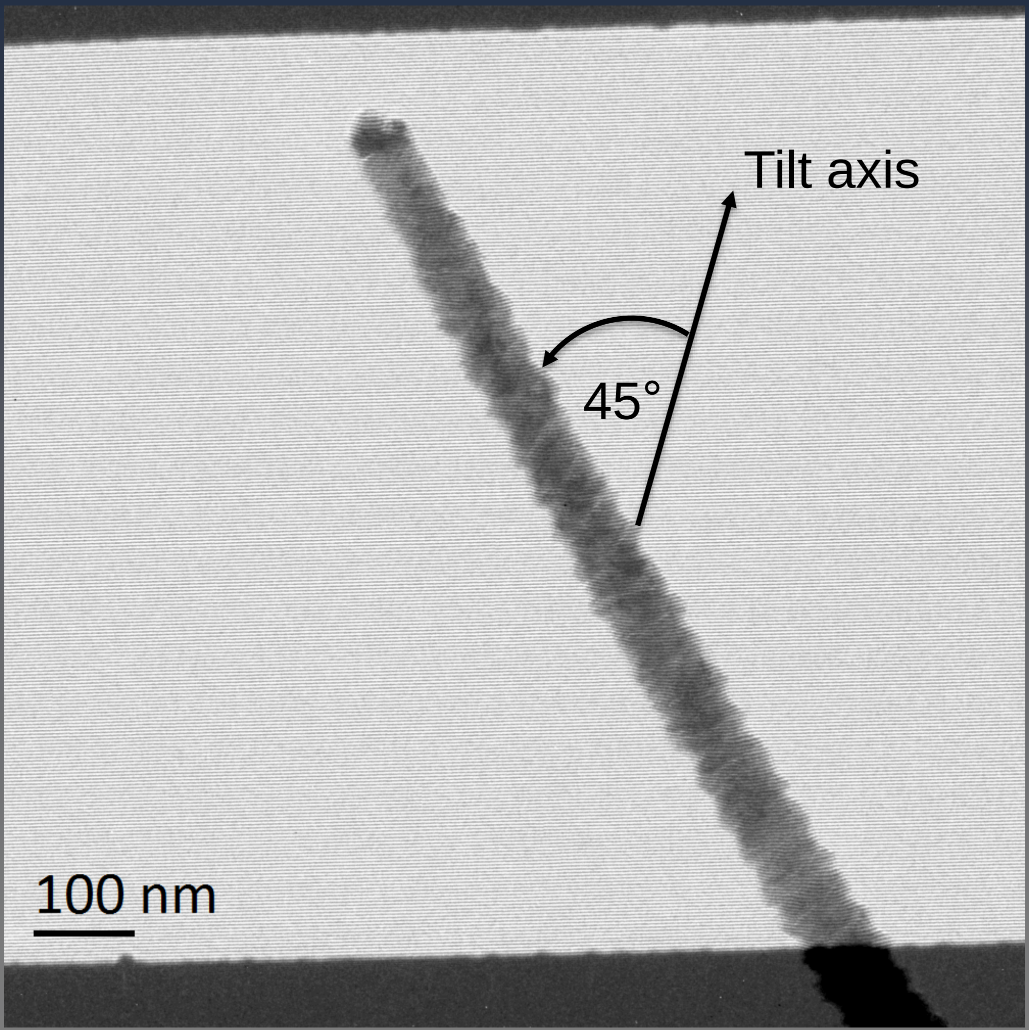

+ tilt series
flipped upside-down

Vectorfield tomography of Cu/Co multi-stacked NWs: Hologram tilt series

Tilt range -69° to +72°

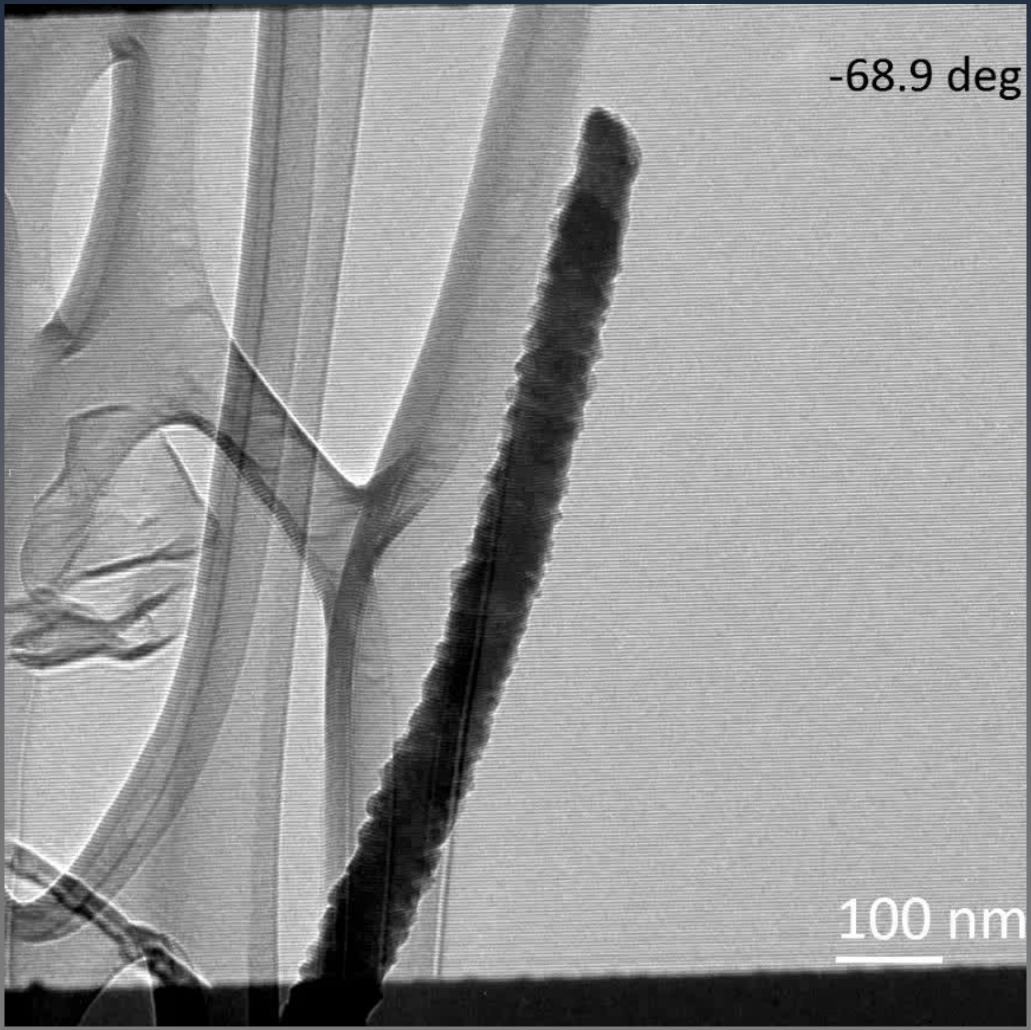

Rotated 90° in-plane: Tilt range -69° to +72°

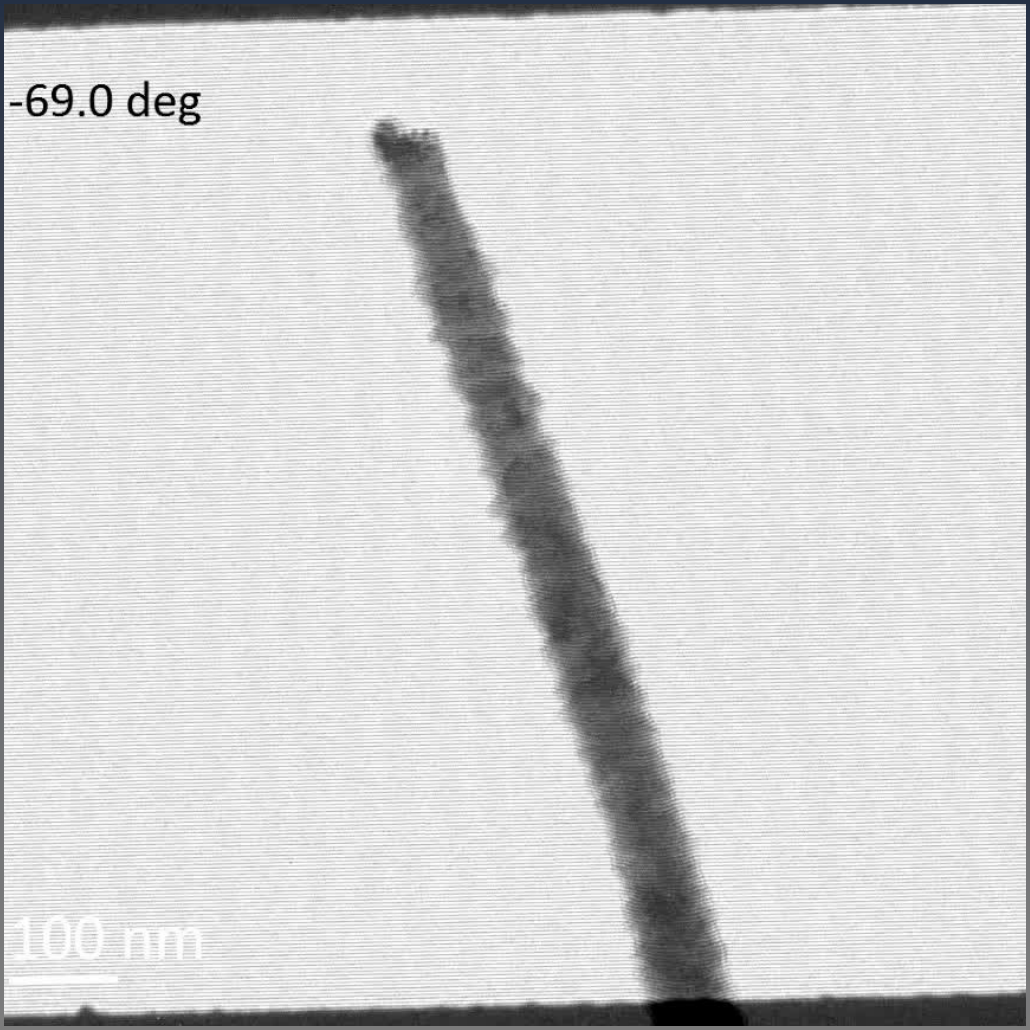

Vectorfield tomography of Cu/Co multi-stacked NWs: Phase tilt series

Electric phase shift

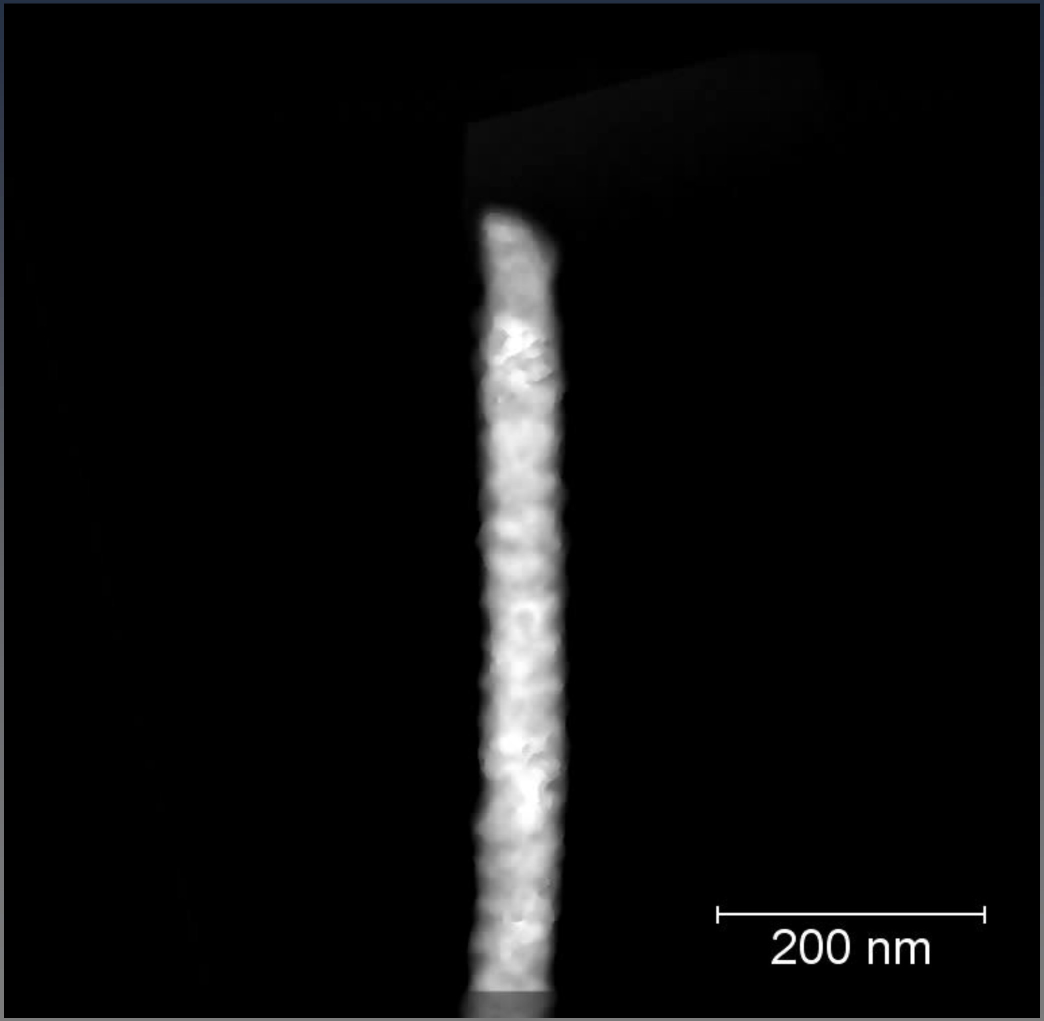

Magnetic phase shift (smoothed)

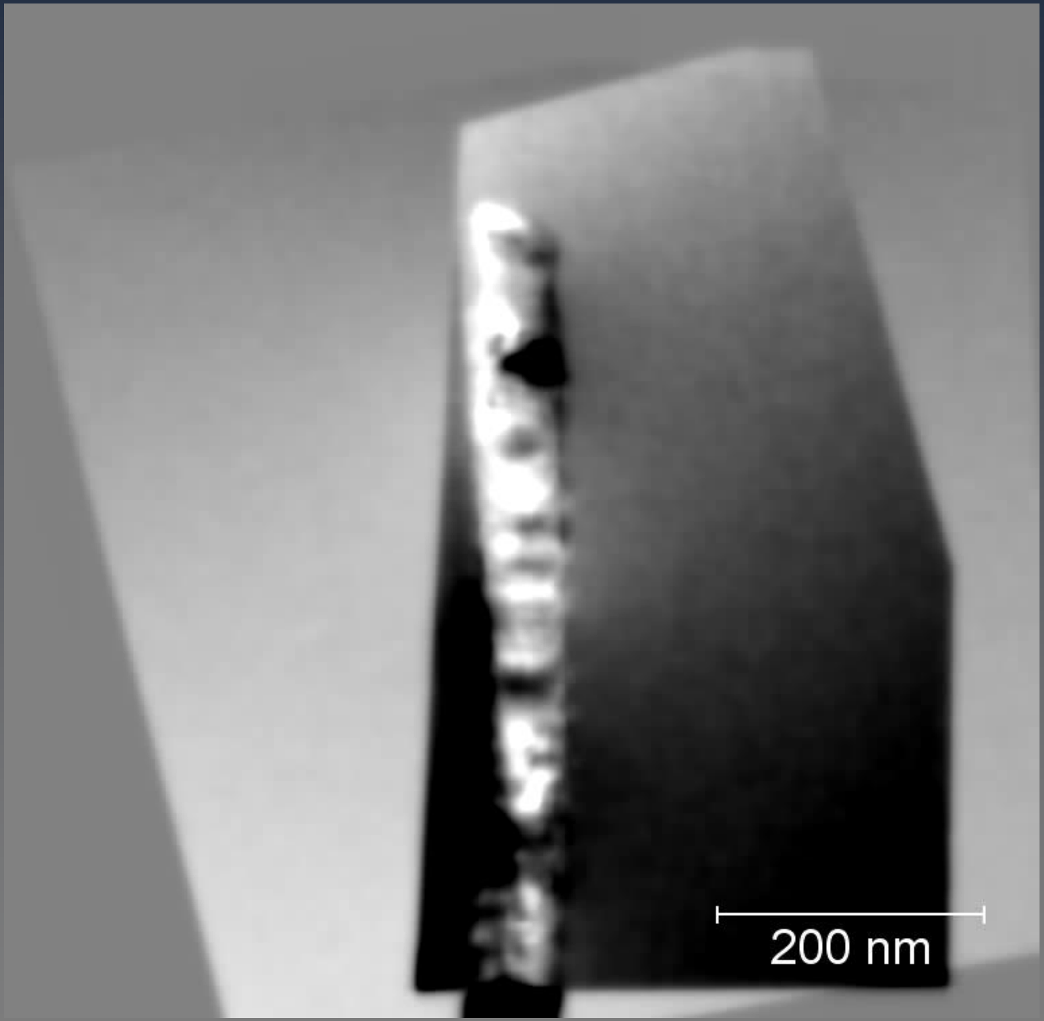

Electrostatic 3D potential of Cu/Co multi-stacked NW

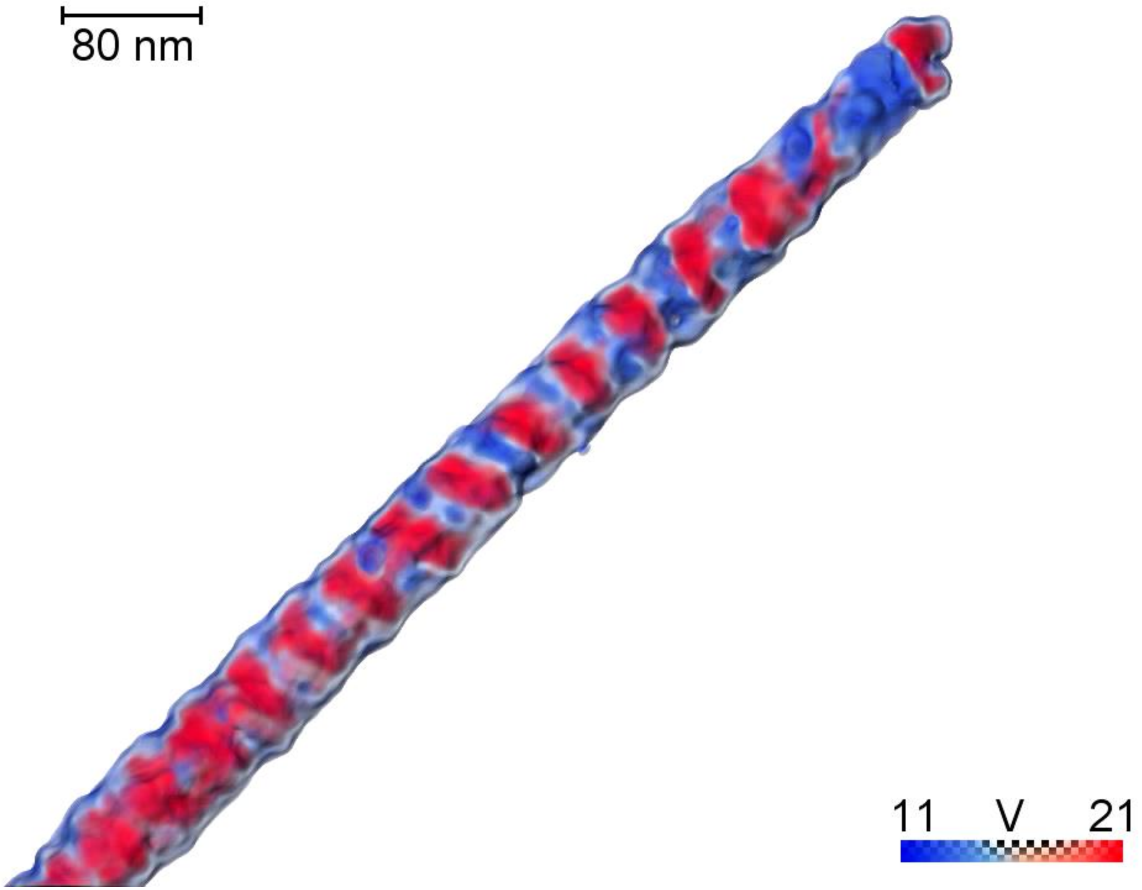

- 3D reconstruction from electrostatic phase shift (Average of two tilt series)

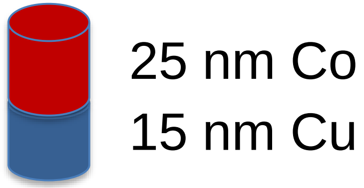

Electrostatic 3D potential of Cu/Co multi-stacked NW: Quantification

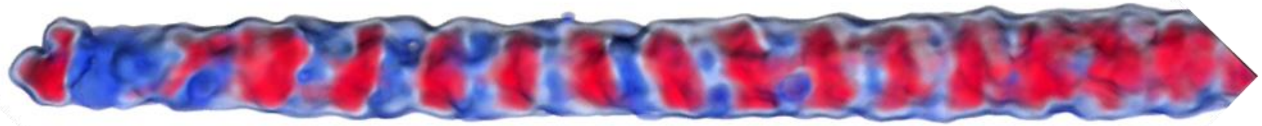

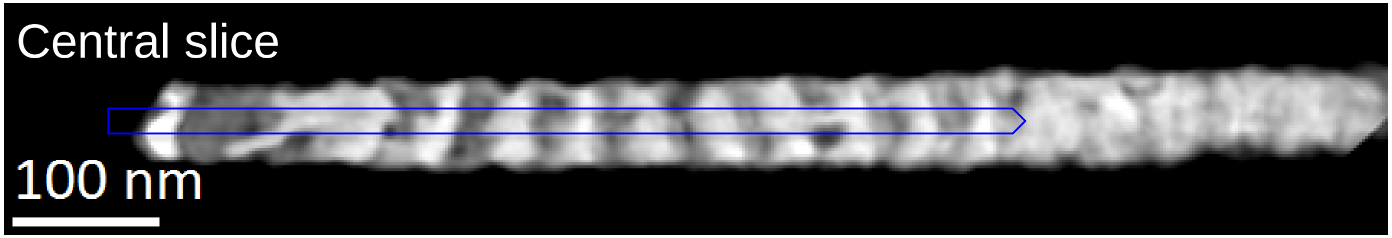

25 nm Co 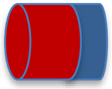 15 nm Cu

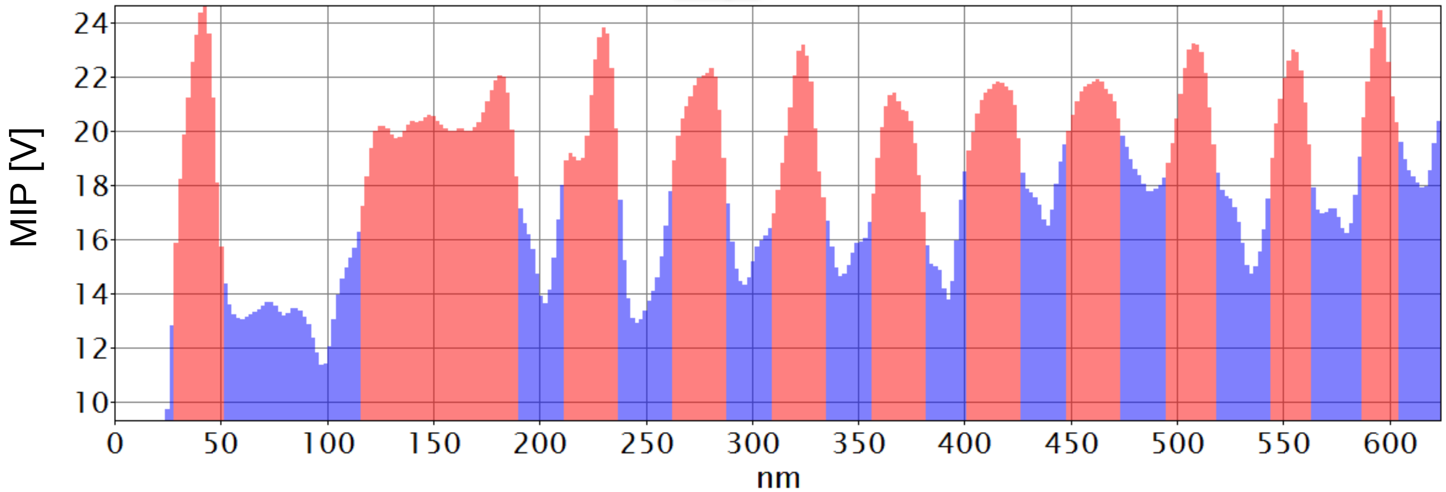

Histogram

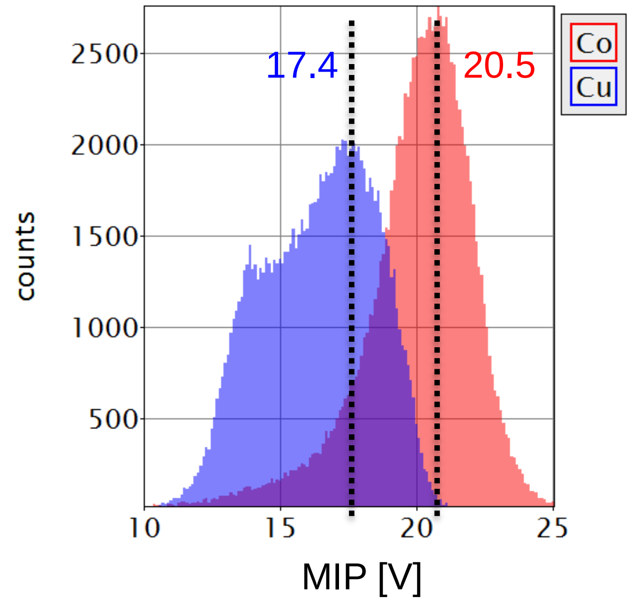

MIPs reduced
due to low purity (voids);
15% Cu amount in Co

Reconstructed magnetic configurations in Cu-Co NW

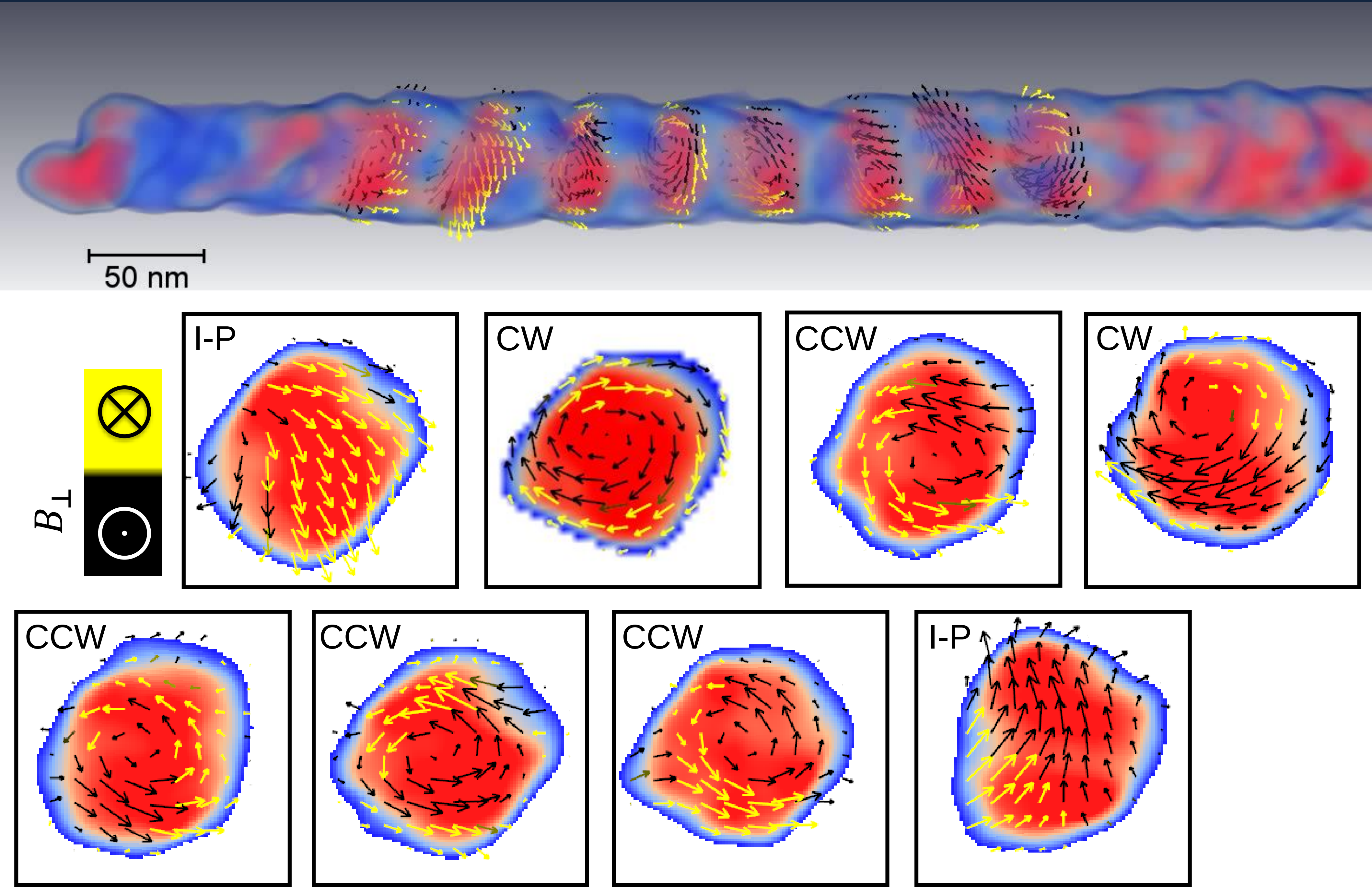

Nanoscale mapping for better understanding of 3D nanomagnetism

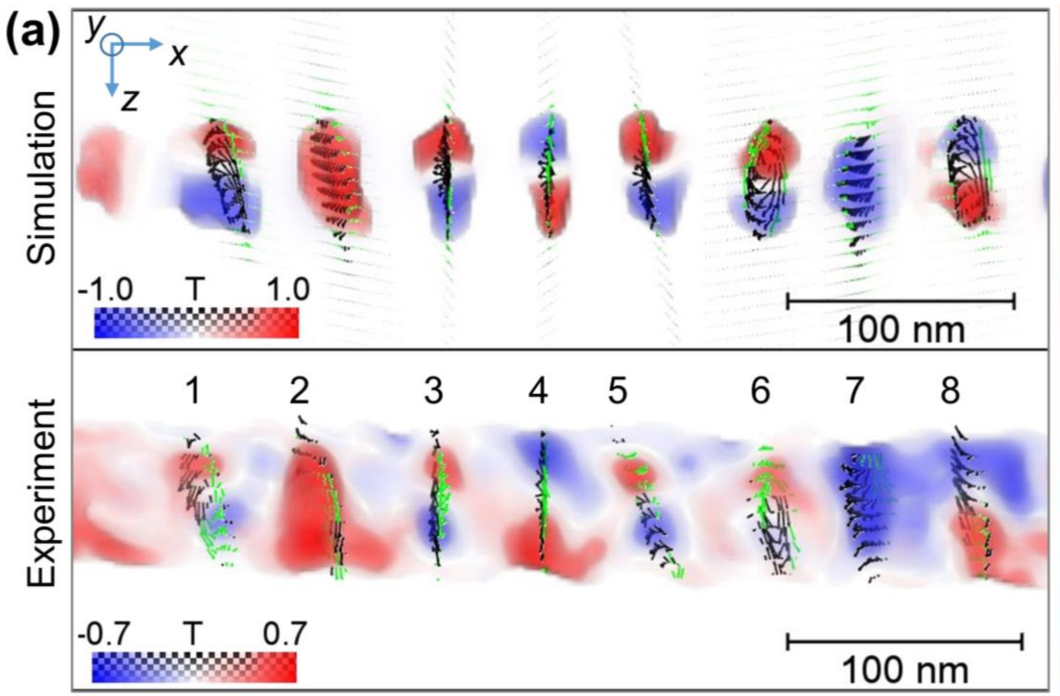

$$M_S = 1200 \times 10^3 \ {}^{A}/_{m}$$
$$A = 22 \times 10^{-12} \ {}^{J}/_{m}$$
$$H_k = 100 \times 10^3 \ {}^{J}/_{m^3}$$

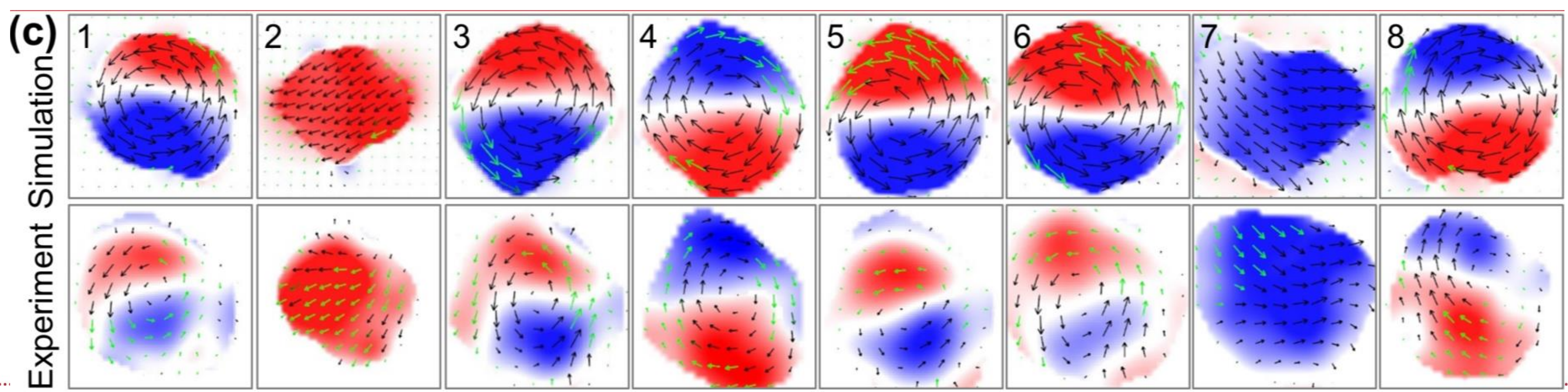

Nanoscale mapping for better understanding of 3D nanomagnetism

+ structural, chemical data

Reyes et al., Nano Lett. 16 (2016) 1230

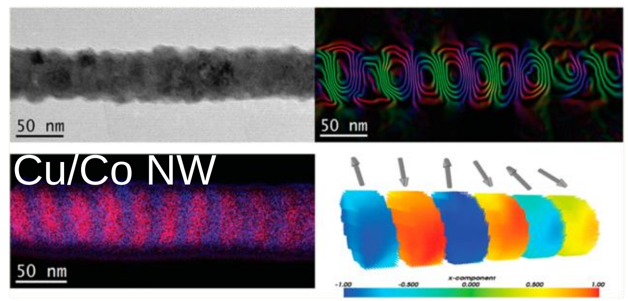

3D reconstruction by electron holographic vector field tomography of B-fields

3D modelling of M,B (eg. micromagnetic simulation)

Biziere et al., Nano Lett. 13 (2013) 2053

Comparison